

UCLA

UCLA Electronic Theses and Dissertations

Title

Parent-of-Origin Sex Chromosome Effects on the Immune and Central Nervous System During Experimental Autoimmune Encephalomyelitis

Permalink

<https://escholarship.org/uc/item/2dq3d1sq>

Author

Du, Sienmi

Publication Date

2015

Peer reviewed|Thesis/dissertation

UNIVERSITY OF CALIFORNIA

Los Angeles

Parent-of-Origin Sex Chromosome Effects on the Immune and Central Nervous System During
Experimental Autoimmune Encephalomyelitis

A dissertation submitted in partial satisfaction of the requirements
for the degree Doctor of Philosophy
in Molecular, Cellular, and Integrative Physiology

by

Sienni Du

2015

ABSTRACT OF THE DISSERTATION

Parent-of-Origin Sex Chromosome Effects on the Immune and Central Nervous System During
Experimental Autoimmune Encephalomyelitis

by

Siemi Du

Doctor of Philosophy in Molecular, Cellular, and Integrative Physiology

University of California, Los Angeles, 2015

Professor Rhonda Renee Voskuhl, Chair

Multiple sclerosis (MS) is an autoimmune demyelinating disease characterized by increased susceptibility in women. However, when men get the disease, they demonstrate more rapid disease progression, thus presenting a clinical enigma of the pathogenic events in MS susceptibility and progression. Of the sex-related factors that may contribute to MS susceptibility, much of the literature on the MS model, experimental autoimmune encephalomyelitis (EAE), has focused on the role of sex hormones in immune responses. While sex hormones have been demonstrated to affect autoimmune responses and neurodegeneration in EAE, it does not preclude sex chromosome effects. Indeed, previous work from our lab has demonstrated that the sex chromosome complement of immune cells affected autoimmune responses, with the XX sex chromosome complement, as compared to XY, leading to greater

encephalitogenicity during auto-antigen stimulation. These results are consistent with human clinical observations of increased autoimmunity in women vs. men. This dissertation builds upon this finding by exploring the nature of sex chromosome effects in the female bias in autoimmunity through the use of transgenic sex chromosome mouse models that include the following genotypes: XX, XY, X_mY^{*x} and X_pY^{*x} . Through a series of experiments, I demonstrate that parental imprinting of the X chromosome gene, forkhead box P3 (*Foxp3*), a master-regulator of T regulatory (T_{reg}) cell development, results in increased $FoxP3^+ T_{regs}$ in XY mice vs. XX mice.

While sex chromosome effects have been identified in the immune system, it remained unclear if there were separate sex chromosome effects in the target organ, the CNS, response to an immune attack during EAE. This question is addressed in another portion of my dissertation. I created a bone marrow chimera model with mice bearing a common immune system, but varying sex chromosome complement in the CNS using the aforementioned transgenic sex chromosome mouse models, to examine the effects of sex chromosomes in the CNS during neurodegeneration. Through a series of experiments, I demonstrated that mice with CNS cells expressing XY sex chromosome complement, as compared to XX, led to greater neurodegeneration. Further, increased neurodegenerative response in the XY CNS was due to the maternal X allele. Together, these results demonstrated for the first time an affect of parental imprinting resulting in female bias on the autoimmune responses, and male bias in neurodegeneration during EAE. These findings may bear relevance to the clinical observations of female bias in susceptibility, but increased disability progression in men with MS.

The dissertation of Sienmi Du is approved.

M. Carrie Miceli

Barney A. Schlinger

Allan Mackenzie-Graham

Arthur P. Arnold

Rhonda Renee Voskuhl, Committee Chair

University of California, Los Angeles

2015

This dissertation is dedicated to my family, friends, colleagues and the many wonderful teachers I have learned from over the years.

TABLE OF CONTENTS

CHAPTER 1. Introduction & Background	1
1.1 Sex differences in multiple sclerosis and EAE	1
1.2 Sex hormones in EAE susceptibility	3
1.3 Sex chromosomes in EAE susceptibility	3
1.4 Epigenetics in MS	4
1.5 Four core genotype and XY ^{*x} mouse models	6
1.6 Overview of Experiments	7
CHAPTER 2. Sex Chromosome Complement Effects in the CNS During EAE	
2.1 Introduction	9
2.2 Reconstitution efficiency in the four-core genotype bone marrow chimera model	11
2.3 EAE disease severity in SJL and C57BL/6 mice with XY vs. XX CNS	12
2.4 Spinal cord and cerebellar pathology in SJL mice with XY vs. XX CNS	16
2.5 Cerebral cortical pathology in SJL mice with XY vs. XX CNS	19
2.6 Tlr7 expression in the cerebral cortex of SJL mice with XY vs. XX CNS	20
2.7 Sex chromosome effects in the immune system in the bone marrow chimera model	23
2.8 Tlr7 in the autoimmune response of XX vs. XY ⁻ mice	26
2.9 Discussion	28

CHAPTER 3. Parent-of-Origin Sex Chromosome Effects in the CNS During EAE	33
3.1 Introduction	33
3.2 EAE disease severity in C57BL/6 mice with XY ^{*x} , XY ⁻ , and XX CNS	36
3.3 Neuropathology in the spinal cord, cerebellum and cerebral cortex in C57BL/6 mice with XY ^{*x} , XY ⁻ , and XX CNS	38
3.4 EAE disease severity in C57BL/6 mice with X _m Y ^{*x} vs. X _p Y ^{*x} CNS	42
3.5 <i>Tlr7</i> methylation in C57BL/6 mice with X _m Y ^{*x} vs. X _p Y ^{*x} cerebral cortex	44
3.6 Discussion	45
CHAPTER 4. Parent-of-Origin Sex Chromosome Effects in the Immune System During Autoimmune Responses	48
4.1 Introduction	48
4.2 FOXP3 expression and function in SJL XY ⁻ vs. XX mice	50
4.3 FOXP3 expression and function in SJL X _m Y ^{*x} , X _m Y, and X _m X _p mice	52
4.4 <i>Foxp3</i> methylation in SJL X _m Y ^{*x} , X _m Y, and X _m X _p mice	53
4.5 FOXP3 expression in SJL X _m Y ^{*x} vs. X _p Y ^{*x} mice	58
4.6 <i>Foxp3</i> methylation in SJL X _m Y ^{*x} vs. X _p Y ^{*x} mice	59
4.7 Expression and methylation status of X chromosome genes <i>Tlr7</i> and <i>Cd40l</i> in CD4 ⁺ T cells of XX, XY ⁻ , X _m Y ^{*x} , and X _p Y ^{*x} mice	63
4.8 Discussion	71
CHAPTER 5. Conclusions	76
5.1 The maternal X allele leads to a more neurodegenerative response to injury	76

5.2 Parental imprinting of <i>Foxp3</i> on the X chromosome affects T regulatory cells during autoimmunity	77
5.3 Preferential methylation of paternal X chromosome genes in the CNS and immune system in the adult mouse during EAE	77
CHAPTER 6. Methods	80
6.1 Animals	80
6.2 Karyotyping	81
6.3 Ovariectomy	82
6.4 Bone Marrow Chimera	82
6.5 EAE Induction and Scoring	83
6.6 Adoptive Transfer and Tlr7 Immune Studies	84
6.7 Histological Preparation	84
6.8 Fluorescence Immunohistochemistry	85
6.9 Chromagen Immunohistochemistry	85
6.10 Fluorescence <i>in-situ</i> Hybridization	86
6.11 Reconstitution Efficiency	87
6.12 Microscopy	87
6.13 Quantification of Microscopy	87
6.14 Cell Culture	88
6.15 Flow Cytometry	89
6.16 Cell Sorting and DNA Isolation	89
6.17 T _{reg} Suppression Assay	90

6.18 DNA Methylation Studies	91
6.19 RNA Isolation	91
6.20 Quantitative Real-Time Polymerase Chain Reaction	92
6.21 Statistical Analysis	93
CHAPTER 7. Limitations	94
7.1 Lack of mouse models to evaluate X dosage effects without confounding effects of parental imprinting	94
7.2 The Y ^{*x} chromosome in the XY ^{*x} mouse model may carry some NPX genes adjacent to the X PAR boundary	95
BIBLIOGRAPHY	97

LIST OF FIGURES

<i>Figure</i>		<i>Page</i>
1	Bone marrow chimera model to examine the effects of sex chromosomes in the CNS without confounding effects of sex chromosomes in the immune system	12
2	SJL mice with XY CNS, compared with XX CNS, have greater clinical EAE disease severity	14
3	C57BL/6 mice with XY CNS, compared with XX CNS, have greater clinical EAE disease severity	16
4	Mice with XY CNS, compared with XX CNS, have greater spinal cord and cerebellar pathology	18
5	Mice with XY CNS, compared with XX CNS, have greater synaptic loss in the cerebral cortex	20
6	Mice with XY CNS, compared with XX CNS, have more Tlr7 expressing cortical neurons in EAE	22
7	No differences in spinal cord inflammation in BMCs with varying sex chromosome complement in the CNS and a common immune system	23
8	No differences in peripheral immune cytokine responses in BMCs with varying sex chromosome complement in the CNS and a common immune system	24
9	No differences in clinical EAE disease severity in mice with varying sex chromosome complement in the immune system and a common CNS	25
10	No differences in Tlr7 expression on immune cells during the induction phase	27

	of EAE in non-chimeric SJL mice	
11	Mice with XY ^{*x} and XY CNS, compared with XX CNS, have greater clinical EAE disease severity	37
12	Mice with XY ^{*x} and XY CNS, as compared to XX, have fewer axons and less myelin staining intensity in the spinal cord during EAE	38
13	Mice with XY ^{*x} and XY CNS, as compared to XX, have less myelin staining intensity and fewer Purkinje cells in the cerebellum during EAE	40
14	Mice with XY ^{*x} and XY CNS, as compared to XX, have more Tlr7 expressing neurons during EAE	41
15	Mice with X _m Y ^{*x} CNS, as compared to X _p Y ^{*x} , have greater clinical disease severity during EAE	43
16	No differences in methylation of the <i>Tlr7</i> promoter in the cerebral cortex of mice with X _m Y ^{*x} vs. X _p Y ^{*x} CNS	44
17	XY ⁻ cells as compared to XX have higher percentage of CD4 ⁺ CD25 ⁺ FoxP3 ⁺ T _{reg} cells during induction of immune responses	51
18	X _m Y ^{*x} cells as compared to X _m X _p have higher percentage of CD4 ⁺ CD25 ⁺ FoxP3 ⁺ T _{reg} cells	53
19	XX mice, as compared to XY ⁻ , have higher DNA methylation of the <i>Foxp3</i> upstream enhancer region in CD4 ⁺ lymph node cells during induction of immune responses	55
20	X _m Y ^{*x} cells as compared to X _p Y ^{*x} have higher percentage of CD4 ⁺ CD25 ⁺ FoxP3 ⁺ T _{reg} cells during the induction of encephalitogenic immune responses	59

21	$X_m Y^{*x}$ cells, as compared to $X_p Y^{*x}$, have lower methylation of the <i>Foxp3</i> enhancer in $CD4^+$ lymph node cells during induction of immune responses	60
22	No Differences in CD40L and TLR7 expression during encephalitogenic immune responses	63
23	$X_m Y^{*x}$ cells, as compared to $X_p Y^{*x}$, have lower methylation of the <i>Cd40l</i> enhancer in $CD4^+$ lymph node cells during induction of immune responses	66
24	$X_m Y^{*x}$ cells, as compared to $X_p Y^{*x}$, have lower methylation of the <i>Tlr7</i> enhancer in $CD4^+$ lymph node cells during induction of immune responses	68

LIST OF TABLES

<i>Table</i>		<i>Page</i>
1	Breeding schematic to examine the role of X and Y dosage in the CNS neurodegenerative response to injury	34
2	Breeding schematic to examine the role of parental imprinting in the CNS neurodegenerative response to injury	35
3	Bisulfite sequencing results demonstrating significant differences between XY and XY ^{*x} vs. XX in the methylation of 17 CG sites located in the <i>Foxp3</i> upstream enhancer region	56
4	Bisulfite sequencing results demonstrating significant differences between X _m Y ^{*x} vs. X _p Y ^{*x} in the methylation of 17 CG sites located in the <i>Foxp3</i> upstream enhancer region	61
5	Bisulfite sequencing results demonstrating significant differences between X _m Y ^{*x} vs. X _p Y ^{*x} in the methylation of 7 out of 11 CG sites located in the <i>Cd40l</i> promoter region	67
6	Bisulfite sequencing results demonstrating significant differences between X _m Y ^{*x} vs. X _p Y ^{*x} in the methylation of 7 out of 8 CG sites located in the <i>Tlr7</i> promoter region	67
7	Breeding schematic to examine X dosage in immune responses and neurodegeneration is confounded by parental X imprinting	92

ACKNOWLEDGEMENTS

First, I would like to thank my advisor, Dr. Rhonda R. Voskuhl, for her scientific expertise, consistent support and encouragement, and for giving me the opportunity to grow in her lab through various exciting projects. Many professors have been very helpful throughout my graduate studies, but I would especially like to thank my committee members: Drs. Arthur P. Arnold, Barney A. Schlinger, Allan MacKenzie Graham, and M. Carrie Miceli. Dr. Arnold has been an invaluable mentor, a friendly voice, a trove of knowledge on sex differences research, welcoming me to his lab meetings, and taking the role of an academic grandfather to me.

I am grateful to the past and present members of the Voskuhl Lab for their technical support, discussions, and friendship through this long process: Noriko Itoh, Elizabeth Umeda, Dr. Deb Smith-Bouvier, Dr. Stefan Gold, Dr. R. Scott Peterson, Dr. Rory Spence, Dr. Marina Ziehn, Dr. Sasidhar Manda, Roy Kim, Laura Kammel, as well as the invaluable team of undergraduate researchers: Kelly Wong, Andi Bernardoni, Mavis Peng, Hadley Johnsonbaugh, Emma Difilippo, Sahar Askarinam, Francisco Sandoval, Alexandra Cappiello, Christina Keenan, and Haley Hill. I would also like to thank the MCIP director and advisor, Dr. Jim Tidball and Michael Carr.

I would like to thank my family for their unwavering support and love. My parents, Bao and Quyen, have believed in me even when I doubted myself, and have thrown all their financial and mental support behind me in pursuing a Ph.D., and in the near future, and M.D. They are such strong role models for me, living examples of what one can achieve with hard work and patience. I'd like to thank my wonderfully creative, spunky, and beautiful sister, Sienree, who is always there for me when I need her, and who inspires me to do achieve my goals. She is a

walking embodiment of the phrase, “live life to the fullest.” I would like to thank my in-laws, Debbie, Bob, and Keith Lutkenhoff for welcoming me into their family with such open arms, for loving me, and providing moral support and encouragement throughout my milestones.

Lastly, I would like to thank my husband, my better half, Evan. You are my rock (the more valuable one ☺). You have been such a wonderfully positive force in my life, supporting my career goals, and encouraging my growth. Thanks for walking the puppies and cooking on those nights I had to study or work late, and sewing up all those chewed up pillows and torn sheets from our beloved puppy. I don’t know how I would have done all this without you. I love you.

On the non-human front, I would like to thank my canine companions, Wrigley and Tank. Wrigley was the best first dog I could ever ask for, always a companion by my side. Tank has provided countless comedic relief and cuddling comfort when I needed it. He is truly a bully breed ambassador. Thank you for loving me, puppies.

Chapter 2 is a version of Sienmi Du, Noriko Itoh, Sahar Askarinam, Haley Hill, Arthur P. Arnold, & Rhonda R. Voskuhl. (2014). XY sex chromosome complement, compared with XX, in the CNS confers greater neurodegeneration during experimental autoimmune encephalomyelitis. *Proceedings of the National Academy of Sciences of the United States of America*, *111*(7), 2806-2811. doi: Doi 10.1073/Pnas.1307091111. In this chapter, SD and RRV designed the experiments, NI bred and maintained the four-core genotypes, SD and NI created the bone marrow chimeras, SD, SA, and HH performed the experiments, SD and RRV analyzed the results; SD wrote the manuscript, with critical revisions by RRV, and APA provided intellectual insight on the FCG model.

Chapter 3 is a version of Sienmi Du, Noriko Itoh, Mavis Peng, Kelly Wong, Andi

Bernardoni, Emma DiFilippo, Hadley Johnsonbaugh, Arthur P. Arnold, Amr H. Sawalha, Rhonda R. Voskuhl. (2015). The maternal X allele leads to a more neurodegenerative response to injury. *In preparation for submission*. In this chapter, SD and RRV designed the experiments; NI, MP, KW, JH, ED, and HJ bred and maintained the four-core genotypes, XY^{*}, and XY^{*x} breeding colonies; SD and NI created the bone marrow chimeras, SD performed the experiments with help from KW, and AB; AHS performed bisulfite sequencing experiments; SD and RRV analyzed the results; APA provided intellectual insight on the FCG, XY^{*}, and XY^{*x} models.

Chapter 4 is a version of Sienmi Du, Noriko Itoh, Mavis Peng, Kelly Wong, Emma DiFilippo, Hadley Johnsonbaugh, Arthur P. Arnold, Amr H. Sawalha, Rhonda R. Voskuhl. (2015). Parental imprinting of *Foxp3* on the X chromosome affects T regulatory cells during autoimmunity. *In preparation for submission*. In this chapter, SD and RRV designed the experiments; AHS performed bisulfite sequencing experiments, SD performed all other experiments; APA designed the X_mY^{*x} and X_pY^{*x} breeding scheme; NI and MP bred and maintained all mouse colonies and performed gonadectomies; NI, MP, KW, ED, HJ, and JH karyotyped the mice; SD and RRV analyzed the results.

The support for this work was provided by National Institutes of Health (NIH) grants R21 NS071210 and K24 NS062117 to RRV, National MS Society grant RG 4857A17 to RRV, and NIH F31NS080437 to SD. SD was supported by NIH T32HD007228. This work was also supported by the Conrad N. Hilton Foundation, the Jack H. Skirball Foundation, and the Sherak Family Foundation.

VITA

EDUCATION

- 2000 - 2005 BS, Neuroscience
University of California, Los Angeles, Los Angeles, CA
- 2007-2009 MS, Physiological Sciences
University of California, Los Angeles, Los Angeles, CA

ACTIVITIES

- 2008-2009 Teaching Associate, Foundations in Physiological Science, Department of Physiological Sciences, University of California, Los Angeles
- 2012, 2014 Teaching Fellow, Sex: From Biology to Gendered Society, Department of Undergraduate Education Initiatives
University of California, Los Angeles
- 2012, 2015 Graduate Student Instructor, Sex differences in multiple sclerosis and other diseases, Department of Undergraduate Education Initiatives, University of California, Los Angeles

AWARDS

- 2010 Trainee, National Institutes of Health (NIH) Institutional Predoctoral National Research Service Award (NRSA) in Molecular, Cellular, and Integrative Physiology, University of California, Los Angeles
- 2012 Trainee, NIH Institutional Predoctoral NRSA in Neuroendocrinology and Sex Differences, University of California, Los Angeles
- 2013 NIH, National Institute of Neurological Disorders and Stroke (NINDS) Individual Predoctoral NRSA in Sex Differences in the CNS During EAE, University of California, Los Angeles
- 2013 Office of Instructional Development Faculty Mini-Grant
University of California, Los Angeles
- 2013 Elizabeth Young New Investigator Award
Organization for the Study of Sex Differences
- 2013 Florence P. Haseltine Award, Honorable Mention
Organization for the Study of Sex Differences
- 2013 Whitaker Scholar for Multiple Sclerosis Research
Americas Committee for Treatment and Research in Multiple Sclerosis
- 2013 Consortium for Multiple Sclerosis Research Scholarship

PUBLICATIONS

Smith DL, Dong X, Du S, Oh M, Singh RR, Voskuhl RR. A female preponderance for chemically induced lupus in SJL/J mice. *Clinical Immunology*, 122(1):101-7, 2007. (PMCID: PMC2291542)

Smith-Bouvier, D., Divekar, A., Sasidhar, M., Du, S., Tiwari-Woodruff, S., King, J., Arnold, A., Singh, R.R., Voskuhl, R.R. A Role for Sex Chromosome Complement in the Female Bias in Autoimmune Disease. *Journal of Experimental Medicine*, 205:1099-1108, 2008. (PMCID: PMC2373842)

Gold, S., Manda, S., Morales, L., Du, S., Sicotte, N., Tiwari-Woodruff, S., Voskuhl, R.R. Estriol treatment decreases matrix metalloproteinase (MMP)-9 in autoimmune demyelinating disease through estrogen receptor alpha. *Laboratory Investigation*, 89: 1076-1083, 2009. (PMCID: PMC2753699).

Du, S., Sandoval, F., Trinh, P., R. Voskuhl, R.R. Additive effects of combination treatment with anti-inflammatory and neuroprotective agents in experimental autoimmune encephalomyelitis. *J. Neuroimmunology*, 219:64-74, 2010. (PMCID: PMC3037186).

Crawford, D., Mangiardi, M., Song, B., Patel, R., Du, S., Sofroniew, M., Voskuhl, R., Tiwari-Woodruff, S. Oestrogen receptor β ligand: A novel treatment to enhance endogenous functional remyelination. *Brain*, 133:2999-3016, 2010. (PMCID: PMC2947430).

Du, S., Sandoval, F., Trinh, P., R., Umeda, E., Voskuhl, R.R. Estrogen receptor-beta ligand treatment modulates dendritic cells in the target organ during autoimmune demyelinating disease. *Eur. J. Immunology*, 41:140-150, 2011. (PMCID: PMC3042725).

Mangiardi, M., Crawford, D., Xia, X., Du, S., Simon-Freeman, R., Voskuhl, R., and Tiwari-Woodruff, S. An Animal Model of Cortical and Callosal Pathology in Multiple Sclerosis. *Brain Pathology*, 21:263-278, 2011.

Rory D. Spence, Mary E. Hamby, Elizabeth Umeda, Sienmi Du, Noriko Itoh, Galyna Bondar, Jeanie Lam, Yan Ao, Amy Wisdom, Yuan Cao, Francisco Sandoval, Michael V. Sofroniew, Rhonda R. Voskuhl. Neuroprotection mediated through estrogen receptor alpha on astrocytes. *Proceedings of the National Academy of Sciences (PNAS)*, 108:8867-8872, 2011. (PMCID: PMC3102368)

Matthew Fuxjager, Julia Barske, Sienmi Du, Barney A. Schlinger. Androgens regulate gene expression in avian skeletal muscles. *PLoS One*, 7(12):e51482, 2012. (PMCID: 23284699)

Sienmi Du, Noriko Itoh, Sahar Askarinam, Haley Hill, Arthur P Arnold, Rhonda R Voskuhl. Sex chromosome genes directly affect the CNS response to injury. *PNAS*, 111(7):2806-11, 2014.

Chapter 1: Introduction & Background

1.1 Sex differences in multiple sclerosis and EAE

Disease susceptibility. Women are more likely to develop autoimmune (AI) diseases than men (Whitacre, 2001). In multiple sclerosis (MS), the female to male ratio for incidence is 2:1 to 3:1, although this ratio seems to have increased in recent years. The average age of onset for females is between 18-30, whereas males tend to have a later onset, between 30-40 years old. A female bias is also found in other autoimmune diseases, including other cell-mediated autoimmune responses such as rheumatoid arthritis, as well as humoral-mediated responses, such as systemic lupus erythematosus (SLE). The female preponderance in a broad spectrum of AI diseases implies that there may be a common sex-related factor affecting immune responses among female biased autoimmune diseases.

Fortunately, there are animal models of some AI diseases that have a natural female bias in which to study this phenomenon. In the most widely used MS mouse model, experimental autoimmune encephalomyelitis (EAE), the SJL strain has a female bias for the disease that is consistent with increased female incidence in MS (R. R. Voskuhl, PitchekianHalabi, MacKenzieGraham, McFarland, & Raine, 1996). The NZW strain also demonstrated a female bias in incidence, but not in disease severity during EAE (Papenfuss et al., 2003). On the other hand, some strains of mice, such as B10.PL and PL/J, demonstrated more severe acute EAE in males than in females, with additional studies implicating physiological ovarian hormones in the female protection against the disease (Papenfuss et al., 2003). There are also some strains, such as the C57BL/6 and NOD/Lt, that demonstrated no difference in incidence or disease severity between females and males (Okuda, Okuda, & Bernard, 2002).

Disease progression. Women demonstrate greater responses to various immune challenges, including autoantigen-stimulated responses skewing from Th2 to Th1 cytokines, with increased IL-5 and decreased IFN γ production in female MS patients (Moldovan, Cotleur, Zamor, Butler, & Pelfrey, 2008; Pelfrey, Cotleur, Lee, & Rudick, 2002). In accord with these findings, another group found a polymorphism in the *IFN γ* gene that is associated with MS susceptibility in men but not women (Orhun H. Kantarci et al., 2008). However, there seems to be a disconnect between immune responses and progression of disease, as evidenced by studies of natural history of MS patients demonstrating faster progression to disability in men (Confavreux, Vukusic, & Adeleine, 2003), particularly those demonstrating a primary progressive disease course (Wolinsky, Shochat, Weiss, Ladkani, & Grp, 2009). Further, another natural history study found that men with MS demonstrated a shorter time to conversion between a relapse-remitting to secondary progressive disease course (Koch, Kingwell, Rieckmann, Tremlett, & Neurologists, 2010).

In summary, epidemiological and natural history studies on the susceptibility and progression of MS in female and male patients have revealed a clinical enigma: women demonstrate higher incidence of MS with more robust immune responses, but disease progression, accumulation of permanent disability, and neurodegeneration, may be faster in men. As such, there should be strong consideration for sex-related factors contributing to sex differences in disease susceptibility and progression, as well as the possibility that these factors may be opposed in the immune system and the CNS.

1.2 Sex hormones in EAE susceptibility

The female bias in MS susceptibility could theoretically result from deleterious effects of female sex hormones or protective effects of male sex hormones. The results have been conflicting in the EAE model with regard to cyclical levels of ovarian sex hormones, with some groups demonstrating that ovariectomy worsens clinical disease (Jansson, Olsson, & Holmdahl, 1994; Matejuk et al., 2001), and others showing no effect (R. R. Voskuhl & Palaszynski, 2001). However, if endogenous low levels of cycling ovarian levels were protective, then contrary to clinical observations, one would reasonably expect to observe greater incidence of MS in men than women.

In contrast, physiological levels of testicular hormones have been demonstrated to be protective in EAE. Sex differences in EAE were abolished after castration of male mice in a strain characterized by a female bias for EAE (Palaszynski, Loo, Ashouri, Liu, & Voskuhl, 2004). This finding suggests that the protective effects of physiological levels of testicular hormones (e.g. testosterone) may partially account for the decreased male susceptibility in strains demonstrating sex differences in susceptibility to EAE.

1.3 Sex chromosomes in EAE susceptibility

Apart from sex hormones, sex differences in MS and EAE may be influenced by another sex-related factor, namely sex chromosomes. It is important to note that findings of sex hormone effects do not preclude independent effects of sex chromosomes on EAE disease susceptibility and progression. With the advent of the four-core genotype mouse model (see Chapter 1.5), our lab was able to examine the role of sex chromosome complements in the susceptibility to EAE. The XX sex chromosome complement, as compared with the XY, resulted in greater disease

severity in EAE and pristane-induced SLE (Palaszynski et al., 2005), as well as in auto-antigen stimulated encephalitogenic immune responses during EAE and spontaneous SLE (Sasidhar, Itoh, Gold, Lawson, & Voskuhl, 2012; Smith-Bouvier et al., 2008). However, it remained unknown whether these findings are caused by X dosage, Y dosage, or parent-of-origin of the X chromosome. It was also unknown whether effects of sex chromosome complement in immune responses could be projected to sex chromosome effects in the CNS during neurodegeneration. This is particularly relevant to MS because all current disease-modifying treatments target inflammation without offering any neuroprotection. Despite anti-inflammatory drug treatment, MS patients inevitably accumulate permanent disability and neurodegeneration over time. Thus, while we have uncovered some interesting roles for sex chromosomes in immune responses during EAE, there should be more efforts toward understanding the sex bias in disability progression. Since men with MS demonstrate a faster progression to disability, this warrants examination of sex-related factors such as sex chromosomes in the CNS neurodegenerative response to injury.

1.4 Epigenetics in MS

Parent-of-origin effects, particularly those related to the human leukocyte antigen (HLA) background, have been ascribed sex-specific MS transmission. For example, female MS patients are more likely to carry the *HLA-DRB1*15+* haplotype than male MS patients with preferential transmission from mother-to-daughter, rather than mother-to-son or father-to-daughter or -son, suggesting maternal imprinting effects on the female bias in MS susceptibility (Chao et al., 2010).

Population-based studies have also identified maternal parent-of-origin effects with increased incidence in female offspring in families through avuncular pair studies. Affected females are more likely to have an affected maternal aunt or uncle (Herrera et al., 2008). Additional studies in half siblings with MS, extended pedigrees of MS families, and interracial admixture populations with MS also suggest transmission through the maternal lineage (Ebers et al., 2004; Hoppenbrouwers et al., 2008; Ramagopalan et al., 2009). Specifically, half siblings and extended families with MS are more likely related through their mother (Ebers et al., 2004; Hoppenbrouwers et al., 2008). Also, in a specific Canadian interracial admixture of less susceptible North American Aboriginals and more susceptible Northern European ancestry, affected patients more likely have mothers of Northern European descent rather than North American Aboriginal, suggesting a maternal parent-of-origin effect on MS transmission (Ramagopalan et al., 2009).

Thus far, the parent-of-origin effects leading to a female bias in susceptibility to MS have been linked to an HLA polymorphism and an *IFN γ* allelic variant (Chao et al., 2010; Orhun H. Kantarci et al., 2008). No studies have examined parent-of-origin effects on MS disability and progression. This may have resulted from a lack of focus on epigenetic mechanisms in MS, and an overemphasis on linkage studies focused on gene mutations and polymorphisms. As such, methods used to detect polymorphisms, such as genome wide association studies (GWAS), would not have detected epigenetic changes like DNA methylation and histone modification that were relevant to disease risk.

1.5 Four core genotype and XY^{*x} mouse models

In order to study the role of sex chromosomes in the female bias of MS and EAE susceptibility and the male bias of MS progression, I used three sex chromosome transgenic mouse lines: XX and XY⁻ four-core genotype, X_mY^{*x}, and X_pY^{*x} mice.

Four-core genotypes. The four-core genotype mouse model has been instrumental in moving past sex hormone-based explanations of biological sex differences and to begin to consider sex chromosome effects (Arnold, 2012). In this model, the testis-determining factor *Sry*, was spontaneously deleted from the Y chromosome (denoted Y⁻), and then reintroduced back to chromosome 3 (Itoh et al., 2015), resulting in XY⁻(+*Sry*). The breeding of XY⁻(+*Sry*) yields mice of four genotypes: ovary-bearing XX or XY⁻, or testis-bearing XX or XY⁻. Using XX and XY⁻ mice with a common gonadal background, one can examine the effects of sex chromosome complement on a given phenotype while simultaneously eliminating possible confounding effects of sex hormones (A. P. Arnold & X. Chen, 2009). For example, since sex hormones can modulate EAE disease through actions in the immune system, the four-core genotype model becomes particularly relevant to EAE studies examining the role of sex chromosome complement on immune responses.

*X_mY^{*x} mice.* The X_mY^{*x} mice is ovary bearing and essentially has 1 X chromosome and 0 Y chromosome. This mouse results from breeding XY^{*} mice (gonadal male), with WT XX mice. A spontaneous mutation of the paternal Y^{*} chromosome yields several aberrant Y^{*} chromosomes, one of which is a Y^{*x} chromosome, comprised of mostly pseudoautosomal region (PAR) of maternal and paternal origin, several non-PAR X (NPX) genes from the X-PAR boundary, and no non-PAR Y genes (NPY). Thus, the X chromosome follows a maternal inheritance. The X_mY^{*x} genotype is essential to determine whether the presence or absence of

the Y chromosome is responsible for an observed difference between XX and XY⁻ sex chromosome complement (see Table 1). The X_mY^{*x} mouse also inherits the X chromosome through the maternal lineage, and when compared with X_pY^{*x}, is useful in determining whether parental imprinting effects are responsible for observed differences between XX or XY⁻ sex chromosome complement.

*X_pY^{*x} mice.* The X_pY^{*x} is essential for examining the effects of parent-of-origin of the X chromosome on a phenotype. This mouse results from the cross of X_mY^{*x} with WT XY, with maternal Y^{*x} inheritance and paternal X inheritance. X_pY^{*x} will be compared against X_mY^{*x} mice to determine whether parental imprinting of the X chromosome accounts for sex differences in immune responses or neurodegeneration. Since both X_mY^{*x} and X_pY^{*x} have 1 Y^{*x}, one can examine the effect of maternal X vs. paternal X imprint without possible confounding effects of X or Y dosage (see Table 2). To control for other genetic variations when comparing across litters, one can use XX mice, which is a common progeny among the four-core genotype, X_mY^{*x}, and X_pY^{*x} colonies.

1.6 Overview of Experiments

In this dissertation, I used the four-core genotype and the XY^{*x} models to first address the role of sex chromosomes in the CNS during neurodegenerative response to injury, considering in particular the role of sex chromosome complement, Y dosage, and parental imprinting of the X chromosome. Since sex chromosome complement affects EAE susceptibility and auto-antigen induced immune responses (Palaszynski et al., 2005; Sasidhar et al., 2012; Smith-Bouvier et al., 2008), I created bone marrow chimeras (BMCs) with a common immune system, and varying sex chromosomes in the CNS (e.g. XX, XY⁻, X_mY^{*x}, or X_pY^{*x}). As EAE ensued, I evaluated

clinical disease and neuropathology in these mice. To evaluate the role of sex chromosome complement on neurodegeneration, I compared BMCs with XX and XY CNS. If there were an effect of sex chromosome complement in the CNS, then I compared BMCs with XX, X_mY , X_mY^{*x} CNS to determine whether these effects were due to the presence or absence of Y chromosome. To address the possibility of parental X imprinting on neurodegeneration, I compared BMCs with X_mY^{*x} and X_pY^{*x} CNS.

I used the same comparisons of four-core genotype and the XY^{*x} models to further examine the role of sex chromosomes during autoimmune responses, also considering effects sex chromosome complement, Y dosage, and parental X imprinting, like in the CNS studies. However, since I was examining the induction phase of autoimmune responses before the animals exhibit clinical signs, I did not create bone marrow chimeras to control of sex chromosome complement in the CNS.

Chapter 2: Sex Chromosome Complement Effects in the CNS

During EAE

2.1 Introduction

Most autoimmune diseases affect females more than males in both humans and mice. In addition to multiple sclerosis (MS), other examples include systemic lupus erythematosus (SLE), rheumatoid arthritis, and Hashimoto's thyroiditis (Whitacre, Reingold, O'Looney, & Task Force Gender Multiple Sclerosis, 1999). This enhanced susceptibility in females compared to males has also been observed in animal models such as experimental autoimmune encephalomyelitis (EAE) in SJL mice, spontaneous SLE, chemically induced lupus, adjuvant arthritis, and thyroiditis (Whitacre et al., 1999). Most studies on sex differences in autoimmune diseases have focused on sex hormones (Rhonda R. Voskuhl & Gold, 2012). However, a role for sex hormones does not exclude a contribution of sex chromosomes to the female bias in susceptibility to these autoimmune diseases. Further, while MS is more prevalent in females with more robust immune responses, some data have suggested that men with MS demonstrate a more progressive neurodegenerative course (Antulov et al., 2009; Confavreux et al., 2003; Pozzilli et al., 2003; Savettieri et al., 2004; Weinshenker, 1994; Weinshenker et al., 1991) (reviewed in (Rhonda R. Voskuhl & Gold, 2012)). Thus, we hypothesized that there could be sex-related factors that have opposing effects on the immune system versus the CNS, causing female MS patients to have more robust peripheral immune responses, but a more resilient CNS response to injury. A comprehensive understanding of sex differences could lead to therapies in sex-biased autoimmune or neurodegenerative diseases.

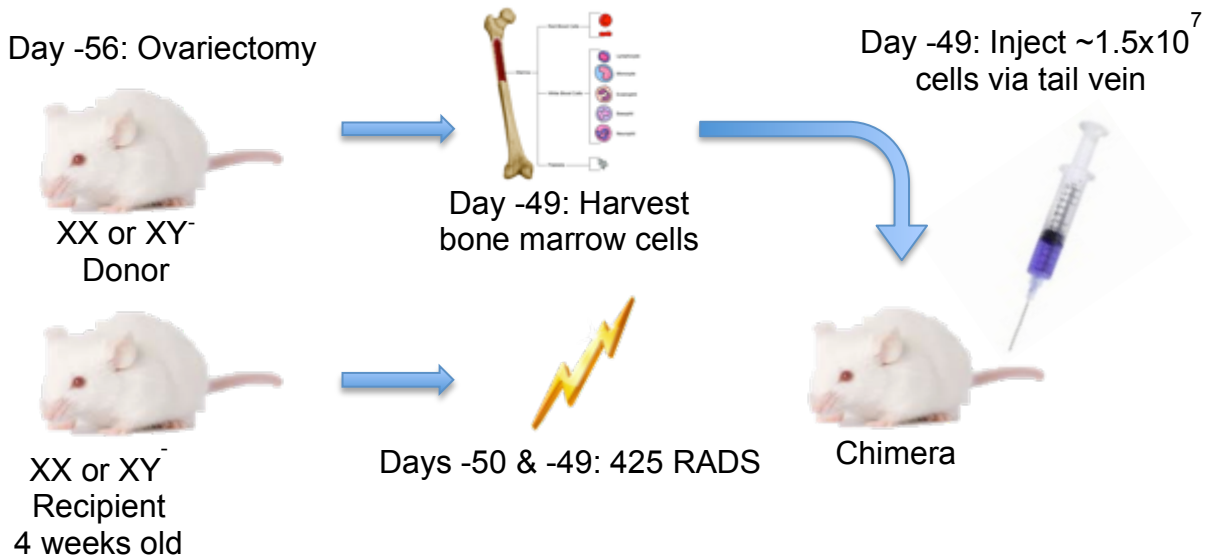
In our lab's previously published work we found that sex chromosome complement affected EAE susceptibility. Our lab used SJL transgenic mice, known as four-core genotypes (FCG), in which the testis-determining factor *Sry* has been deleted from the Y chromosome (denoted Y^-). XY^- mice with an autosomal *Sry* transgene, denoted $XY^- (Sry^+)$, are fertile and are fathers to ovary-bearing XX and XY^- females. Comparisons between XX and XY^- mice revealed effects of sex chromosomes not confounded by differences in types of gonadal hormones since they are both gonadally female. When PLP 139-151 sensitized lymph node cells (LNCs) derived from either XX or XY^- immunized mice were adoptively transferred into a common recipient, there was a dramatic difference in EAE severity, with those receiving XX cells having much more severe EAE than those receiving XY^- cells (Smith-Bouvier et al., 2008). This demonstrated a sex chromosome effect on the induction of encephalitogenic immune responses during immunization of adult mice with PLP 139-151. However, it remained unknown whether there were sex chromosome effects in the CNS response to injury.

Previous work suggests that sex chromosomes may play a role in CNS plasticity. Gene expression array studies in mice and humans have shown that a significantly higher proportion of genes on sex chromosomes, as compared to genes on autosomes, are preferentially expressed in the brain compared to other somatic tissues (Gregg, Zhang, Weissbourd, et al., 2010; Nguyen & Disteche, 2006). Additionally, neurons with different sex chromosome complements develop differently, regardless of gonadal sex (Carruth, Reisert, & Arnold, 2002). These findings are consistent with the observations of anatomically dimorphic brain regions between females and males in the human and mouse (Dorr, Lerch, Spring, Kabani, & Henkelman, 2008; Luders, Gaser, Narr, & Toga, 2009; Spring, Lerch, & Henkelman, 2007). While many hypothesize that sex hormones may contribute to the sexual dimorphism in a number of neurological diseases,

such as Parkinson's disease, Alzheimer's disease, and schizophrenia, a role for sex chromosomes has not been excluded (Cahill, 2006). To test whether sex chromosomes may directly influence the CNS response to injury, we generated bone marrow chimeras (BMC) of XX and XY⁻ gonadal female mice in which the sex chromosome complement of the reconstituted immune system was varied independently of that in the brain. This allowed us to examine sex chromosome effects in the CNS during EAE without confounding effects of differences in sex chromosome complement in the immune system.

2.2 Reconstitution efficiency in the four-core genotype bone marrow chimera model

We generated FCG BMCs in the following combinations: 1) XX immune system, XX CNS, 2) XX immune system, XY⁻ CNS, 3) XY⁻ immune system, XX CNS, 4) XY⁻ immune system, XY⁻ CNS (Fig 1). We first determined the reconstitution efficiency of the BMCs by marking X and Y chromosomes in splenocytes using DNA fluorescence *in situ* hybridization. As a positive control, XX chimeric mice reconstituted with XX BM cells (XX→XX; donor BM genotype before arrow and recipient after arrow) and XY⁻ chimeric mice reconstituted with XY⁻ immune cells (XY⁻→XY⁻) were labeled with an X chromosome (red) and Y chromosome (green) probe mixture. Both X and Y labeling was present in DAPI⁺ cells in XY⁻→XY⁻ chimeras (Fig 2A), while Y labeling was absent in DAPI⁺ cells in XX→XX chimeras (Fig 2B). The reconstitution percentage was then determined to be in the range of 87-94% (Fig 2C) in chimeric mice with XX CNS reconstituted with XY⁻ BM cells (XY⁻→XX) and chimeric mice with XY⁻ CNS reconstituted with XX BM cells (XX→XY⁻).



- Bone marrow chimeras**
- Group 1) XX immune → XX CNS
 - Group 2) XX immune → XY⁻ CNS
 - Group 3) XY⁻ immune → XX CNS
 - Group 4) XY⁻ immune → XY⁻ CNS

Figure 1. Bone marrow chimera model to examine the effects of sex chromosomes in the CNS without confounding effects of sex chromosomes in the immune system. Five-week old donor of a single genotype, as well as recipient mice of either XX or XY⁻ genotype are ovariectomized and then allowed to recover for a week. Recipient mice are then irradiated and injected with 1.5×10^7 donor bone marrow cells to reconstitute their immune system. Mice are allowed to recover from irradiation for seven weeks, after which they are immunized to induce EAE. Detailed protocol can be found in Chapter 6: Methods.

2.3 EAE disease severity in SJL and C57BL/6 mice with XY vs. XX CNS

To determine the role of sex chromosome complement in the CNS independent of sex chromosome effects on the immune system, we compared PLP 139-151 peptide induced active EAE in SJL BMCs that had been reconstituted with the same immune system and had a common hormonal background (all females), but differed in their sex chromosome complement in the

CNS ($XX \rightarrow XX$ vs. $XX \rightarrow XY^-$, and $XY^- \rightarrow XX$ vs. $XY^- \rightarrow XY^-$). As shown in Fig 2D and 2E, mice with XY^- sex chromosome complement in the CNS, as compared with XX , had worse standard EAE disease severity scores late in EAE ($p < 0.0001$, $XX \rightarrow XX$ vs. $XX \rightarrow XY^-$, and $p < 0.0001$, $XY^- \rightarrow XX$ vs. $XY^- \rightarrow XY^-$, repeated measures one-way ANOVA with Bonferroni post-hoc test). Additionally, mice were subjected to rotarod testing, a more sensitive measure of coordination. Consistent with EAE scores, mice with XY^- CNS were able to stay on the rotarod for fewer seconds as compared to mice with XX CNS (Fig 2F and 2G, $p < 0.0001$, $XX \rightarrow XX$ vs. $XX \rightarrow XY^-$, and $p < 0.0001$, $XY^- \rightarrow XX$ vs. $XY^- \rightarrow XY^-$, repeated measures one-way ANOVA with Bonferroni post-hoc test). Notably, this sex difference in the CNS runs counter to those found in the induction phase of adoptive EAE in SJL mice where autoantigen specific XX immune cells were more encephalitogenic than XY^- . Together, this indicates that sex chromosome effects in disease can be tissue-specific.

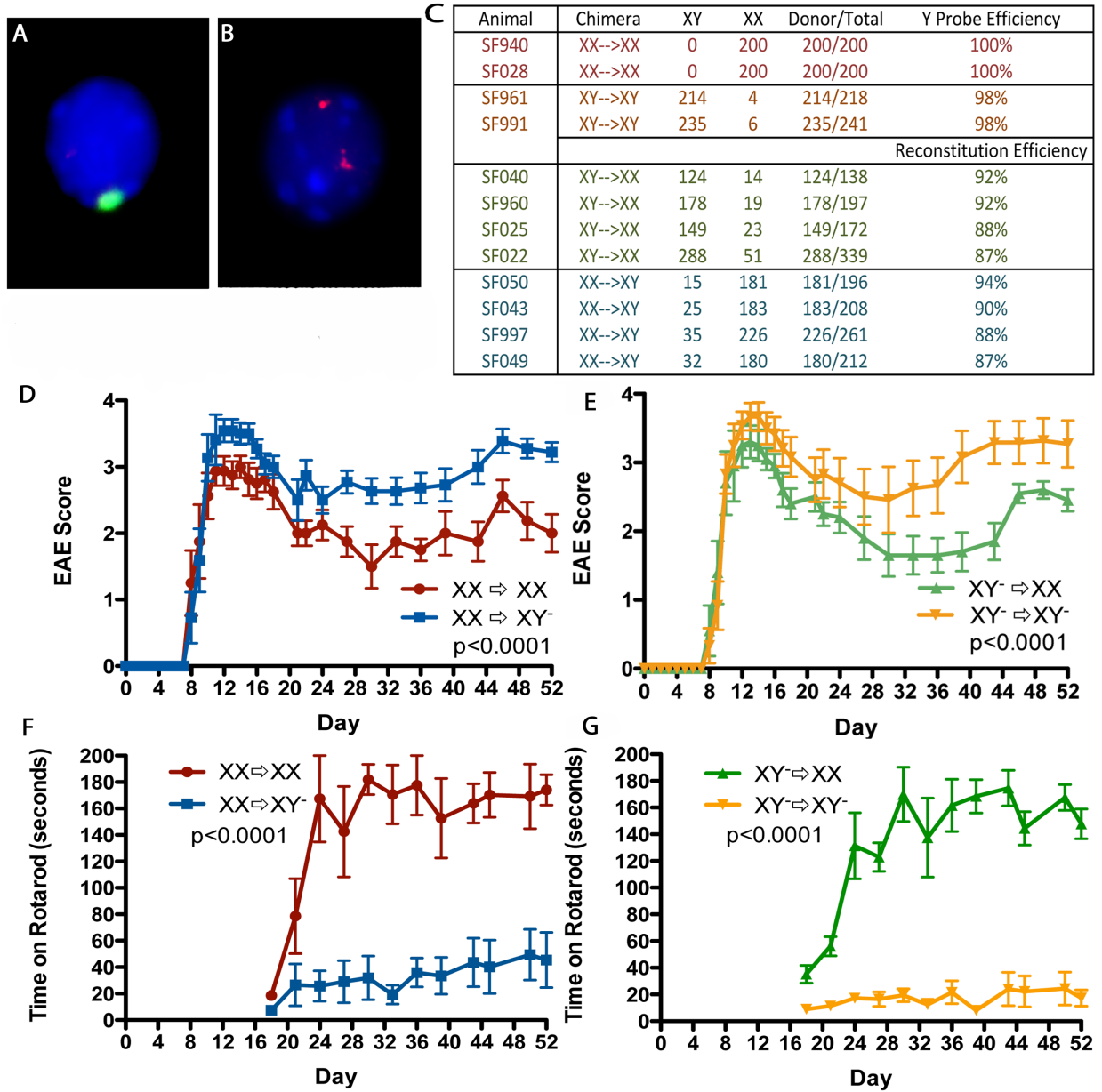


Figure 2. SJL mice with XY CNS, compared with XX CNS, have greater clinical EAE disease severity. (A-C) Representative 100x captures of splenocytes from XY \rightarrow XY \rightarrow XY \rightarrow XY (A; Notations detail bone marrow donor before arrow and irradiated recipient after arrow) and XX \rightarrow XX (B) mice stained for X (red) and Y (green) probes, and DAPI (blue) nuclear stain. A single red and green label identified XY, whereas two red labels and no green labels identified XX. Nearly all DAPI $^{+}$ XY \rightarrow XY \rightarrow XY \rightarrow XY cells had one red and one green label, whereas most DAPI $^{+}$ XX \rightarrow XX cells had two red and no green labels. (C) Chart summarizing the probe staining efficiency in representative XX \rightarrow XX (red) and XY \rightarrow XY \rightarrow XY \rightarrow XY (orange) BMCs, and the reconstitution efficiency of XY \rightarrow XX (green) and XX \rightarrow XY \rightarrow XY \rightarrow XY (blue) BMCs. The reconstitution efficiency

was calculated by taking the proportion of donor cells in a sample (donor/total x 100) normalized by the staining efficiency of the Y probe in a known control (98% in $XY^- \rightarrow XY^-$). For example, using sample SF040, Reconstitution Efficiency = $(124/138) \times 100 / 98 = 92\%$. By this method, the reconstitution efficiency ranged from 87-94%. (D-G) BMCs, XY genotype in the host CNS, compared to XX, had greater disease severity at late timepoints (i.e., had higher EAE scores) ($p < 0.0001$, $XX \rightarrow XX$ (n=9) vs. $XX \rightarrow XY^-$ (n=12), and $p < 0.0001$, $XY^- \rightarrow XX$ (n=12) vs. $XY^- \rightarrow XY^-$ (n=13), repeated measures one-way ANOVA with Bonferroni post-hoc test), and had worse rotarod performance (i.e., spent less time on the rotarod = lower scores) ($p < 0.0001$, $XX \rightarrow XX$ vs. $XX \rightarrow XY^-$, and $p < 0.0001$, $XY^- \rightarrow XX$ vs. $XY^- \rightarrow XY^-$, repeated measures one-way ANOVA with Bonferroni post-hoc test). Data are displayed as mean clinical scores \pm SEM. Data are representative of three repeated experiments.

To determine whether or not the results were limited to one strain of mouse, we next used C57BL/6 mice of the four core genotypes. We compared MOG 35-55 peptide induced active EAE in C57BL/6 BMCs that had been reconstituted with the same immune system and had a common hormonal background (all females), but differed in their sex chromosome complement in the CNS as above. We observed similar results in the C57BL/6 background as in the SJL background, whereby mice with XY^- CNS, as compared with XX, had worse EAE scores (Fig 3A and 3B, $p < 0.05$, $XX \rightarrow XX$ vs. $XX \rightarrow XY^-$ and $p < 0.001$, $XY^- \rightarrow XX$ vs. $XY^- \rightarrow XY^-$, repeated measures one-way ANOVA with Bonferroni post-hoc test) and rotarod performance (Fig 3C and 3D, $p < 0.001$, $XX \rightarrow XX$ vs. $XX \rightarrow XY^-$, and $p < 0.0001$, $XY^- \rightarrow XX$ vs. $XY^- \rightarrow XY^-$, repeated measures one-way ANOVA with Bonferroni post-hoc test). Together, data in two different mouse strains demonstrates that chimeras with XY^- CNS, when compared with XX, have more clinical disability late in EAE.

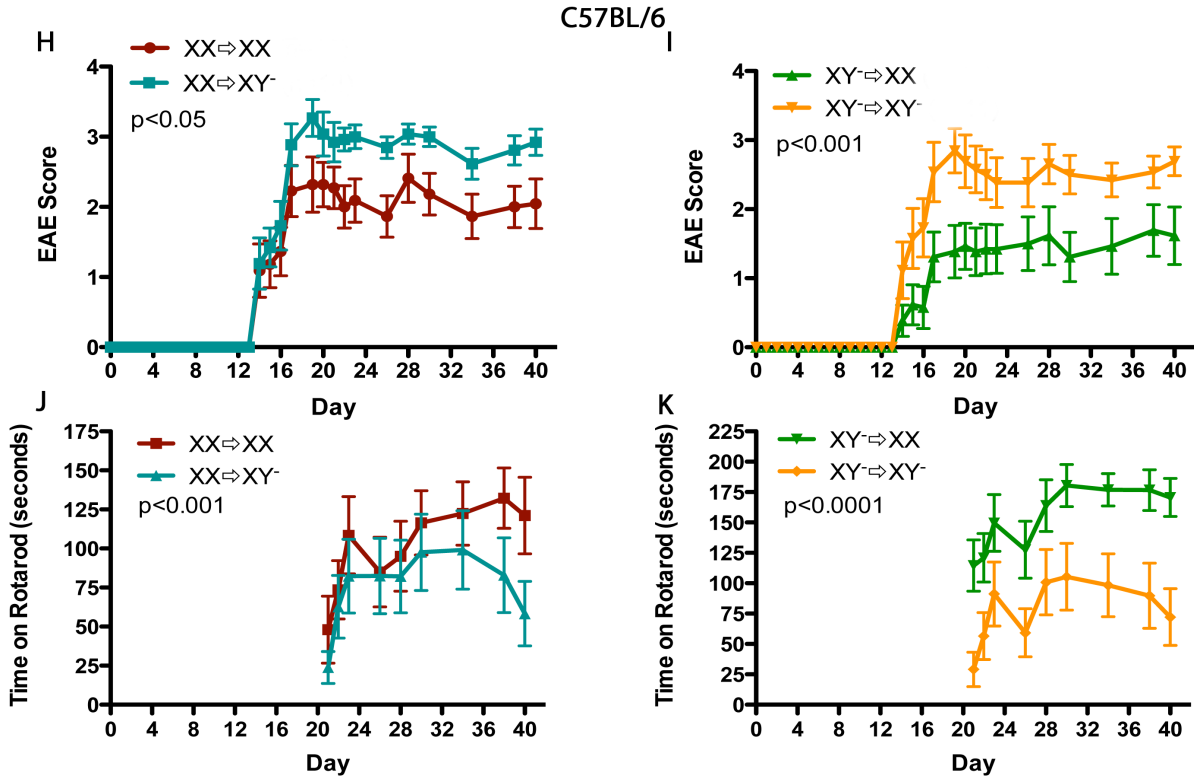


Figure 3. C57BL/6 mice with XY CNS, compared with XX CNS, have greater clinical EAE disease severity. (A-D) In the C57BL/6 strain, XY genotype in the host CNS, compared to XX, had greater disease severity at late timepoints (i.e., had higher EAE scores) ($p < 0.05$, $XX \rightarrow XX$ ($n=12$) vs. $XX \rightarrow XY^-$ ($n=14$), and $p < 0.001$, $XY^- \rightarrow XX$ ($n=13$) vs. $XY^- \rightarrow XY^-$ ($n=11$), repeated measures one-way ANOVA with Bonferroni post-hoc test), and had worse rotarod performance (i.e., spent less time on the rotarod = lower scores) ($p < 0.001$, $XX \rightarrow XX$ vs. $XX \rightarrow XY^-$, and $p < 0.0001$, $XY^- \rightarrow XX$ vs. $XY^- \rightarrow XY^-$, repeated measures one-way ANOVA with Bonferroni post-hoc test). Data are displayed as mean clinical scores \pm SEM. Data are representative of three repeated experiments.

2.4 Spinal cord and cerebellar pathology in SJL mice with XY vs. XX CNS

At the endpoint of disease, we examined the chimeric SJL EAE mice for neuropathology related to ambulation and coordination, in spinal cord and cerebellum, respectively. Consistent with clinical disability results, mice with XY^- CNS, compared with XX, had more demyelination

(Fig 4A vs. 4B, $p < 0.001$, $XX \rightarrow XX$ vs. $XX \rightarrow XY^-$, and 4C vs. 4D, $p < 0.05$, $XY^- \rightarrow XX$ vs. $XY^- \rightarrow XY^-$, two-way ANOVA) and greater axonal loss (Fig 4E vs. 4F, $p < 0.01$, $XX \rightarrow XX$ vs. $XX \rightarrow XY^-$, and 4G vs. 4H, $p < 0.001$, $XY^- \rightarrow XX$ vs. $XY^- \rightarrow XY^-$, two-way ANOVA) in the spinal cords when assessed by anti-myelin-basic protein (MBP) antibody staining and anti-neurofilament-200 (NF200), respectively. Cerebellar pathology was examined by quantifying the degree of white matter demyelination with anti-MBP antibody, and the number of healthy Purkinje cell bodies stained with anti-Calbindin D28-K. Mice with XY^- CNS, when compared with XX , had more demyelination in the white matter of the cerebellum (Fig 4I vs. 4J, $p < 0.05$, $XY^- \rightarrow XX$ vs. $XY^- \rightarrow XY^-$, and 4K vs. 4L, $p < 0.05$, $XX \rightarrow XX$ vs. $XX \rightarrow XY^-$, two-way ANOVA) and lower numbers of healthy Purkinje cells characterized by full-bodied, balloon-like cell bodies with clearly visible dendritic arborization (Fig 4M vs. 4N, $p < 0.01$, $XY^- \rightarrow XX$ vs. $XY^- \rightarrow XY^-$, and 4O vs. 4P, $p < 0.01$, $XX \rightarrow XX$ vs. $XX \rightarrow XY^-$, two-way ANOVA).

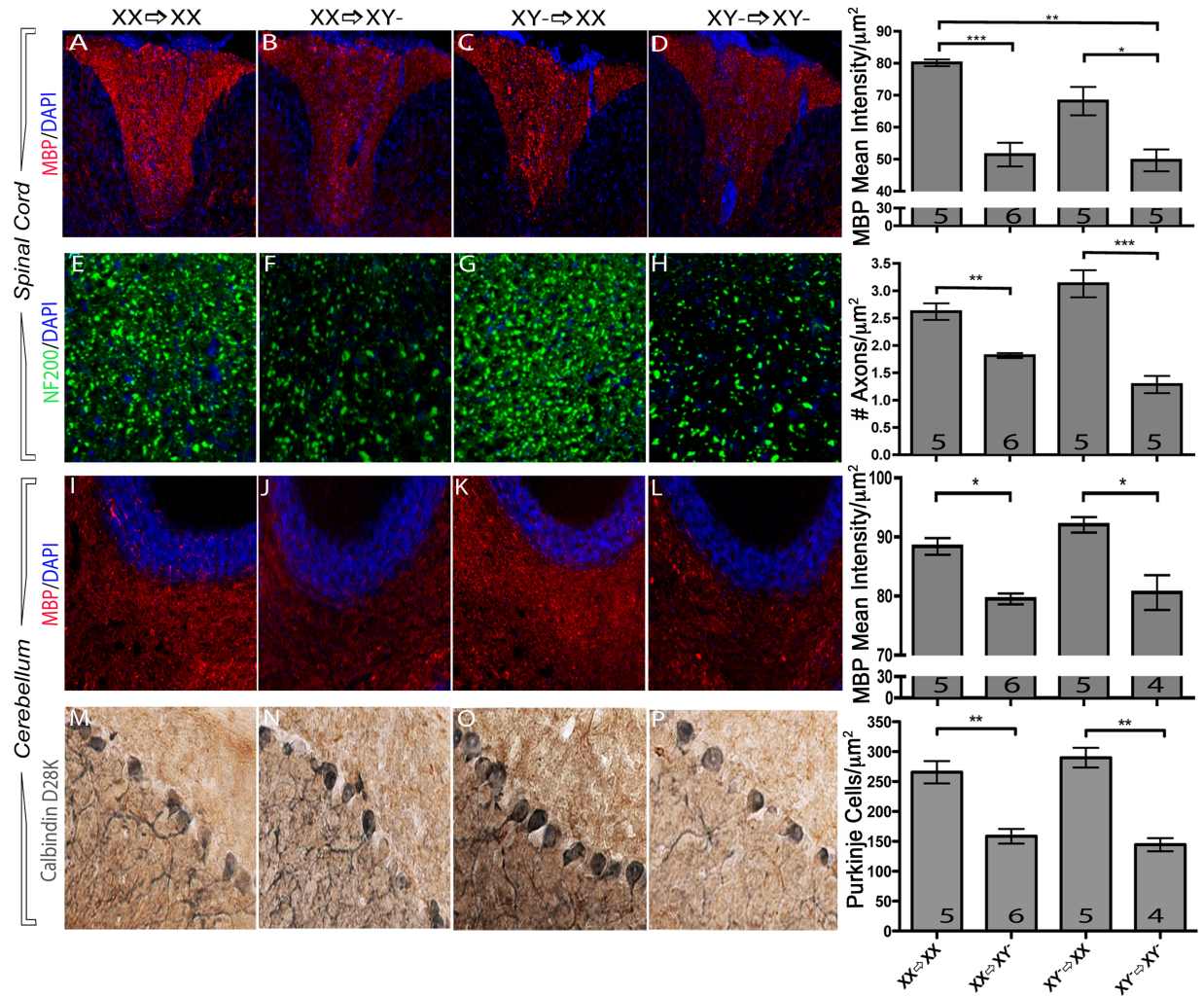


Figure 4. Mice with XY CNS, compared with XX CNS, have greater spinal cord and cerebellar pathology. (A-D) Representative 10x captures of myelin stained with MBP (red) in the dorsal column of the thoracic spinal cord. SJL mice with XY CNS have less myelin staining intensity compared to mice with XX CNS in the setting of the same immune system ($p < 0.001$, XX \rightarrow XX vs. XX \rightarrow XY $^-$, and $p < 0.05$, XY $^-$ \rightarrow XX vs. XY $^-$ \rightarrow XY $^-$, two-way ANOVA, top right). Tissues were counterstained with DAPI (blue). (E-H) Representative 40x captures of axons stained with NF200 (green) and DAPI at the lateral funiculus of the thoracic spinal cord at day 52 of active EAE. Mice with XY CNS have fewer number of axons compared to mice with XX CNS ($p < 0.01$, XX \rightarrow XX vs. XX \rightarrow XY $^-$, and $p < 0.001$, XY $^-$ \rightarrow XX vs. XY $^-$ \rightarrow XY $^-$, two-way ANOVA, second row right). (I-L) Representative 10x captures of mid-sagittal cerebellar white matter stained with MBP (red) and granule cell layer stained with DAPI (blue). Mice with XY CNS have less MBP staining intensity in the cerebellar white matter compared to mice with XX CNS ($p < 0.05$, XY $^-$ \rightarrow XX vs. XY $^-$ \rightarrow XY $^-$, and XX \rightarrow XX vs. XX \rightarrow XY $^-$,

two-way ANOVA, third row right). (M-P) Representative 20x captures of Purkinje cells stained with Calbindin-D28K (black) in the mid-sagittal plane of the cerebellum. Mice with XY CNS have less organized and fewer number of Purkinje cells compared to mice with XX CNS in the setting of the same immune system ($p < 0.01$ for $XY^- \rightarrow XX$ vs. $XY^- \rightarrow XY^-$, and $XX \rightarrow XX$ vs. $XX \rightarrow XY^-$, two-way ANOVA, bottom right). Graphs are displayed as mean \pm SEM. * $p < 0.05$, ** $p < 0.01$, *** $p < 0.001$. Data are representative of two repeated experiments.

2.5 Cerebral cortical pathology in SJL mice with XY vs. XX CNS

We next examined the integrity of the cerebral cortex, focusing on the primary somatosensory strip representing the hindlimbs (S1HL; Franklin & Paxinos, Bregma -1.23 to -1.31 mm, Plates 41-42) and adjacent primary motor cortex (M1) because these regions process afferent sensory information from spinal cord and convey efferent motor behavior that are continuously modified by cerebellar input. Since cortical synaptic loss is one of the earliest signs of neurodegeneration in several neurological diseases including EAE (MacKenzie-Graham et al., 2012; Rasmussen et al., 2007; Ziehn, Avedisian, Dervin, O'Dell, & Voskuhl, 2012; Ziehn, Avedisian, Dervin, Umeda, et al., 2012), we assessed pre- and post-synaptic loss with antibodies to Synapsin1 and post-synaptic density protein 95 (PSD-95), respectively. Mice with XY CNS, compared to XX, had less PSD-95 expression in the S1HL and M1 region (Fig 5A vs. 5B, $p = 0.05$, $XX \rightarrow XX$ vs. $XX \rightarrow XY^-$, 5C vs. 5D, $p < 0.001$, $XY^- \rightarrow XX$ vs. $XY^- \rightarrow XY^-$, two-way ANOVA, and Fig 5E). Mice with XY CNS, compared to XX, also demonstrated a trend of lower Synapsin 1 expression, but this did not reach statistical significance (Fig 5F).

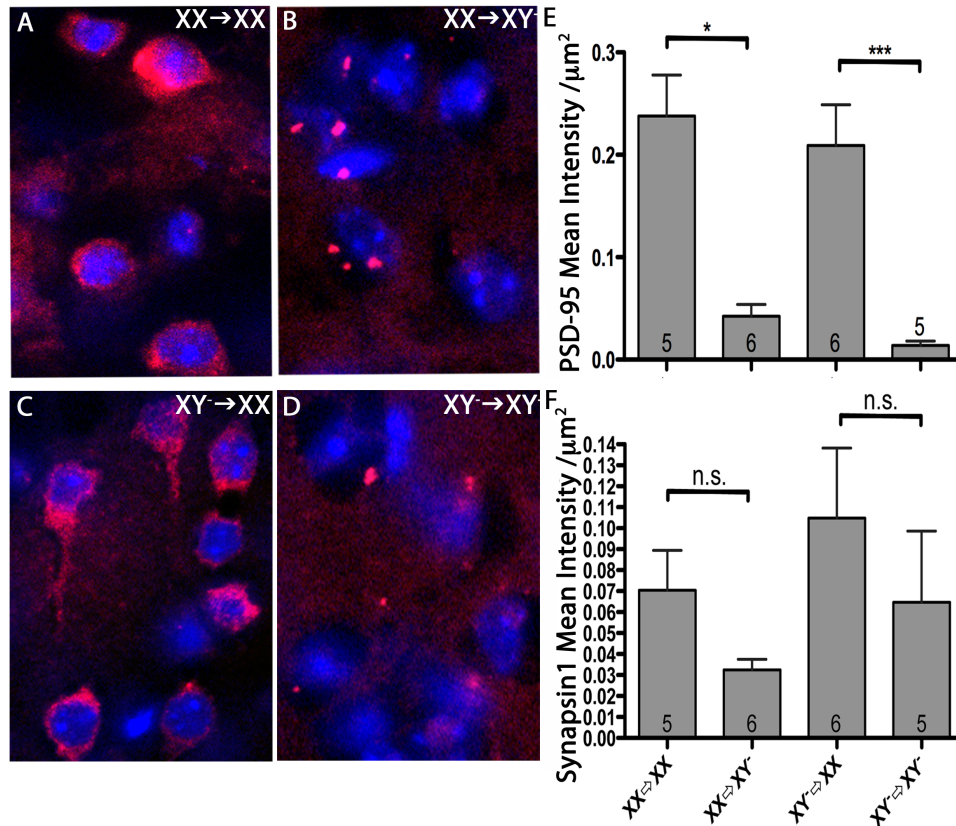


Figure 5. Mice with XY CNS, compared with XX CNS, have greater synaptic loss in the cerebral cortex. (A-D) Representative 60x captures of PSD-95 protein staining (red) in cortical neurons of the S1HL region of the cerebral cortex. Tissues were counterstained with DAPI (blue). (E) Mice with XY CNS have less PSD-95 staining intensity compared to mice with XX CNS ($p=0.05$, XX \rightarrow XX vs. XX \rightarrow XY, and $p<0.001$, XY \rightarrow XX vs. XY \rightarrow XY, two-way ANOVA). (F) Trend of less Synapsin 1 staining in mice with XY CNS compared to mice with XX CNS.

2.6 Tlr7 expression in the cerebral cortex of SJL mice with XY vs. XX CNS

Since the molecular pattern recognition receptor toll-like receptor 7 (Tlr7) is X-linked and its signaling in neurons has been shown to cause neurodegeneration (Sabrina M. Lehmann et al., 2012), we examined the levels of Tlr7 expression in the cerebral cortex. Tlr7 was abundantly expressed in the cerebral cortex of EAE mice (Fig 6A-E, $p<0.05$, XX \rightarrow XX vs. XX \rightarrow XY, and

$p < 0.01$, $XY^- \rightarrow XX$ vs. $XY^- \rightarrow XY^-$, two-way ANOVA), particularly in cortical neurons in layers I-VI (Fig 6F-H). Notably, mice with XY CNS, compared with XX, had higher percentages of Tlr7 expressing cortical neurons, as evidenced by Tlr7 and NeuN colocalization (Fig 6F-I, $p < 0.05$, $XX \rightarrow XX$ vs. $XX \rightarrow XY^-$, and $p < 0.001$, $XY^- \rightarrow XX$ vs. $XY^- \rightarrow XY^-$, two-way ANOVA). Because Tlr7 has a widely known role in innate immune responses in antigen presenting cells of the immune system, and Tlr7 signaling in microglia can lead to neurodegeneration, we also examined Tlr7 in microglia. Interestingly, Tlr7 was minimally expressed in microglia in the cerebral cortical layers I-VI (Fig 6J-L), and there were no sex chromosome effects on Tlr7 expression in microglia (Fig 6M). Together our data suggest that increased Tlr7 expression in neurons of XY^- mice leads to more neuronal degeneration as compared to XX during EAE. This conclusion would be consistent with observations by others that neuronal Tlr7 expression can cause neurodegeneration (S. M. Lehmann et al., 2012). However, further experiments using neuronal Tlr7 conditional knock outs backcrossed onto the four core genotype sex chromosome model would be required to show a causal relationship between increased Tlr7 in neurons and increased neurodegeneration in the XY^- CNS.

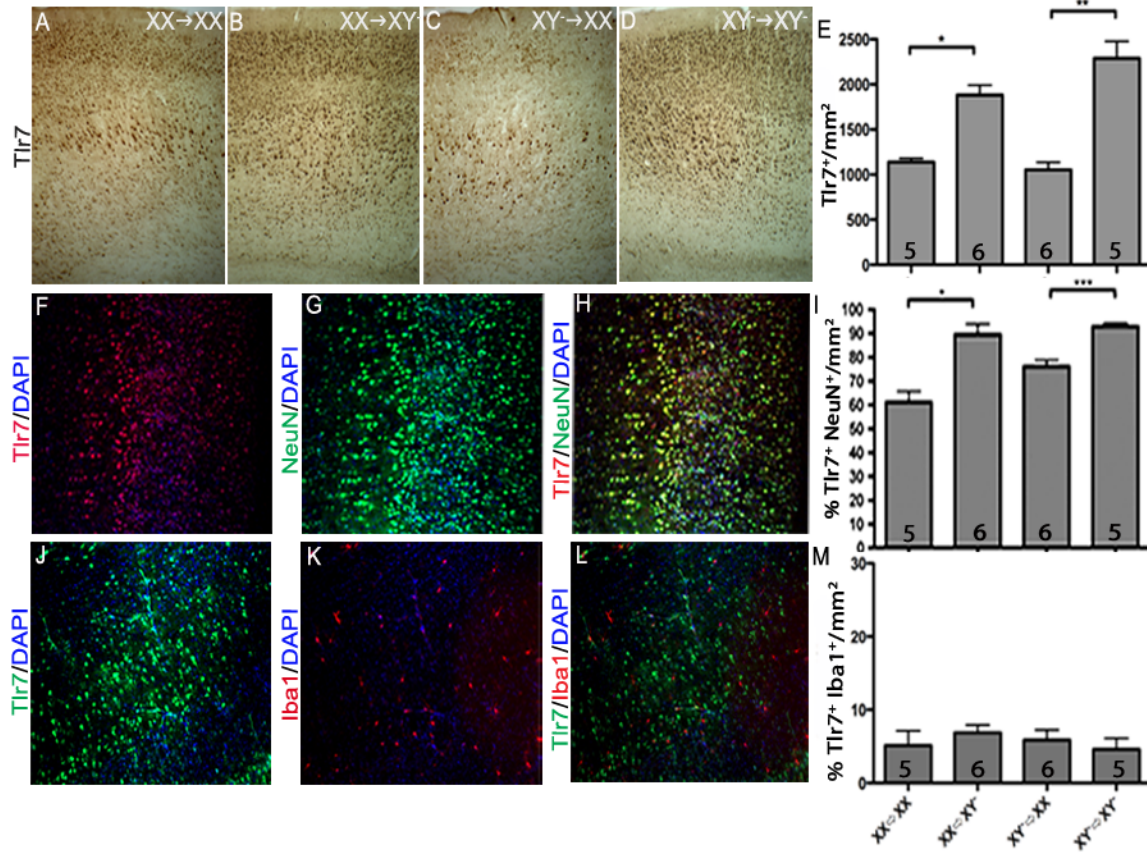


Figure 6. Mice with XY CNS, compared with XX CNS, have more Tlr7 expressing cortical neurons in EAE. (A-D) Representative 10x capture of coronal sections of cerebral cortical layers I-VI stained with Tlr7 in XX→XX, XX→XY, XY→XX, and XY→XY bone marrow chimeras. (E) SJL mice with XY CNS, compared to XX, have more Tlr7⁺ expressing cells in the cerebral cortex ($p < 0.05$, XX→XX vs. XX→XY, and $p < 0.01$, XY→XX vs. XY→XY, two-way ANOVA). (F-H) Representative 10x confocal capture of a coronal section of cerebral cortical layers I-VI stained with Tlr7 (red) and NeuN (green), where (F) represents red channel only, (G) represents the green channel only, and (H) represents a merged image. Tissues were counterstained with DAPI (blue). (I) SJL mice with XY CNS, compared to XX, have a higher percentage of Tlr7⁺ expressing cortical neurons ($p < 0.05$, XX→XX vs. XX→XY, and $p < 0.001$, XY→XX vs. XY→XY, two-way ANOVA). (J-K) Representative 10x confocal capture of a coronal section of cerebral cortical layers I-VI stained with Tlr7 (green) and Iba1 (red), where (J) represents green channel only, (K) represents the red channel only, and (L) represents a merged image. Tissues were counterstained with DAPI (blue). (M) There were few Tlr7⁺ microglia in cortical layers I-VI, and no differences in the number of Tlr7⁺ microglia were observed between all groups.

2.7 Sex chromosome effects in the immune system in the bone marrow chimera model

To rule out an effect of sex chromosomes in the immune system in our comparisons, spinal cords were assessed for the quantity of infiltrating T-cells and macrophages based on anti-CD3 and anti-CD68 antibody staining, respectively. There were no effects of sex chromosomes in the CNS on CD3⁺ T-cell (Figs 7A and 7B) or CD68⁺ macrophage infiltration (Figs 7C and 7D).

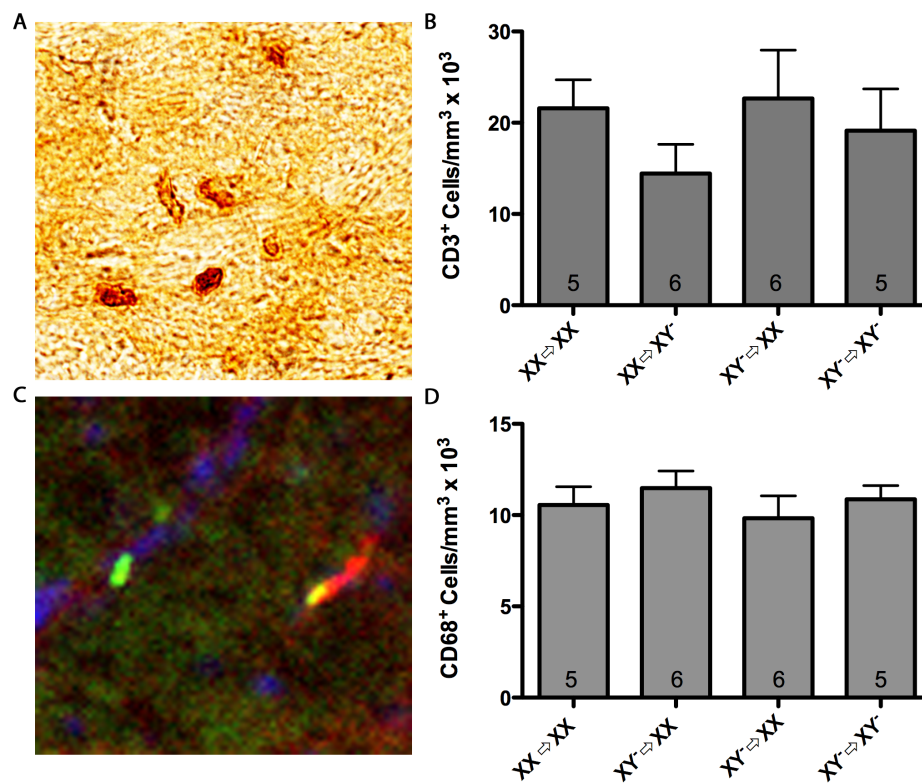


Figure 7. No differences in spinal cord inflammation in BMCs with varying sex chromosome complement in the CNS and a common immune system. (A) Representative 40x capture of infiltrating CD3⁺ T-cells in the cross-section of the thoracic spinal cord of SJL EAE mice. (B) No differences were observed in quantities of CD3⁺ T-cells between any groups. (C) Representative 40x capture of CD68⁺ macrophages (green, arrows) in the cross-section of the thoracic spinal cord. DAPI, blue; CD45, red. (D) No differences were observed in quantities of CD68⁺ macrophages between any groups. Data are representative of two repeated experiments.

Then, we examined cytokine production in *ex vivo* auto-antigen stimulated splenocytes. There were no differences between any groups in IFN γ , TNF α , IL-6, IL-2, IL-12p40, IL-17, IL-27, IL-4, IL-5, IL-10, and IL-13 cytokine levels, as well as MMP-9 (Fig 8).

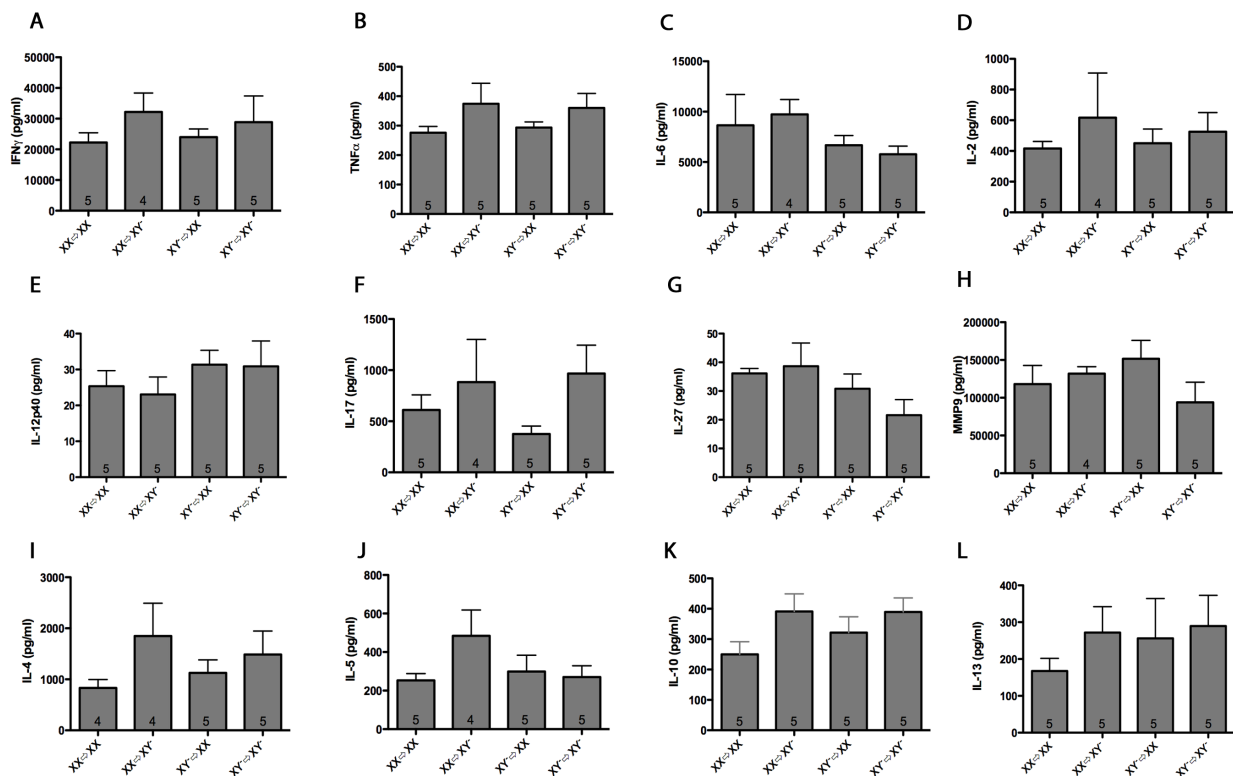


Figure 8. No differences in peripheral immune cytokine responses in BMCs with varying sex chromosome complement in the CNS and a common immune system. (A-L) Cytokine levels (IFN γ , TNF α , IL-6, IL-2, IL-12p40, IL-17, IL-27, IL-4, IL-5, IL-10, and IL-13) as well as MMP-9 in supernatants of XX→XX, XX→XY, XY→XX, and XY→XY SJL bone marrow chimera splenocytes after 72 h of autoantigen stimulation.

Our experimental design also allowed us to examine the role of sex chromosomes in the immune system without confounding variation in sex chromosomes in the CNS. We compared clinical EAE data between BMC reconstituted with XX versus XY immune systems in the setting of the same CNS ($XX \rightarrow XX$ vs. $XY^- \rightarrow XX$, and $XX \rightarrow XY^-$ vs. $XY^- \rightarrow XY^-$). Interestingly, these comparisons revealed no difference in clinical EAE when assessing for effects of sex chromosome complement in the immune system in these chimeras (Figs 9A and 9B).

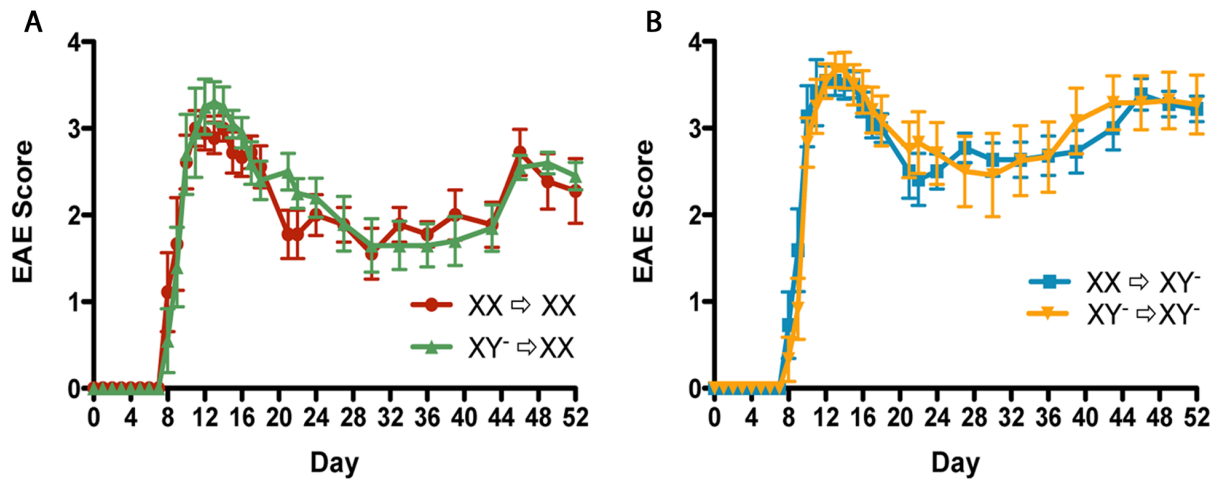


Figure 9. No differences in clinical EAE disease severity in mice with varying sex chromosome complement in the immune system and a common CNS. (A-B) Comparisons were made between SJL $XX \rightarrow XX$ vs. $XY^- \rightarrow XX$, and $XX \rightarrow XY^-$ and $XY^- \rightarrow XY^-$ BMCs from the same experiment as in Figure 1. Data are representative of three repeated experiments.

2.8 TLR7 in the autoimmune response of XX vs. XY⁻ mice

We next asked whether differential expression of the same sex chromosome gene that is related to worse neurodegeneration in XY⁻ mice might also be responsible for the increase in adaptive immune responses in XX mice that were previously observed in our publication (Smith-Bouvier et al., 2008). Specifically, we wondered whether the former is an effect of higher TLR7 expression in neurons of XY⁻ mice, and the latter an effect of higher TLR7 expression in immune cells of XX mice. Notably, the place to look for differential expression of TLR7 playing a role in sex chromosome effects in the immune system would be where we had previously found an effect of sex chromosomes in the immune system, namely in LNCs from autoantigen immunized adult mice (Smith-Bouvier et al., 2008). We would not want to assess TLR7 in the immune system of bone marrow cells developed in irradiated hosts, since there was no effect of sex chromosomes in those immune cells. Thus, we repeated the adoptive EAE results from our previous paper (Smith-Bouvier et al., 2008), whereby adoptively transferred autoantigen stimulated XX LNCs conferred greater encephalitogenicity as compared to XY⁻ LNCs (Fig 10A). In parallel, separate aliquots of these same LNCs were examined for TLR7 expression including subpopulations of T lymphocytes, B lymphocytes, and macrophages. We found that TLR7 expression levels were no different between LNCs derived from XX versus XY⁻ in any immune cell subset (Fig 10B). Given the numerous genes expressed on sex chromosomes, particularly the X chromosome, it is not surprising that a single gene (e.g. *Tlr7*) would not be responsible for both the effect of sex chromosomes on the CNS and the effect of sex chromosomes on adaptive immune responses.

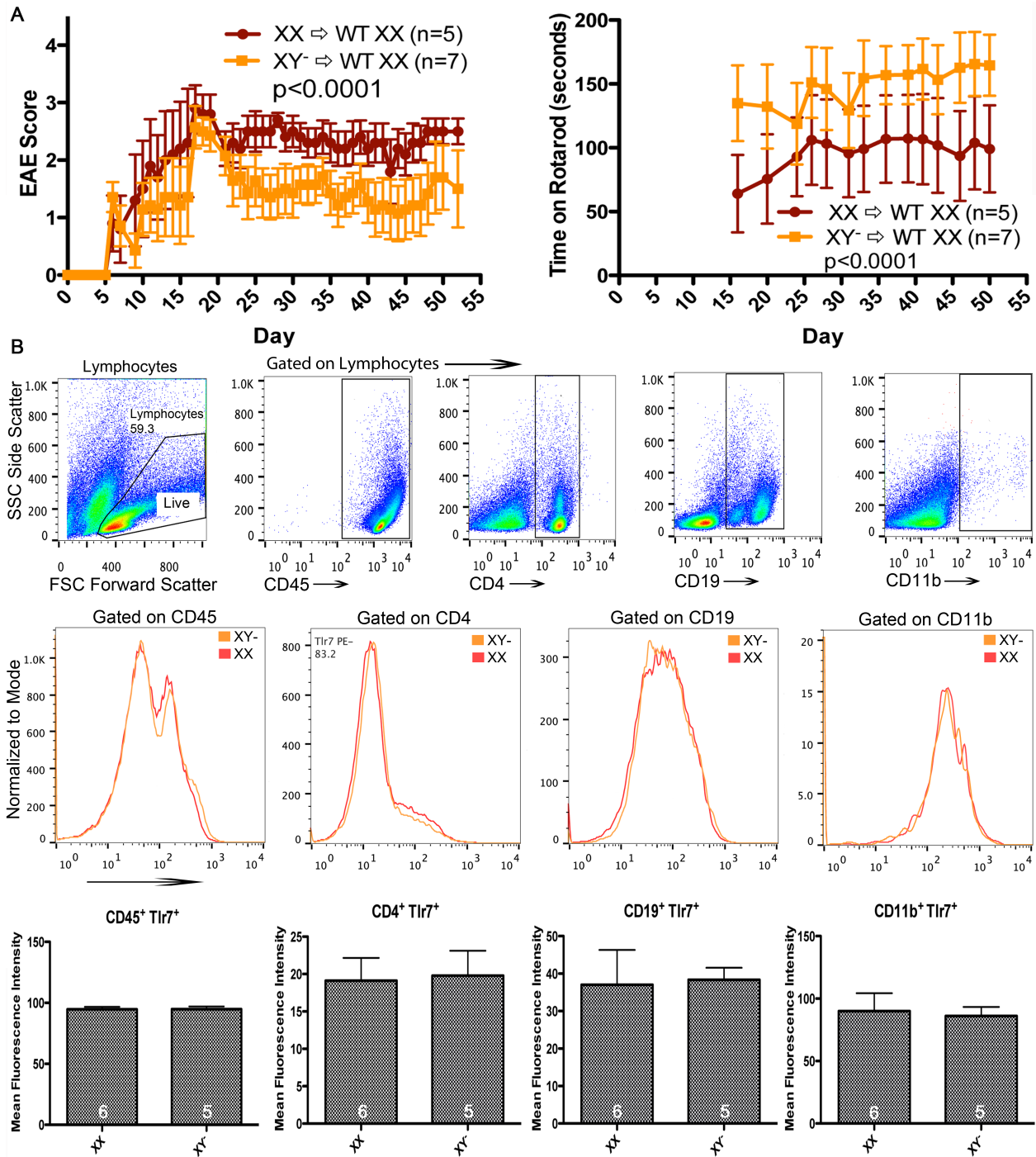


Figure 10. No differences in Tlr7 expression on immune cells during the induction phase of EAE in non-chimeric SJL mice. A) Adoptive transfer of lymph node immune cells harvested on day 12 of PLP 139-151 immunization and restimulated *ex vivo* for 72 hours. Left. Standard EAE scores were worse in mice that received XX lymph node cells (red), compared to mice that received XY lymph node cells (orange). Right. Mice that received XX lymph node cells (red)

performed worse on the rotarod, compared to mice that received XY cells (orange). B) Tlr7 expression on lymph node immune cells harvested on day 12 of PLP 139-151 immunization and restimulated *ex vivo* for 72 hours. No differences were observed in Tlr7 expression in CD45⁺ pan-immune cells, CD4⁺ T cells, CD19⁺ B cells, and CD11b⁺ macrophages.

2.9 Discussion

This is the first report demonstrating an effect of sex chromosome complement in the CNS response to injury. Specifically, having an XY CNS, as opposed to XX, results in more axonal and neuronal loss and greater demyelination in the spinal cord and cerebellum during an immune mediated injury. An XY CNS compared to XX also resulted in greater synaptic loss in the cerebral cortex during EAE, particularly in the somatosensory and primary motor strip. Synaptic loss is one of the earliest signs of neurodegeneration in several neurological disorders, particularly Alzheimer's and Huntington's disease and in EAE (MacKenzie-Graham et al., 2012; Masliah et al., 2001; Rasmussen et al., 2007; Usdin, Shelbourne, Myers, & Madison, 1999; Ziehn, Avedisian, Dervin, O'Dell, et al., 2012; Ziehn, Avedisian, Dervin, Umeda, et al., 2012).

Much of the literature on the origins of sex-biased neurological diseases has focused on the role of sex steroid hormones, particularly the role of estrogens and testosterone in neuroprotection (Bourque, Dluzen, & Di Paolo, 2009; Pike, Carroll, Rosario, & Barron, 2009; Spence & Voskuhl, 2012; Wise, 2002; Ziehn, Avedisian, Dervin, O'Dell, et al., 2012; Ziehn, Avedisian, Dervin, Umeda, et al., 2012). The increased female bias for MS could theoretically result from deleterious effects of physiologic levels of female sex hormones or protective effects of male sex hormones. In the MS model, no studies have shown deleterious effects endogenous estrogens as would be evidenced by improved EAE in ovariectomized versus sham-operated mice. Rather, one group showed that endogenous levels of estradiol protect from EAE since

ovariectomized were worse than sham-operated groups (Matejuk et al., 2001), while other groups found no effect of ovariectomy (Jansson et al., 1994; R. R. Voskuhl & Palaszynski, 2001). Very high, pregnancy levels of estrogens are clearly protective in EAE (Jansson et al., 1994; Kim, Dalal, & Voskuhl, 1998), but there is a dose effect whereby lower doses, similar to those present during the menstrual cycle, may not be high enough to provide significant protection (Jansson et al., 1994), reviewed in (Rhonda R. Voskuhl & Gold, 2012). In contrast, endogenous circulating levels of testosterone in males have clearly been shown to be protective in EAE, with numerous groups having shown that castrated young males show worse EAE scores in mouse strains characterized by a female bias (Palaszynski, Loo, et al., 2004), reviewed in (Rhonda R. Voskuhl & Gold, 2012). Together, there is no evidence that endogenous circulating levels of estrogens are deleterious in females, but there is evidence that endogenous levels of testosterone may be protective in males. Thus, testosterone mediated protection could contribute to sex differences in EAE. However, this protective effect of endogenous testosterone in males does not exclude an additional role of sex chromosomes.

Our finding of sex chromosome complement effects in the CNS during EAE has implications for the role of sex chromosomes in MS as well as other neurological disorders with a sex bias, such as Alzheimer's disease, Parkinson's disease, schizophrenia, and stroke. Our results suggest that other sex-related factors can play a role and have been underappreciated. Indeed, a large proportion of sex chromosome genes, particularly those on the X chromosome, are involved in brain development and function (Nguyen & Distèche, 2006). Our current studies suggest that there are sex chromosome genes expressed in the CNS in mouse and humans that may affect the progression of sex-biased neurological diseases.

Ultimately, in intact mice and humans, sex differences will be due to the contribution of both sex hormones and sex chromosomes. Here, it is fascinating that the XY sex chromosome complement is associated with more neurodegeneration in EAE, since testosterone treatment is known to be neuroprotective in both EAE and cuprizone induced chronic demyelination (Hussain et al., 2013; Ziehn, Avedisian, Dervin, Umeda, et al., 2012). A yin-yang, or compensatory, effect between sex hormones and sex chromosomes has been previously postulated and found in other systems (De Vries, 2004; Palaszynski et al., 2005). Together, it is tempting to speculate that the XY sex chromosome complement may drive greater neurodegeneration in CNS diseases, but this is held in check in young males with high levels of testosterone. This protection is eventually lost however as testosterone levels begin to wane gradually during andropause, which initially starts at approximately age 30 in humans.

Our comparison of XX vs. XY reveals differences in the non-pseudoautosomal regions (non-PAR) of X vs. Y, as opposed to genes on the terminal recombining PAR that are shared between X and Y. Since this is a relative comparison, a gene on non-PAR Y could lead to more neurodegeneration or a gene on non-PAR X could lead to CNS resilience. The first possibility is somewhat unlikely since there are very few genes on non-PAR Y that relate to processes other than reproduction and most sex chromosome effects published to date are X chromosome effects (AP, X, JC, Y, & K., 2013; Burgoyne, 1998).

Regarding an effect of a gene on non-PAR X promoting resilience, this could occur in two ways. First, a gene on the X chromosome that escapes X inactivation would be expressed at increased dosage (twice in females vs. once in males) and this X gene could promote neuroprotection. If differential Tlr7 expression indeed causes neurodegeneration, our data showing higher Tlr7 expression in XY CNS compared to XX is not consistent with X dosage.

Had *Tlr7* escaped X-inactivation in XX mice, we would have observed the opposite results, with XX mice having higher levels of Tlr7 expression compared to XY⁻. Second, a gene on the X chromosome that is X-inactivated, but has differential imprinting (paternal vs. maternal) would be differentially expressed in X^mX^p vs. X^mY mice (Arnold, 2009; William Davies, Isles, Humby, & Wilkinson, 2007). Specifically, all cells from XY⁻ mice express the maternal imprint, while half of cells in XX mice express the maternal imprint and half the paternal imprint. Such unique mosaicism in X gene expression occurs in XX individuals due to the random inactivation of either the maternal or paternal X on a cell-to-cell basis. In our model, mice with one copy of the X chromosome (XY) have greater expression of the X gene *Tlr7* in neurons than mice with two copies of the X chromosome (XX). This indicates that differential *Tlr7* expression is not due to X dosage, but more likely due to parental imprinting. Specifically, the paternally imprinted X chromosome has reduced *Tlr7* expression, resulting in less Tlr7 in X^mX^p as compared to X^mY mice. Consistent with this hypothesis, another gene on X, *Xlr3b*, has been shown to be affected by imprinting, is expressed in frontal cortex and hippocampus, and plays a role in cognitive function in mice (W. Davies et al., 2005). Specifically, the paternal imprint has reduced *Xlr3b* expression, with higher levels of expression driven by the maternal imprint inducing neurodegeneration.

Our data demonstrating no sex chromosome effects in the immune system of BMCs in the setting of the same CNS further extend our previously published findings of an effect of XX, as compared to XY, autoantigen stimulated LNCs being more encephalitogenic in the induction phase of adoptive EAE. In the present data, sex chromosome effects were not observed in hematopoietic stem cells derived from bone marrows of five-week old XX versus XY⁻ mice used to reconstitute age-matched host immune systems seven weeks prior to active EAE induction. In

contrast, previously, sex chromosome effects were observed in XX versus XY lymphocytes derived from lymph nodes of 8-week old PLP-immunized mice that were then stimulated *ex vivo* with autoantigen and adoptively transferred to naïve recipients (Smith-Bouvier et al., 2008). Together, these two complementary findings show that the earlier observation of a sex chromosome effect on the immune system, specifically on the adaptive immune response, is not inherently present in bone marrow cells of juvenile mice, but rather becomes evident either after these bone marrow cells undergo maturation or upon immunization to induce the adaptive immune response. Further studies defining when and how sex chromosomes affect the immune system are now warranted.

In summary, sex chromosomes may independently affect the CNS response to a given immune mediated injury, potentially bearing some relevance on the fact that despite increased MS susceptibility in females, males tend to have more disability progression (Antulov et al., 2009; Confavreux et al., 2003; Pozzilli et al., 2003; Savettieri et al., 2004; Rhonda R. Voskuhl & Gold, 2012; Weinshenker, 1994; Weinshenker et al., 1991). Further, our data indicate that it is important to consider a potential role for sex chromosome genes in future studies of sex differences in neurological diseases. Finally, the model described herein will be an important tool in examining sex differences in a variety of CNS diseases since most CNS diseases have an immune component.

Chapter 3: Parent-of-Origin Sex Chromosome Effects in the CNS

During EAE

3.1 Introduction

In the previous chapter, we demonstrated that mice with CNS cells expressing the XY sex chromosome complement, as compared to XX, led to greater clinical EAE disease severity and neuropathology (Du et al., 2014). It remained unknown whether increased neurodegeneration in mice with XY⁻ CNS was due to X dosage, the presence or absence of Y, or maternal versus paternal X imprinting.

With respect to X dosage, an imbalance in X gene expression between XX and XY individuals can occur when an X gene is expressed in double doses in XX individuals when it escapes X-inactivation, an evolutionary mechanism to equalize the dosage of X genes between XX and XY individuals. In the mouse, approximately 3% of X genes escape X-inactivation, as compared to 15% in humans (Berletch, Yang, Xu, Carrel, & Disteche, 2011). It is well documented that X genes including *Ddx3x*, *Eif2s3x*, and *Kdm5c* escape X inactivation and thus are candidates for contributing to reduced neurodegeneration in XX mice during EAE (Agulnik et al., 1994; Ehrmann et al., 1998; Greenfield et al., 1998).

Another possibility is that Y genes could have an indirect transregulatory effect on X gene expression. The Y chromosome has been demonstrated to contain regulatory elements that shape autosomal immune cell transcriptomes, although a possible role in regulating X gene expression was not shown (L. K. Case et al., 2013). Here, we differentiated between the above possible mechanisms by comparing mice with XY⁻ and XX CNS, and included a third genotype,

mice with XY^{*x} CNS. XY^{*x} mice are essentially XO, with the Y^{*x} chromosome containing only pseudoautosomal genes and no known X or Y specific genes (X. Chen et al., 2008). Comparison of XY^{*x} (1 X, 0 Y) with XY (1 X, 1 Y) and XX (2 X, 0 Y) mice allows for the examination of whether greater neurodegeneration in mice with XY CNS as compared to XX are due to X dosage versus the presence or absence of Y (Table 1).

Parents	Progeny Genotype	NPY dose	NPX dose
XX x XY ⁻ (+Sry)	XY ⁻	1	1
XX x XY [*]	XY ^{*x} (XO)	0	1+
XX x XY ⁻ (+Sry)	XX	0	2
XX x XY [*]	XX	0	2

Table 1. Breeding schematic to examine the role of X and Y dosage in the CNS neurodegenerative response to injury.

Mating XY⁻ (+Sry) males with WT XX females produces XY⁻ and XX progenies. The Y^{*x} chromosome consists of mostly pseudoautosomal genes and several adjacent NPX genes, hence the “+” notation in NPX dosage. Mating XY^{*} males with WT XX females produces XY^{*x} and XX progenies. Comparison between XY⁻ and XY^{*x} (XO) mice (green) allows for the examination of effects of Y dosage. Comparison between XX and XY^{*x} (XO) mice (orange) allows for the examination of effects of X dosage. XX littermates were generated from both breeding schemes to serve as appropriate controls. All progenies in this table are ovary-bearing. NPY, non- pseudoautosomal Y; NPX, non-pseudoautosomal X; Sry, sex-determining region of the Y.

Further, an additional mechanism that could account for the increased disease and neuropathology in mice with XY⁻ CNS as compared to XX is differences parental imprinting of the X chromosome. Parental imprinting is an epigenetic mechanism of gene regulation that is passed on in a parent-of-origin manner and has been shown to cause differential gene expression.

Since XX mice undergo random X inactivation in each cell, half the cells in XX mice would express the maternal X (X_m), while the other half expresses the paternal X (X_p). In contrast, XY mice, possessing only the maternal X, would express X_m in all cells. Our results of greater neurodegeneration in X_mY compared to X_mX_p are consistent with the possibility that the maternal imprint increases expression of a deleterious gene relative to the paternal imprint. To directly address whether greater neurodegeneration in mice with XY as compared to XX CNS was due to parental imprinting of the X chromosome, we further examined clinical EAE disease in XY^{*x} mice that either inherited a maternal X (X_mY^{*x}) or a paternal X (X_pY^{*x}) chromosome (Table 2).

Throughout the above experiments, to control for known effects of sex chromosomes on autoimmune responses, we created bone marrow chimeras in which mice with varying sex chromosome complements in the CNS are reconstituted with a common immune system.

Parents	Progeny Genotype	X_m	X_p
XX x XY^*	X_mY^{*x}	1+	0
XY^{*x} x XY	X_pY^{*x}	0	1+
XX x XY^*	X_mX_p	1	1
XY^{*x} x XY	X_mX_p	1	1

Table 2. Breeding schematic to examine the role of parental imprinting in the CNS neurodegenerative response to injury.

Mating XY^* males with WT XX females produces X_mY^{*x} and X_mX_p progenies. The Y^{*x} chromosome consists of mostly pseudoautosomal genes and several adjacent NPX genes, hence the “+” notation in NPX dosage. Mating X_mY^{*x} females with WT XY males produces X_pY^{*x} and X_mX_p progenies. Comparison between X_mY^{*x} and X_pY^{*x} (blue) allows for the examination of the effect of parental X imprinting. XX littermates were generated from both breeding schemes to serve as appropriate controls. All progenies in this table are ovary-bearing. X_m , maternal X; X_p , paternal X.

3.2 EAE disease severity in C57BL/6 mice with XY^{*x}, XY⁻, and XX CNS

To determine whether the dosage of Y genes contributed to the increased neurodegeneration in mice with XY⁻ CNS as compared to XX, we compared EAE clinical disease in bone marrow chimera mice with XY^{*x} (1X, 0Y), XY (1X, 1Y), and XX (2X, 0Y) CNS. All mice were reconstituted with a common immune system to eliminate confounding effects of sex chromosome complement on the immune system. As shown in Fig 11A, mice with XY^{*x} had similar clinical EAE disease scores as mice with XY⁻ CNS, with both groups demonstrating greater disease severity when compared with mice with XX CNS ($p < 0.0001$, XX \rightarrow XY⁻ vs. XX \rightarrow XX, and XX \rightarrow XY^{*x} vs. XX \rightarrow XX, repeated measures one-way ANOVA, Bonferonni post test). In another measure of motor impairment, the rotarod behavioral test corroborated clinical EAE results, with mice with XY^{*x} and XY⁻ CNS ambulating for fewer seconds than mice with XX CNS (Fig 11B, $p < 0.0001$, XX \rightarrow XY⁻ vs. XX \rightarrow XX, and XX \rightarrow XY^{*x} vs. XX \rightarrow XX, repeated measures one-way ANOVA, Bonferonni post test). These results indicate that the greater neurodegeneration in mice with XY⁻ CNS as compared to XX were due to X, not Y, gene effects.

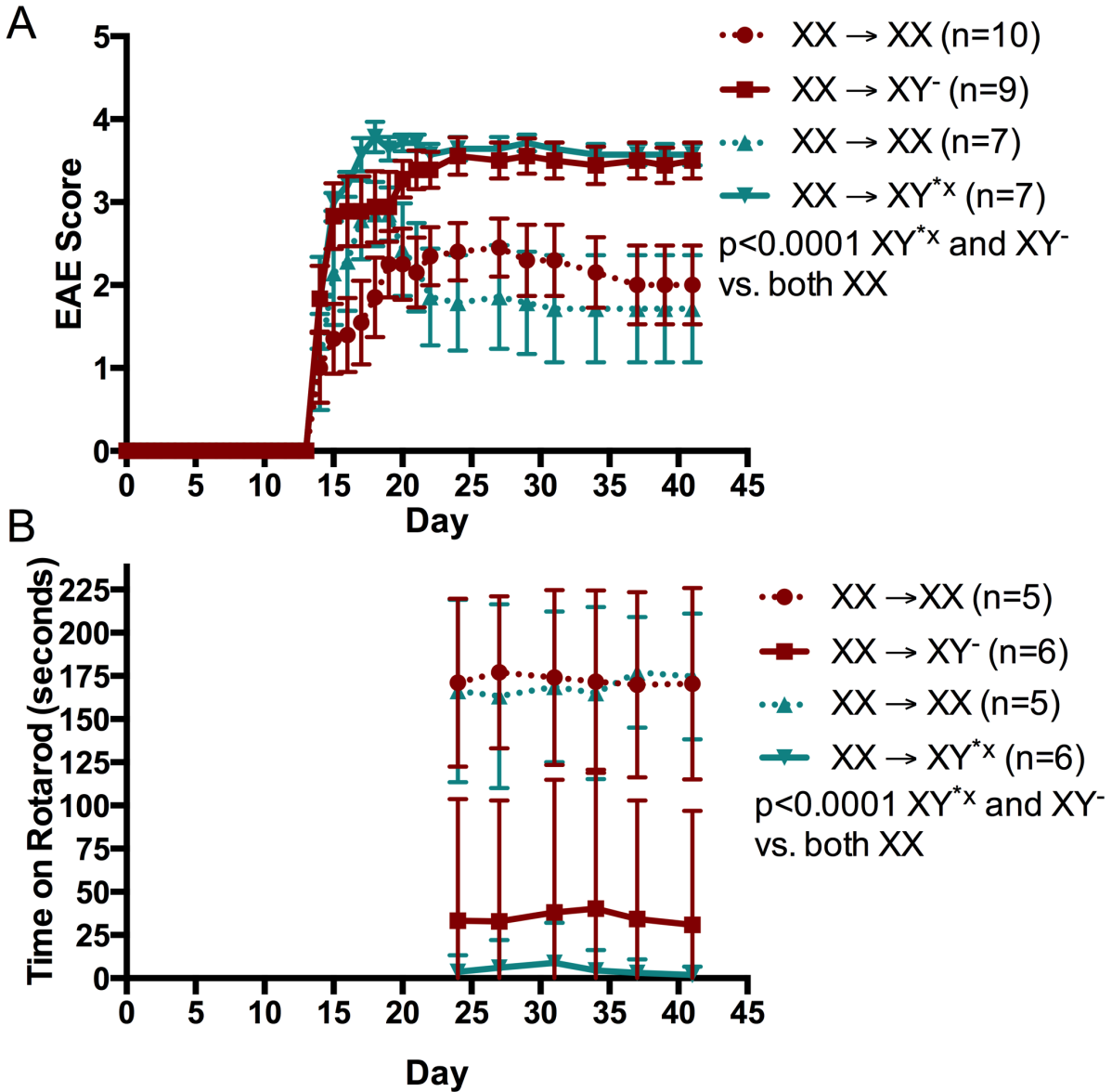


Figure 11. Mice with XY^{*x} and XY⁻ CNS, compared with XX CNS, have greater clinical EAE disease severity. Mice with XY^{*x} or XY⁻ genotype in the host CNS, compared to XX, had greater disease severity (had higher EAE scores) (A; p<0.0001, XX→XY⁻ and XX→XY^{*x} vs. XX→XX, repeated measures one-way ANOVA with Bonferroni post-hoc test), and had worse rotarod performance (i.e., spent less time on the rotarod = lower scores) (B; p<0.0001, XX→XY⁻ and XX→XY^{*x} vs. XX→XX, repeated measures one-way ANOVA with Bonferroni post-hoc test). XX littermates to XY⁻ and XY^{*x} mice are in hashed lines of the same color. Data are displayed as mean clinical scores ± SEM. Data are representative of three repeated experiments.

3.3 Neuropathology in the spinal cord, cerebellum and cerebral cortex in C57BL/6 mice with XY^{*x}, XY⁻, and XX CNS

At the endpoint of disease, we examined neuropathology by assessing myelin and axonal loss in the spinal cord. Mice with XY^{*x} and XY⁻ CNS has less myelin staining intensity and fewer numbers of axons when compared with mice with XX CNS as evaluated by myelin basic protein (MBP) and neurofilament 200 (NF200) staining, respectively (Fig 12A, $p=0.05$, XX \rightarrow XY⁻ vs. XX \rightarrow XX MBP, $p<0.001$, XX \rightarrow XY^{*x} vs. XX \rightarrow XX MBP; Fig 12B, $p<0.001$, XX \rightarrow XY⁻ and XX \rightarrow XY^{*x} vs. XX \rightarrow XX NF200, two way ANOVA). These data are consistent with the clinical observations of greater disability in mice with XY⁻ and XY^{*x} CNS as compared to XX.

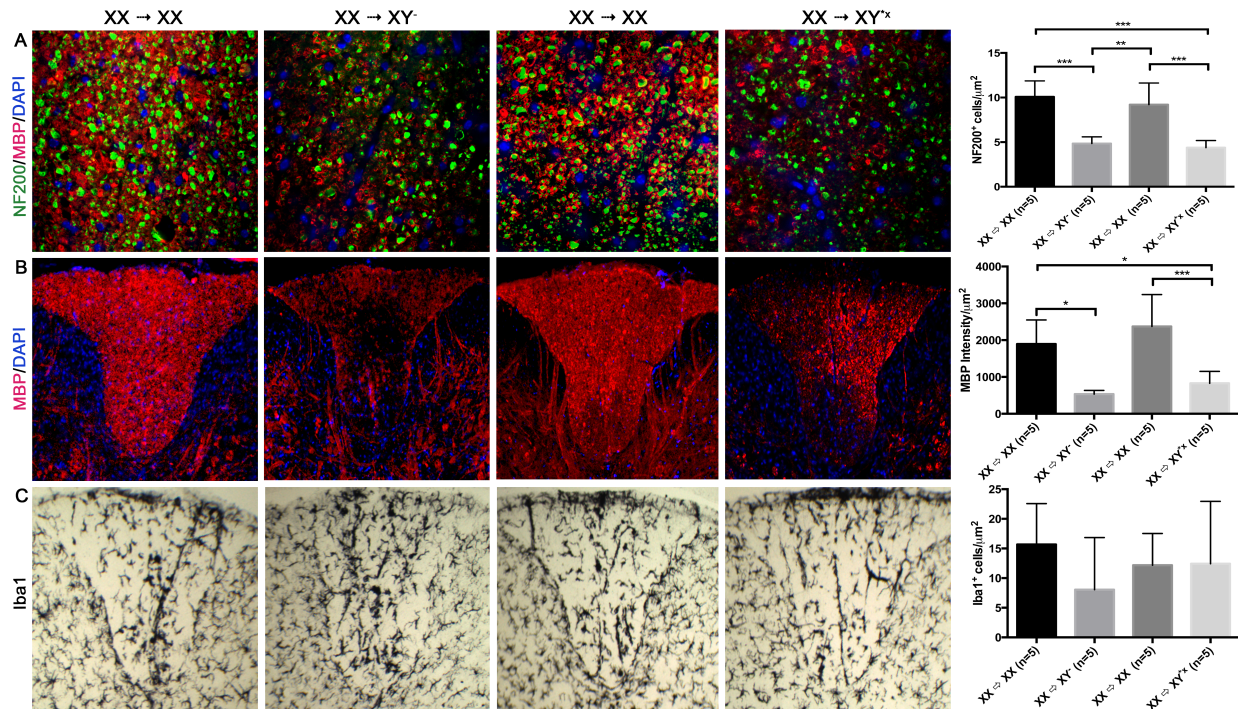


Figure 12. Mice with XY^{*x} and XY⁻ CNS, as compared to XX, have fewer axons and less myelin staining intensity in the spinal cord during EAE. Representative 40x captures of axons stained with NF200 (green) and MBP (red) at the

lateral funiculus of the thoracic spinal cord. Mice with XY^{*x} and XY^- CNS have fewer number of axons compared to mice with XX CNS ($p < 0.001$, $XX \rightarrow XY^-$ vs. $XX \rightarrow XX$ littermates, and $XX \rightarrow XY^{*x}$ vs. $XX \rightarrow XX$ littermates, two-way ANOVA). Tissues were counterstained with DAPI (blue). (B) Representative 10x captures of myelin stained with MBP (red) and DAPI in the dorsal column of the thoracic spinal cord. Mice with XY^{*x} and XY^- CNS have less myelin staining intensity in the spinal cord compared to mice with XX CNS ($p = 0.05$, $XX \rightarrow XY^-$ vs. $XX \rightarrow XX$ littermates; $p < 0.001$ $XX \rightarrow XY^{*x}$ vs. $XX \rightarrow XX$ littermate, two-way ANOVA). (C) Representative 10x captures of microglia stained with Iba1 (dark gray) in the dorsal column of the thoracic spinal cord. Graphs are displayed as mean \pm SEM. * $p = 0.05$, ** $p < 0.01$, *** $p < 0.001$. Data are representative of two repeated experiments.

Since mice demonstrated deficits in motor coordination in the rotarod behavioral test, we next examined cerebellar pathology by assessing demyelination and Purkinje cell quantity in these mice. At the endpoint of disease, mice with XY^{*x} and XY^- CNS, as compared to XX , had less myelin staining intensity in the granule cell layer (Fig 13A, $p < 0.0001$, $XX \rightarrow XY^-$ vs. $XX \rightarrow XX$, $p < 0.001$, $XX \rightarrow XY^{*x}$ vs. $XX \rightarrow XX$, two-way ANOVA) and fewer numbers of Purkinje cells in the cerebellum (Fig 13B, $p < 0.0001$, $XX \rightarrow XY^-$ and $XX \rightarrow XY^{*x}$ vs. $XX \rightarrow XX$, two-way ANOVA), as evaluated by MBP and calbindin staining, respectively. These results corroborate our observation of increased clinical EAE severity and worse rotarod performance in mice with XY^{*x} and XY^- CNS as compared to XX .

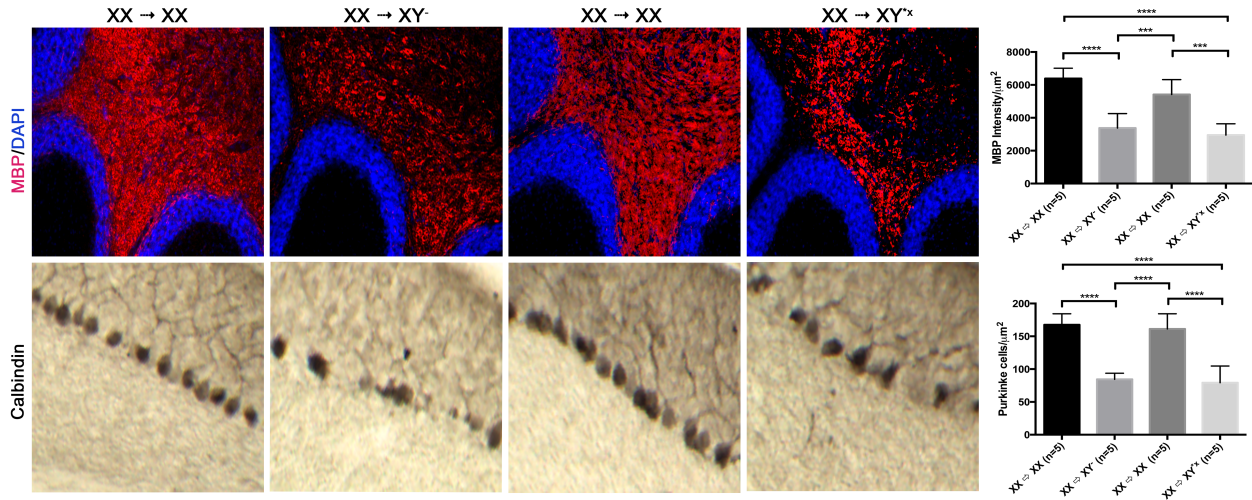


Figure 13. Mice with XY^{*x} and XY^- CNS, as compared to XX , have less myelin staining intensity and fewer Purkinje cells in the cerebellum during EAE. (A) Representative 10x captures of myelin stained with MBP (red) and DAPI in the white matter of the cerebellum. Mice with XY^{*x} and XY^- CNS have less myelin staining intensity in cerebellar white matter compared to mice with XX CNS ($p < 0.001$, $XX \rightarrow XY^-$ vs. $XX \rightarrow XX$ littermates and $XX \rightarrow XY^{*x}$ vs. $XX \rightarrow XX$ littermate, two-way ANOVA). (B) Representative 40x captures of Purkinje cells stained with calbindin (dark gray) in the cerebellum. Mice with XY^{*x} and XY^- CNS have fewer Purkinje cells compared to mice with XX CNS ($p < 0.0001$, $XX \rightarrow XY^-$ vs. $XX \rightarrow XX$ littermates and $XX \rightarrow XY^{*x}$ vs. $XX \rightarrow XX$ littermate, two-way ANOVA). Graphs are displayed as mean \pm SEM. *** $p < 0.001$, **** $p < 0.0001$. Data are representative of two repeated experiments.

Since *Tlr7* is located on the X chromosome and its expression in neurons has been linked to neurodegeneration (Sabrina M. Lehmann et al., 2012), we next examined *Tlr7* expression in the cerebral cortex. As shown in Fig 14, mice with XY^{*x} and XY^- CNS, as compared to XX , had more *Tlr7* expressing neurons in the cerebral cortex (Fig 14, middle right, $p < 0.001$, $XX \rightarrow XY^-$ and $XX \rightarrow XY^{*x}$ vs. $XX \rightarrow XX$, two-way ANOVA). The increased expression of *Tlr7* in XY^- and XY^{*x} mice as compared to XX was not due to relative neuronal loss because all groups had similar numbers of cortical neurons (Fig 14, bottom right). Our findings of increased *Tlr7*

expressing neurons in XY^{*x} and XY^- mice, compared to XX , as well as our previous finding of increased Tlr7 expression in XY^- relative to XX (Du et al., 2014), are consistent with previous findings of Tlr7 expression in neurons leading to neurodegeneration.

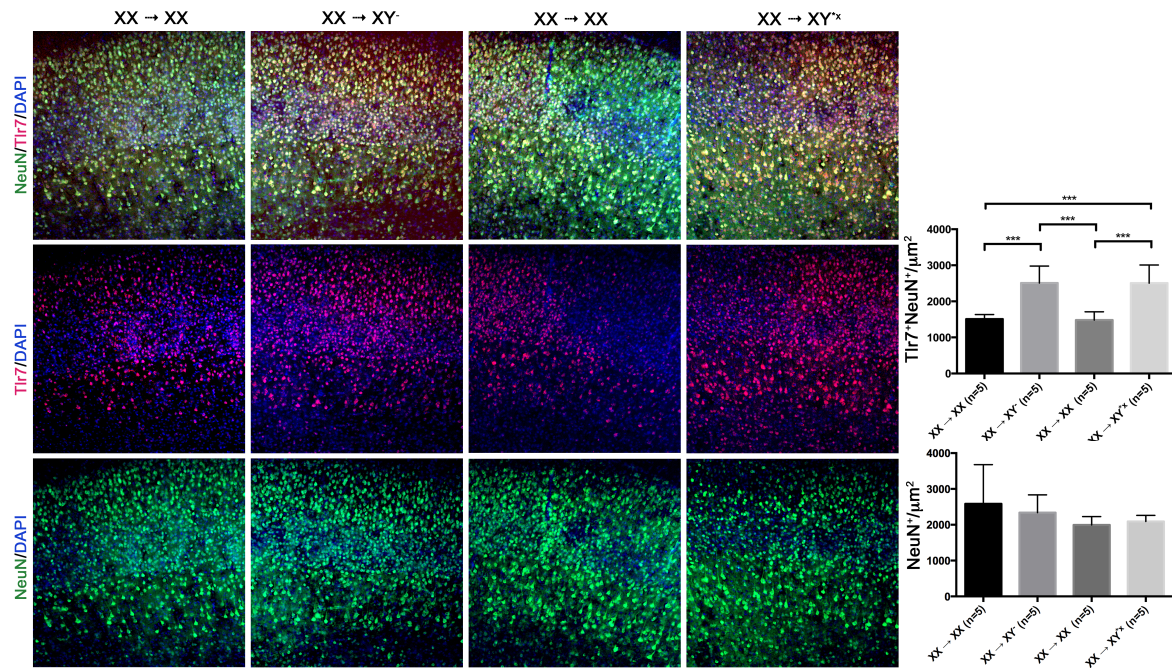


Figure 14. Mice with XY^{*x} and XY^- CNS, as compared to XX , have more Tlr7 expressing neurons during EAE. (A) Representative 10x capture of coronal sections of cerebral cortical layers I-VI stained with Tlr7 (red) and NeuN (green) in $XX \rightarrow XX$, $XX \rightarrow XY^-$, $XX \rightarrow XX$ (littermates to XY^{*x}), and $XX \rightarrow XY^{*x}$ bone marrow chimeras. Top row represents merged Tlr7, NeuN, and DAPI; middle row represents Tlr7 only; bottom row represents NeuN only. All sections were counterstained with DAPI (blue). (B) Mice with XY^- and XY^{*x} CNS, compared to XX , have more Tlr7⁺ expressing cells in the cerebral cortex ($p < 0.001$, $XX \rightarrow XX$ vs. $XX \rightarrow XY^-$ and $XX \rightarrow XY^{*x}$, two-way ANOVA), with no significant differences in the number of cerebral cortical cells. Data are representative of two repeated experiments. *** $p < 0.001$.

3.4 EAE disease severity in C57BL/6 mice with X_mY^{*x} vs. X_pY^{*x} CNS

Since both XY^- and XY^{*x} mice expressed X_m in all cells and had greater disease as compared to XX mice that expressed the X_m in half the cells, and X_p in the other half, we next determined if X imprinting could account for this observation. We generated XY^{*x} mice which inherited either the maternal X (X_mY^{*x}) or paternal X (X_pY^{*x}). As shown in Fig 15, mice with X_mY^{*x} CNS, as compared to X_pY^{*x} , have greater clinical disease severity during EAE (Fig 15A, $p < 0.0001$, $XX \rightarrow X_mY^{*x}$ vs. $XX \rightarrow X_pY^{*x}$, repeated measures one-way ANOVA) and stayed on the rotarod for fewer seconds (Fig 15B, $p = 0.05$, $XX \rightarrow X_mY^{*x}$ vs. $XX \rightarrow X_pY^{*x}$, repeated measures one-way ANOVA). Our results indicate that parental imprinting of the X chromosome contributes to sex differences in the CNS response to injury in a given immune attack. Specifically, the maternal X imprint increases neurodegeneration relative to the paternal X imprint.

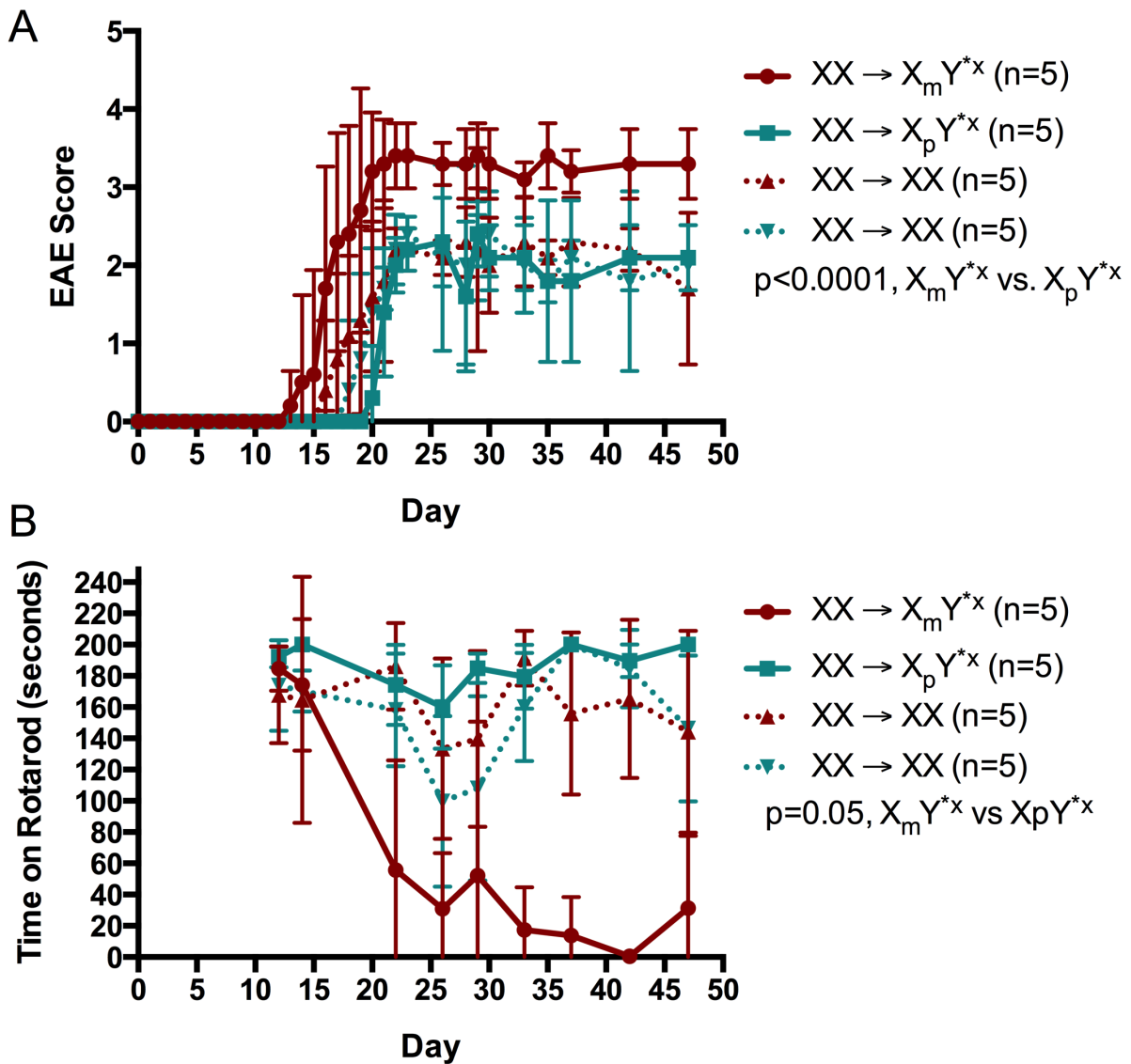


Figure 15. Mice with $X_m Y^{*x}$ CNS, as compared to $X_p Y^{*x}$, have greater clinical disease severity during EAE. Mice with $X_m Y^{*x}$ genotype in the host CNS, compared to $X_p Y^{*x}$, had greater disease severity (had higher EAE scores) (A; $p < 0.0001$, $XX \rightarrow X_m Y^{*x}$ vs. $XX \rightarrow X_p Y^{*x}$, repeated measures one-way ANOVA with Bonferroni post-hoc test), and had worse rotarod performance (i.e., spent less time on the rotarod = lower scores) (B; $p = 0.05$, $XX \rightarrow X_m Y^{*x}$ vs. $XX \rightarrow X_p Y^{*x}$, repeated measures one-way ANOVA with Bonferroni post-hoc test). XX littermates to $X_m Y^{*x}$ and $X_p Y^{*x}$ are coded as hashed lines of the same color. Data are displayed as mean clinical scores \pm SEM. Data are representative of three repeated experiments.

3.5 *Tlr7* methylation in C57BL/6 mice with X_mY^{*x} vs. X_pY^{*x} cerebral cortex

To directly determine whether differential *Tlr7* expression in cortical neurons of X_mY^{*x} and X_mY vs. XX mice during EAE was a result of parental imprinting on *Tlr7*, we examined the methylation status of a CG rich *Tlr7* promoter region in the cerebral cortex of X_mY^{*x} vs. X_pY^{*x} mice at the endpoint of disease. As shown in Fig 16, there was no differences in methylation of *Tlr7* when comparing as compared to X_mY^{*x} and X_pY^{*x} . Together these data show that while X imprinting affects the neurodegenerative response to injury, difference in *Tlr7* expression are the consequence and not the cause of neurodegeneration.

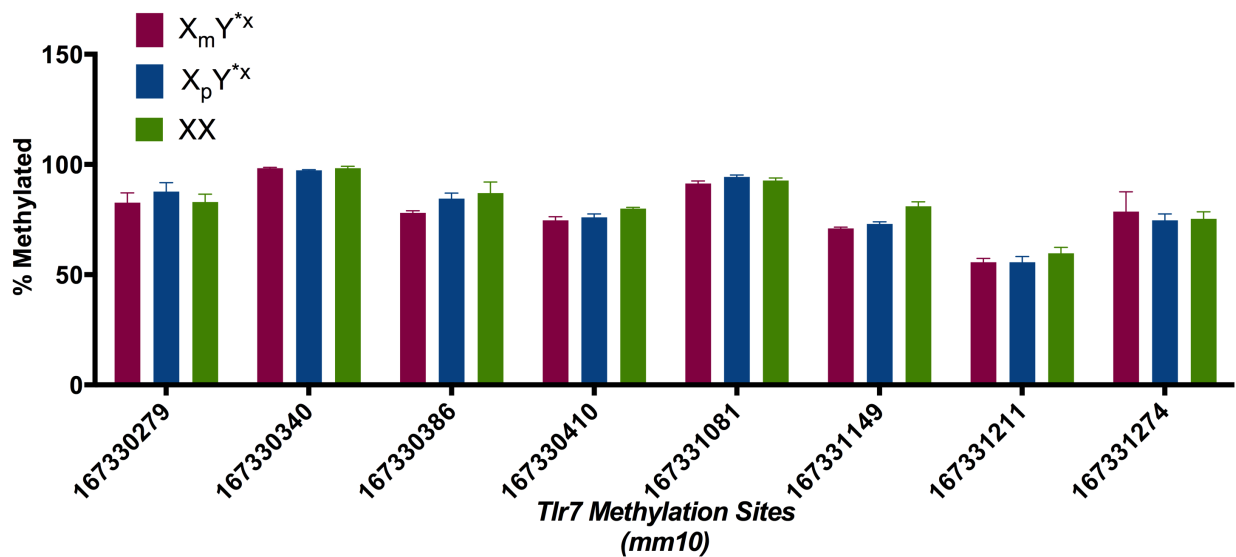


Figure 16. No differences in methylation of the *Tlr7* promoter in the cerebral cortex of mice with X_mY^{*x} vs. X_pY^{*x} CNS. Percent methylation of the *Tlr7* promoter CpG sites in the cerebral cortex of mice with X_mY^{*x} (red), X_pY^{*x} (blue), and XX (green) CNS. No differences in methylation were observed in any of the 8 CpG sites examined.

3.6 Discussion

It is well known that autoimmune diseases like MS occur in women more frequently than men. However, men with MS demonstrate faster disability progression, presenting a clinical enigma in susceptibility and progression in MS (Rhonda R. Voskuhl & Gold, 2012). Previously, our lab demonstrated that mice with CNS cells expressing the XY sex chromosome complement, as compared to XX, had greater neurodegeneration during EAE (Du et al., 2014). This could be due to Y presence or absence, differences in X dosage, or parental imprinting of the X chromosome. Our findings showing no difference in EAE in mice with XY^{*x} (XO) versus XY CNS eliminated the possibility of a Y gene being responsible. Instead, our finding of the maternal X imprint leading to greater disease relative to the paternal imprint demonstrated that the parent-of-origin of the X chromosome accounts for sex differences in the CNS response to injury.

Parental imprinting of the X chromosome leading to preferential gene expression in the mouse neuronal architecture has been documented (Gregg, Zhang, Butler, Haig, & Dulac, 2010), but such has never before been described in a disease. In EAE, epigenetic effects have been limited to autosomal genes affecting the immune system, with none examining the role of sex chromosome genes in the CNS. For example, a recent study identified changes in the parentally imprinted disease-predisposing autosomal gene *Dlk1* during EAE, highlighting a role for epigenetic factors in EAE susceptibility (Stridh et al., 2014). Another study demonstrated that DNA methylation at inflammatory cytokine promoters regulates Th cell differentiation during chronic EAE (Guan, Nagarkatti, & Nagarkatti, 2011). These studies as well as our current findings underscore the importance of epigenetic factors not only in EAE susceptibility, but now also in progression.

X chromosome abnormalities have been consistently linked to aberrant neurological development as exemplified in several X-linked diseases. For example, X chromosome aneuploidies can result in Turner's syndrome (Lepage et al., 2013), or Klinefelter's syndrome (Hong & Reiss, 2014), while mutations in the X chromosome gene *FMR1* leads to Fragile X syndrome (Hong & Reiss, 2014). Additionally, the expanding catalog of 'X-linked mental retardation' (XLMR) genes to over 100, or nearly 10% of the genes on the X chromosome, indicates that an inordinate amount of the X chromosome is devoted to brain development (Gecz, Shoubridge, & Corbett, 2009). Interestingly, the X chromosome gene *MECP2*, in which the mutation causes Rett syndrome, produces MeCP2 protein that acts as a transcription regulator by binding to methylated CG nucleotides (Gonzales & LaSalle, 2010), thus highlighting a role for X genes in the epigenetic control of neurodevelopment and cognition.

The literature on epigenetic effects on neurodegeneration in MS has been sparse, but examination of epigenetic effects on demyelination and remyelination has been explored to some extent. One study demonstrated marked demethylation in the promoter of *peptidylarginine deiminase type-2 (PAD-2)*, leading to overexpression of this myelin-destabilizing protein during demyelination of the white matter of MS patients (Mastronardi, Noor, Wood, Paton, & Moscarello, 2007). Other studies have also found epigenetic changes during remyelination, from substantial histone H3 deacetylation correlating with impaired oligodendrocyte differentiation in early stage MS (Pedre et al., 2011), to increased miRNA expression targeting proteins that maintain myelin and axon integrity in the CNS of MS patients (Junker et al., 2009; Shin, Shin, McManus, Ptacek, & Fu, 2009). Thus, epigenetic changes of critical proteins in myelin integrity are emerging as potential contributors to disruption of myelin and axonal integrity in MS pathogenesis.

To date, no studies have directly examined the role of epigenetics in neuronal degeneration in MS or EAE, although a link between DNA methylation and neuron death in cell culture models has been described. In one study, cultured spinal cord neurons degenerated with overexpression of *Dnmt3a*, a molecule involved in DNA methylation, whereas inhibition of *Dnmt3a* inhibited apoptosis. These results suggested that *Dnmt3a* has pro-apoptotic functions and may serve as another program for cell death, although the specific gene targets of apoptosis-related DNA methylation remained unidentified. Additional studies in samples from ALS patients revealed similar results (Chestnut et al., 2011). Together, these results support a role for epigenetic effects of autosomal genes playing a role in neuronal degeneration, with our results adding a role for epigenetic effects of X chromosome genes participating in disease characterized by a sex difference. Consistent with an important role for epigenetic effects of genes involved in myelin, axonal, and neuronal integrity are results from GWAS studies in MS where significant allelic linkages to CNS genes were not found (Baranzini et al., 2009; Beecham et al., 2013; Sawcer et al., 2011).

In summary, this is the first observation of a parental imprinting effect on neurodegeneration in any disease model that is not characterized by sex chromosome dosage or mutation, thereby extending this phenomenon to the general euploid population. Further, in the MS model, deleterious effects of the maternal X imprint, which are unopposed in males, are consistent with males having faster disability progression as compared to females in MS. Further studies examining epigenetic effects on X genes as well as autosomal genes in MS may reveal novel therapeutic targets to prevent disability progression.

Chapter 4: Parent-of-Origin Sex Chromosome Effects in the Immune System During Autoimmune Responses

4.1 Introduction

In this chapter, I investigate sex chromosome effects in the immune system to address why multiple sclerosis is more prevalent in women than men. Previously, our lab demonstrated that mice bearing XX sex chromosomes in immune cells, as compared to XY, increases autoimmune responses in the mouse model of multiple sclerosis and systemic lupus erythematosus (Sasidhar et al., 2012; Smith-Bouvier et al., 2008). These studies used the four core genotypes (FCG) mouse model that allows for the comparison of two different sex chromosome genotypes with a common sex hormonal background. Specifically, the testis-determining factor, *Sry*, is deleted from the Y chromosome, and translocated to an autosomal location, resulting in: ovary-bearing XX and XY mice, or testis-bearing XX and XY mice (A. P. Arnold & X. Q. Chen, 2009). While the findings demonstrated a role for sex chromosomes in sex differences in immune responses, the genes and mechanisms involved remained unknown. Possible explanations for observed differences between XX vs. XY⁻ mice included the dosage of X chromosomes (1 vs. 2), the presence of Y (1 vs. 0), or differential parental imprinting of X chromosome genes.

There are several X chromosome genes that are known to be involved in immune responses: *Forkhead box p3 (Foxp3)*, *Toll-like receptor 7 (Tlr7)*, and *Cd40lg*. *Foxp3* is a transcription factor found only on CD4⁺CD25^{hi} T regulatory (T_{reg}) cells, a subset of T helper cells that regulate immune responses by countering effector T cell function. *Foxp3* is considered

the “master-regulator” of T_{reg} development and function, with the induction of the *Foxp3* gene sufficient to elicit downstream co-stimulatory molecules and immunosuppressive responses (Fontenot, Gavin, & Rudensky, 2003b; Hori, Nomura, & Sakaguchi, 2003). In EAE, the induction of $FoxP3^+$ T_{regs} has immunosuppressive functions (McGeachy, Stephens, & Anderton, 2005; Yu et al., 2005). FOXP3 expression during the induction of T_{reg} function is regulated by epigenetic mechanisms at the transcriptional level that involves *Foxp3* DNA methylation (Floess et al., 2007; G. Lal et al., 2009; Polansky et al., 2008). Previous findings suggested that T_{regs} contribute to the resistance mechanisms to autoimmunity in male mice (Reddy et al., 2005). T_{reg} populations are also expanded during pregnancy and estrogen treatment, coinciding with a reduced inflammatory phenotype (Polanczyk et al., 2004; Polanczyk, Hopke, Huan, Vandembark, & Offner, 2005; Tai et al., 2008). While T_{reg} development and function can be altered by sex hormones, this does not preclude direct sex chromosome effects.

In addition to a role for *Foxp3* in sex differences in autoimmune diseases, other X chromosome candidates such as *Cd40lg* and *Tlr7* may also be important. *Cd40lg* (or *Cd154*) is expressed primarily on activated $CD4^+$ T cells, and sex differences in CD40L expression have been reported in a spontaneous mouse model of SLE, with XX T cells expressing higher levels relative to XY (Sasidhar et al., 2012). *Tlr7*, expressed in antigen-presenting cells in the immune system, as well as in neurons and glia in the CNS, recognizes pathogen-associated molecular patterns and signals innate immune responses during viral infections (Lalive et al., 2014; Sabrina M. Lehmann et al., 2012). Since *Tlr7* has also been implicated in autoimmunity (Pisitkun et al., 2006; Subramanian et al., 2006), expression of *Tlr7* may also differ between XX and XY⁻ mice.

To examine the nature of sex differences in X chromosome gene expression during autoimmune responses, we returned to the FCG model, XX (2X, 0Y), and XY⁻ (1X, 1Y), to

which we compared XY^{*x} (1X, 0Y) mice, daughters of XY^* males. The XY^{*x} mouse is used to model the XO genotype because it contains one X chromosome and no male-specific region of the Y chromosome (Burgoyne, Mahadevaiah, Perry, Palmer, & Ashworth, 1998; Chen, McClusky, Itoh, Reue, & Arnold, 2013; Isles, Davies, Burrmann, Burgoyne, & Wilkinson, 2004). This additional genotype allowed us to determine which sex chromosome, X or Y, harbors genes that regulate immune function in a sexually dimorphic manner (Table 1). One possibility is X dosage, wherein an X gene is expressed higher in XX than XY cells because it escapes X-inactivation and is expressed from both X chromosomes in XX cells (Arnold, 2012). In the case of an $XX > XY$ bias in autoimmunity, a deleterious X chromosome gene could theoretically escape X-inactivation in XX mice and be expressed in higher dose relative to XY mice. Another possibility is that differential parental imprinting of an X gene in XX vs. XY^- . To further address the latter possibility, we also generated $X_m Y^{*x}$ mice (with a maternal X allele) and $X_p Y^{*x}$ mice (with a paternal X allele) to compare directly maternal vs. paternal imprinting effects on immune responses (Table 2).

4.2 FOXP3 expression and function in SJL XY vs. XX mice

Since *Foxp3* is an X chromosome gene and is involved in development of T_{regs} , we examined *Foxp3* mRNA levels in LNCs of PLP 139-151 immunized XX and XY^- SJL female mice. As shown in Fig 17A, XY^- mice had nearly 8-fold higher levels of *Foxp3* mRNA when compared with XX mice ($p < 0.0001$, one-way ANOVA, Student's t-test). We next examined FOXP3 protein expression gated on $CD4^+ CD25^+$ T cells by flow cytometry (Fig 17B), and found that XY LNCs had higher numbers of $CD4^+ CD25^+ FoxP3^+$ T_{regs} as compared to XX LNCs (Fig 17C, $p < 0.0001$, one way ANOVA, Student's t-test). The functional ability of the

CD4⁺CD25⁺FoxP3⁺ T_{regs} to suppress effector T cells was then confirmed using the standard T_{reg} suppressor assay, with no differences between XY and XX in T_{reg} suppressor function (Fig 17D). Thus, the effect of sex chromosome complement on CD4⁺CD25⁺FoxP3⁺ T_{reg} cells in autoimmunity is quantitative with a higher number of these cells in XY⁻ as compared to XX.

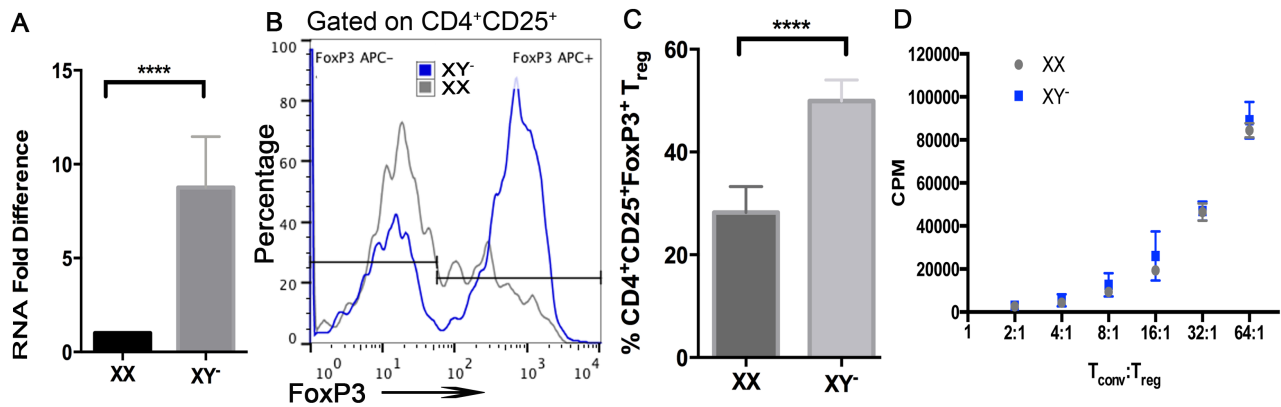


Figure 17. XY⁻ cells as compared to XX have higher percentage of CD4⁺CD25⁺FoxP3⁺ T_{reg} cells during induction of immune responses. (A) Representative lymph node *Foxp3* mRNA levels between XX and XY⁻ mice 10 days after immunization with PLP 139-151. XY⁻ cells expressed higher levels of *Foxp3* mRNA as compared to XX cells ($p < 0.0001$, paired Student's t-test). (B) Representative FACS data showing FoxP3⁺ cells gated on CD4⁺CD25⁺ T cells with quantification in (C) ($p < 0.0001$, Student's t-test). (D) Representative results in the assessment of XX versus XY⁻ T_{reg} suppression activity. XX and XY⁻ T_{reg} do not differ in their ability to suppress T cell activation. CPM, counts per minute; corresponds to [³H]-Thymidine incorporation during proliferation. Data are representative of three separate repeated experiments. **** $p < 0.0001$.

4.3 FOXP3 expression and function in SJL X_mY^{*x} , X_mY , and X_mX_p mice

We next determined whether the differences in FOXP3 expression between XX versus XY⁻ resulted from a direct effect of X chromosome genes or an indirect effect of Y genes. For this, we created XY^{*x} female transgenic mice, essentially with 1X and 0Y chromosomes (Table 1), since the Y^{*x} chromosome possesses pseudoautosomal genes from both the X and Y chromosome, but no X- or Y-specific genes (Xuqi Chen et al., 2008). At day 10 after PLP 139-151 immunization, X_mY^{*x} (1X, 0Y) mice had higher levels of *Foxp3* mRNA in LNCs (Fig 18A, $p < 0.01$, one-way ANOVA, Tukey's post test), as well as higher percentages of CD4⁺CD25⁺FoxP3⁺ T_{reg} cells (Fig 18B and 18C, $p < 0.01$, Tukey's post test), when compared with XX (2X, 0Y) mice. Since X_mY^{*x} (1X, 0Y) mice, which have no Y-specific genes, displayed similar levels of *Foxp3* mRNA and protein expression as compared to X_mY^- (1X, 1Y), this rules out the possibility of a Y-regulatory element driving FOXP3 expression on X. Rather, higher FOXP3 levels in X_mY^{*x} as compared to X_mX_p mice must be due to a direct effect of X chromosome genes. This X chromosome effect could not be due to an X dosage effect with *Foxp3* escaping X-inactivation because higher FOXP3 levels were found in XY⁻, not in XX. Rather, higher levels of FOXP3 in XY⁻ could be due to differences in parental imprinting.

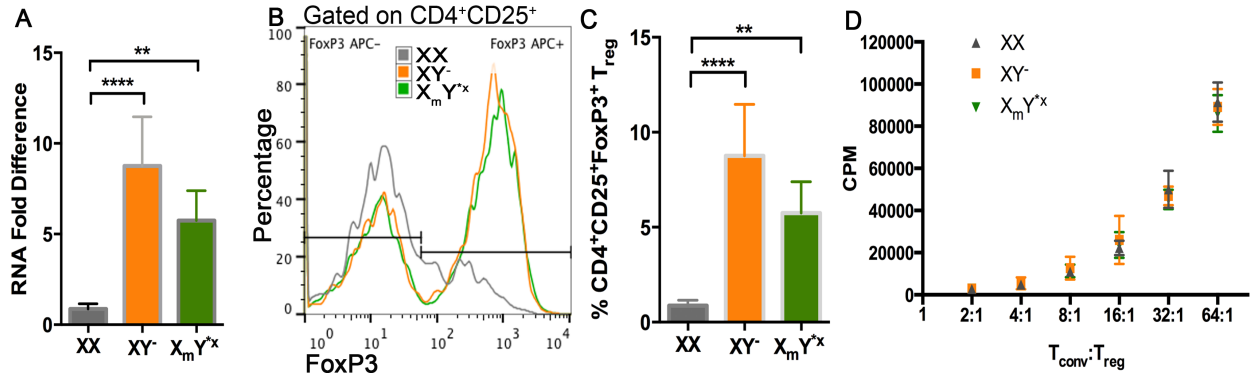


Figure 18. X_mY^{*x} and X_mY⁻ cells, as compared to X_mX_p, have higher percentage of CD4⁺CD25⁺FoxP3⁺ T_{reg} cells. (A) Representative lymph node *Foxp3* mRNA levels between X_mY^{*x} (green), X_mY⁻ (orange), and X_mX_p (gray) mice 10 days after immunization with PLP 139-151. X_mY^{*x} and X_mY⁻, as compared to X_mX_p, expressed higher levels of *Foxp3* mRNA ($p < 0.0001$, X_mX_p vs. X_mY⁻; $p < 0.01$, X_mX_p vs. X_mY^{*x}; N=6 each group, one-way ANOVA, Tukey's post test). (B, C) Relative quantity of FoxP3⁺ cells gated on CD4⁺CD25⁺ T cells as defined by isotype control. X_mY^{*x} and X_mY⁻ cells, as compared to X_mX_p, have a higher percentage of CD4⁺CD25⁺FoxP3⁺ regulatory T cells ($p < 0.0001$, X_mX_p vs. X_mY⁻; $p < 0.01$, X_mX_p vs. X_mY^{*x}; N=6 each group, one-way ANOVA, Tukey's post test). (D) Representative results in the assessment of X_mY^{*x}, X_mY⁻, and X_mX_p T_{reg} suppression activity. X_mY^{*x}, X_mY⁻, and X_mX_p T_{regs} do not differ in their ability to suppress T cell activation, regardless of the T_{conv}:T_{reg} ratio. Data are representative of three separate repeated experiments. ** $p < 0.01$, **** $p < 0.0001$.

4.4 *Foxp3* methylation in SJL X_mY^{*x}, X_mY, and X_mX_p mice

Since sexually dimorphic FOXP3 expression was localized to the X chromosome, we next determined whether increased *Foxp3* mRNA and protein expression levels in XY relative to XX mice could have resulted from parental imprinting. Specifically, FOXP3 expression could be regulated in a parent-of-origin manner via DNA methylation. Thus, we examined the methylation status of a CG rich transcriptionally relevant *Foxp3* upstream enhancer region (Fig 19A). The DNA methylation status of this upstream enhancer has been previously shown to correlate with *Foxp3* expression levels (G. Lal et al., 2009). At day 10 after PLP 139-151 immunization, LNCs from X_mX_p and X_mY⁻ littermates, as well as X_mY^{*x} and X_mX_p littermates,

were harvested and restimulated *ex vivo* with auto-antigen, and DNA was isolated from FACS sorted CD3⁺CD4⁺ T cells for the assessment of *Foxp3* methylation levels via bisulfite sequencing. As shown in Fig 18, X_mY⁻ (1X, 0Y) CD3⁺CD4⁺ T cells had lower percent methylation in *Foxp3* as compared to cells from X_mX_p (1X, 1Y) littermates (p<0.01, Student's t-test). Similarly, CD3⁺CD4⁺ T cells from X_mY^{*x} (1X, 0Y) mice also had lower percent methylation as compared to their X_mX_p (1X, 1Y) littermates (Fig 19, p-values for each CpG site in Table 3). Together, these data show a parental imprinting effect in regulating FOXP3 expression. Specifically, the maternal allele results in lower percent methylation of the *Foxp3* enhancer relative to the paternal allele. These results are consistent with increased FOXP3 expression in X_mY^{*x} and X_mY⁻ mice, which express the maternal allele in all cells, when compared with X_mX_p mice, which expresses the maternal allele in half of cells and the paternal allele in the other half due to random X-inactivation.

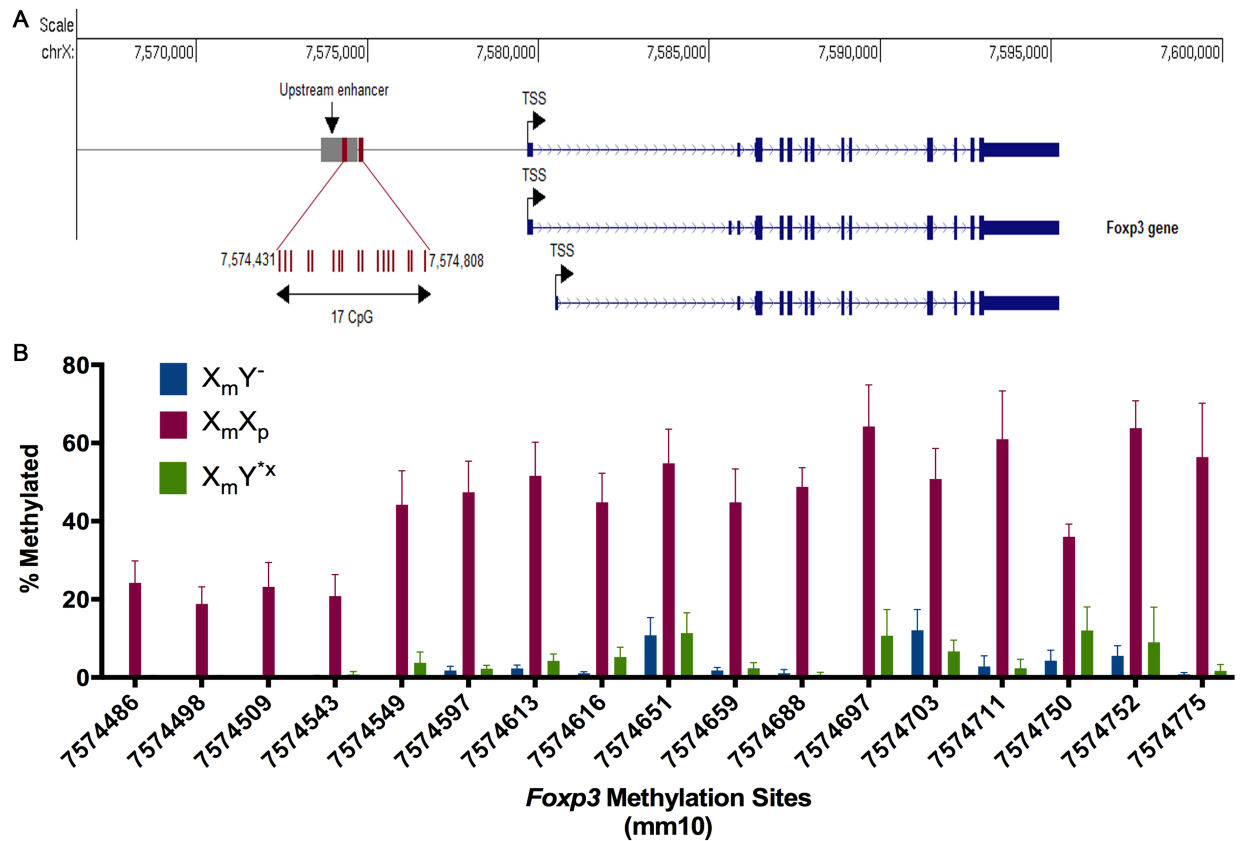


Figure 19. XX mice, as compared to XY^- , have higher DNA methylation of the *Foxp3* upstream enhancer region in $CD4^+$ lymph node cells during induction of immune responses. (A) Schematic map of the X chromosome region containing the *Foxp3* gene (blue) and CpG rich upstream enhancer region (gray). 17 CpG sites (red) in the *Foxp3* upstream enhancer region were examined. TSS, transcription start site. (B) Percent methylation of *Foxp3* enhancer in $CD3^+CD4^+$ T cells derived from LN of PLP 139-151-immunized $X_m Y^{*x}$ (magenta), $X_p Y^{*x}$ (blue), and XX (green) mice. $CD3^+CD4^+$ T cells derived from XX mice have higher *Foxp3* methylation as compared to $CD3^+CD4^+$ T cells derived from $X_m Y^{*x}$ and $X_m Y^-$ mice ($p < 0.0001$, $N = 8$ each group, students t-test). Data are representative of three repeated experiments.

Tukey's multiple comparisons test	Mean Diff.	95% CI of diff.	Significant?	Summary	Adjusted P Value
7574486					
XX vs. XY ⁻	24.2	4.437 to 43.96	Yes	*	0.0119
XX vs. XY ^{*x}	23.95	4.187 to 43.71	Yes	*	0.013
XY ⁻ vs. XY ^{*x}	-0.25	-21.08 to 20.58	No	ns	0.9996
7574498					
XX vs. XY ⁻	18.8	-0.9626 to 38.56	No	ns	0.066
XX vs. XY ^{*x}	18.55	-1.213 to 38.31	No	ns	0.0708
XY ⁻ vs. XY ^{*x}	-0.25	-21.08 to 20.58	No	ns	0.9996
7574509					
XX vs. XY ⁻	23.2	3.437 to 42.96	Yes	*	0.0168
XX vs. XY ^{*x}	23.2	3.437 to 42.96	Yes	*	0.0168
XY ⁻ vs. XY ^{*x}	0	-20.83 to 20.83	No	ns	> 0.9999
7574543					
XX vs. XY ⁻	20.55	0.7874 to 40.31	Yes	*	0.0395
XX vs. XY ^{*x}	20.05	0.2874 to 39.81	Yes	*	0.0459
XY ⁻ vs. XY ^{*x}	-0.5	-21.33 to 20.33	No	ns	0.9982
7574549					
XX vs. XY ⁻	44.2	24.44 to 63.96	Yes	****	< 0.0001
XX vs. XY ^{*x}	40.45	20.69 to 60.21	Yes	****	< 0.0001
XY ⁻ vs. XY ^{*x}	-3.75	-24.58 to 17.08	No	ns	0.9049
7574597					
XX vs. XY ⁻	45.65	25.89 to 65.41	Yes	****	< 0.0001
XX vs. XY ^{*x}	45.15	25.39 to 64.91	Yes	****	< 0.0001
XY ⁻ vs. XY ^{*x}	-0.5	-21.33 to 20.33	No	ns	0.9982
7574613					
XX vs. XY ⁻	49.35	29.59 to 69.11	Yes	****	< 0.0001
XX vs. XY ^{*x}	47.35	27.59 to 67.11	Yes	****	< 0.0001
XY ⁻ vs. XY ^{*x}	-2	-22.83 to 18.83	No	ns	0.972
7574616					
XX vs. XY ⁻	43.8	24.04 to 63.56	Yes	****	< 0.0001
XX vs. XY ^{*x}	39.55	19.79 to 59.31	Yes	****	< 0.0001
XY ⁻ vs. XY ^{*x}	-4.25	-25.08 to 16.58	No	ns	0.8796

7574651					
XX vs. XY ⁻	44.05	24.29 to 63.81	Yes	****	< 0.0001
XX vs. XY ^{*x}	43.47	21.95 to 64.98	Yes	****	< 0.0001
XY ⁻ vs. XY ^{*x}	-0.5833	-23.08 to 21.92	No	ns	0.9979
7574659					
XX vs. XY ⁻	43.05	23.29 to 62.81	Yes	****	< 0.0001
XX vs. XY ^{*x}	42.47	20.95 to 63.98	Yes	****	< 0.0001
XY ⁻ vs. XY ^{*x}	-0.5833	-23.08 to 21.92	No	ns	0.9979
7574688					
XX vs. XY ⁻	47.8	28.04 to 67.56	Yes	****	< 0.0001
XX vs. XY ^{*x}	48.13	26.62 to 69.65	Yes	****	< 0.0001
XY ⁻ vs. XY ^{*x}	0.3333	-22.17 to 22.83	No	ns	0.9993
7574697					
XX vs. XY ⁻	64.2	44.44 to 83.96	Yes	****	< 0.0001
XX vs. XY ^{*x}	53.53	32.02 to 75.05	Yes	****	< 0.0001
XY ⁻ vs. XY ^{*x}	-10.67	-33.17 to 11.83	No	ns	0.5023
7574703					
XX vs. XY ⁻	38.8	19.04 to 58.56	Yes	****	< 0.0001
XX vs. XY ^{*x}	44.13	22.62 to 65.65	Yes	****	< 0.0001
XY ⁻ vs. XY ^{*x}	5.333	-17.17 to 27.83	No	ns	0.8411
7574711					
XX vs. XY ⁻	58.25	38.49 to 78.01	Yes	****	< 0.0001
XX vs. XY ^{*x}	58.67	37.15 to 80.18	Yes	****	< 0.0001
XY ⁻ vs. XY ^{*x}	0.4167	-22.08 to 22.92	No	ns	0.9989
7574750					
XX vs. XY ⁻	31.75	11.99 to 51.51	Yes	***	0.0006
XX vs. XY ^{*x}	24	2.485 to 45.51	Yes	*	0.0247
XY ⁻ vs. XY ^{*x}	-7.75	-30.25 to 14.75	No	ns	0.6944
7574752					
XX vs. XY ⁻	58.3	38.54 to 78.06	Yes	****	< 0.0001
XX vs. XY ^{*x}	54.8	30.15 to 79.45	Yes	****	< 0.0001
XY ⁻ vs. XY ^{*x}	-3.5	-29.01 to 22.01	No	ns	0.9436

7574775					
XX vs. XY ⁻	55.65	35.89 to 75.41	Yes	****	< 0.0001
XX vs. XY ^{*x}	54.73	33.22 to 76.25	Yes	****	< 0.0001
XY ⁻ vs. XY ^{*x}	-0.9167	-23.42 to 21.58	No	ns	0.9949

Table 3: Bisulfite sequencing results demonstrating significant differences between XY⁻ and XY^{*x} vs. XX in the methylation of 17 CG sites located in the *Foxp3* upstream enhancer region.

4.5 FOXP3 expression in SJL X_mY^{*x} vs. X_pY^{*x} mice

To directly determine whether parental imprinting regulates FOXP3 expression, we generated XY^{*x} mice that have either inherited the maternal or paternal X chromosome, resulting in X_mY^{*x} and X_pY^{*x} mice, respectively (Table 2). At day 10 after PLP 139-151 immunization, LNCs were extracted and re-stimulated *ex vivo* with auto-antigen for 72 hours. As shown in Fig 19, X_mY^{*x} mice have 2.5 fold higher levels of *Foxp3* mRNA in LNCs (Fig 20A, p<0.01, one-way ANOVA, Tukey's post test), as well as higher percentages of CD4⁺CD25⁺FoxP3⁺ T_{reg} cells (Fig 20B and 20C, p<0.01, one-way ANOVA, Tukey's post test), upon auto-antigen stimulation when compared with X_pY^{*x} mice. These results indicate that parental imprinting indeed regulates FOXP3 expression with the maternal allele resulting in increased FOXP3 expression relative to the paternal allele.

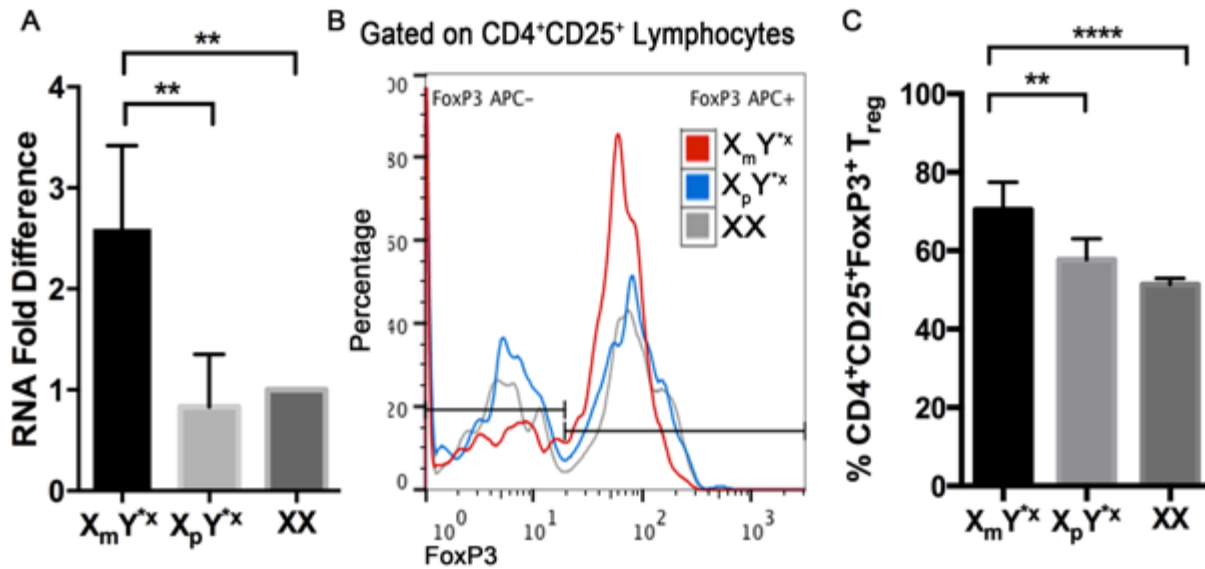


Figure 20. X_mY^{*x} cells as compared to X_pY^{*x} have higher percentage of $CD4^+CD25^+FoxP3^+$ T_{reg} cells during the induction of encephalitogenic immune responses. (A) Representative lymph node *Foxp3* mRNA levels between X_mY^{*x} and X_pY^{*x} mice 10 days after immunization with PLP 139-151. X_mY^{*x} cells expressed higher levels of *Foxp3* mRNA as compared to X_pY^{*x} cells ($p < 0.01$, $N = 5$ each group, paired students t-test). (B, C) Relative quantity of $FoxP3^+$ cells gated on $CD4^+CD25^+$ T cells as defined by isotype control. X_mY^{*x} cells have a higher percentage of $CD4^+CD25^+FoxP3^+$ regulatory T cells as compared to X_pY^{*x} cells ($p < 0.001$, $N = 6$ each group, students t-test). Data are representative of three separate repeated experiments. ** $p < 0.01$, **** $p < 0.0001$.

4.6 *Foxp3* methylation in SJL X_mY^{*x} vs. X_pY^{*x} mice

To directly determine if the differential methylation of *Foxp3* was due to parental imprinting, we examined *Foxp3* methylation in X_mY^{*x} and X_pY^{*x} mice during encephalitogenic immune responses. Both of these mice possessed one X chromosome, either maternal or paternal, with each sharing the Y^{*x} . As shown in Fig 21, X_mY^{*x} $CD3^+/CD4^+$ T cells demonstrated lower percentage methylation in *Foxp3*, as compared to those of X_pY^{*x} , upon auto-antigen stimulation (p -values for each CpG site in Table 4). Combined with earlier bisulfite

sequencing experiments, these results demonstrated that when cells express the maternal X, as in X_mY^- and X_mY^{*x} mice, there is less *Foxp3* methylation corresponding with a higher number of $CD4^+CD25^+FoxP3^+$ T_{reg} cells as compared to cells expressing the paternal X, as in X_pY^{*x} mice.

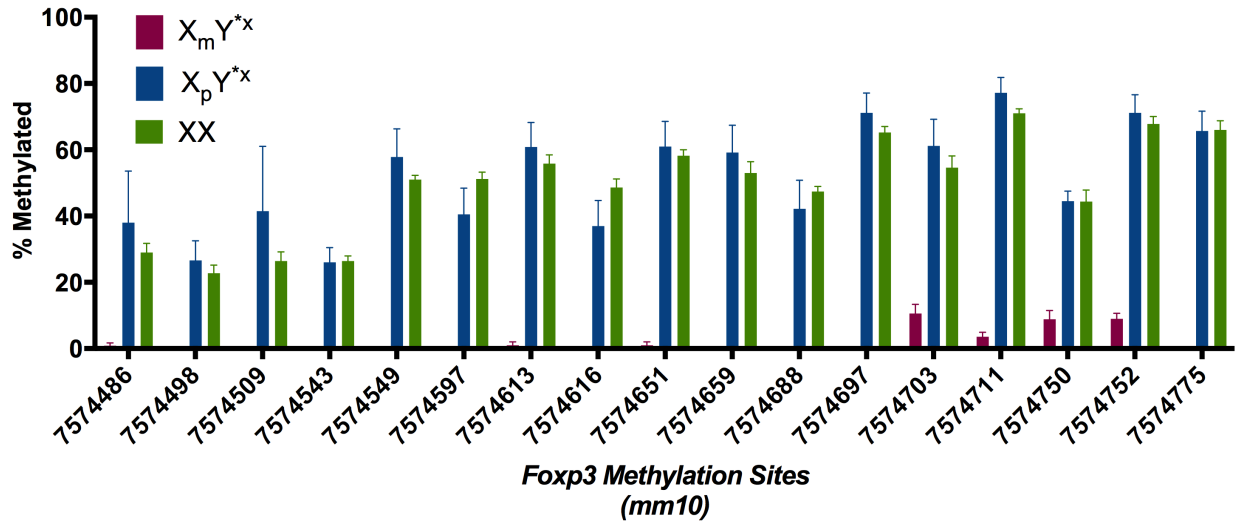


Figure 21. X_mY^{*x} cells, as compared to X_pY^{*x} , have lower methylation of the *Foxp3* enhancer in $CD4^+$ lymph node cells during induction of immune responses. Percent methylation of *Foxp3* enhancer in $CD3^+CD4^+$ T cells derived from LN of PLP 139-151-immunized X_mY^{*x} (red), X_pY^{*x} (blue), and XX (green) mice. $CD3^+CD4^+$ T cells derived from X_mY^{*x} mice have lower *Foxp3* methylation as compared to $CD3^+CD4^+$ T cells derived from X_pY^{*x} mice ($p < 0.0001$, $N=6$ each group, one-way ANOVA). XX littermates to both X_mY^{*x} and X_pY^{*x} showed similar levels of DNA methylation and were thus grouped together.

Tukey's multiple comparisons test	Mean Diff.	95% CI of diff.	Significant?	Summary	Adjusted P Value
7574486					
$X_m Y^{*x}$ vs. XX	-28.14	-45.14 to -11.14	Yes	***	0.0004
$X_m Y^{*x}$ vs. $X_p Y^{*x}$	-37.14	-53.02 to -21.26	Yes	****	< 0.0001
XX vs. $X_p Y^{*x}$	-9	-27.19 to 9.193	No	ns	0.4744
7574498					
$X_m Y^{*x}$ vs. XX	-22.75	-39.75 to -5.751	Yes	**	0.0051
$X_m Y^{*x}$ vs. $X_p Y^{*x}$	-26.6	-42.48 to -10.72	Yes	***	0.0003
XX vs. $X_p Y^{*x}$	-3.85	-22.04 to 14.34	No	ns	0.8719
7574509					
$X_m Y^{*x}$ vs. XX	-26.4	-42.28 to -10.52	Yes	***	0.0003
$X_m Y^{*x}$ vs. $X_p Y^{*x}$	-41.5	-58.50 to -24.50	Yes	****	< 0.0001
XX vs. $X_p Y^{*x}$	-15.1	-33.29 to 3.093	No	ns	0.1252
7574543					
$X_m Y^{*x}$ vs. XX	-26.4	-42.28 to -10.52	Yes	***	0.0003
$X_m Y^{*x}$ vs. $X_p Y^{*x}$	-26	-41.09 to -10.91	Yes	***	0.0002
XX vs. $X_p Y^{*x}$	0.4	-16.02 to 16.82	No	ns	0.9982
7574549					
$X_m Y^{*x}$ vs. XX	-51	-66.88 to -35.12	Yes	****	< 0.0001
$X_m Y^{*x}$ vs. $X_p Y^{*x}$	-57.83	-72.92 to -42.74	Yes	****	< 0.0001
XX vs. $X_p Y^{*x}$	-6.833	-23.26 to 9.589	No	ns	0.5895
7574597					
$X_m Y^{*x}$ vs. XX	-51.2	-67.08 to -35.32	Yes	****	< 0.0001
$X_m Y^{*x}$ vs. $X_p Y^{*x}$	-40.5	-55.59 to -25.41	Yes	****	< 0.0001
XX vs. $X_p Y^{*x}$	10.7	-5.722 to 27.12	No	ns	0.2758
7574613					
$X_m Y^{*x}$ vs. XX	-54.8	-70.68 to -38.92	Yes	****	< 0.0001
$X_m Y^{*x}$ vs. $X_p Y^{*x}$	-59.83	-74.92 to -44.74	Yes	****	< 0.0001
XX vs. $X_p Y^{*x}$	-5.033	-21.46 to 11.39	No	ns	0.7503
7574616					
$X_m Y^{*x}$ vs. XX	-48.46	-64.34 to -32.58	Yes	****	< 0.0001
$X_m Y^{*x}$ vs. $X_p Y^{*x}$	-36.86	-51.95 to -21.77	Yes	****	< 0.0001
XX vs. $X_p Y^{*x}$	11.6	-4.822 to 28.02	No	ns	0.2206

7574651					
$X_m Y^{*x}$ vs. XX	-57.2	-73.08 to -41.32	Yes	****	< 0.0001
$X_m Y^{*x}$ vs. $X_p Y^{*x}$	-60	-75.09 to -44.91	Yes	****	< 0.0001
XX vs. $X_p Y^{*x}$	-2.8	-19.22 to 13.62	No	ns	0.9148
7574659					
$X_m Y^{*x}$ vs. XX	-53	-68.88 to -37.12	Yes	****	< 0.0001
$X_m Y^{*x}$ vs. $X_p Y^{*x}$	-59.17	-74.26 to -44.08	Yes	****	< 0.0001
XX vs. $X_p Y^{*x}$	-6.167	-22.59 to 10.26	No	ns	0.65
7574688					
$X_m Y^{*x}$ vs. XX	-47.11	-62.99 to -31.23	Yes	****	< 0.0001
$X_m Y^{*x}$ vs. $X_p Y^{*x}$	-41.88	-56.97 to -26.79	Yes	****	< 0.0001
XX vs. $X_p Y^{*x}$	5.233	-11.19 to 21.66	No	ns	0.7331
7574697					
$X_m Y^{*x}$ vs. XX	-65.2	-81.08 to -49.32	Yes	****	< 0.0001
$X_m Y^{*x}$ vs. $X_p Y^{*x}$	-71.17	-86.26 to -56.08	Yes	****	< 0.0001
XX vs. $X_p Y^{*x}$	-5.967	-22.39 to 10.46	No	ns	0.6681
7574703					
$X_m Y^{*x}$ vs. XX	-44.03	-59.91 to -28.15	Yes	****	< 0.0001
$X_m Y^{*x}$ vs. $X_p Y^{*x}$	-50.6	-65.68 to -35.51	Yes	****	< 0.0001
XX vs. $X_p Y^{*x}$	-6.567	-22.99 to 9.855	No	ns	0.6137
7574711					
$X_m Y^{*x}$ vs. XX	-67.43	-83.31 to -51.55	Yes	****	< 0.0001
$X_m Y^{*x}$ vs. $X_p Y^{*x}$	-73.6	-88.68 to -58.51	Yes	****	< 0.0001
XX vs. $X_p Y^{*x}$	-6.167	-22.59 to 10.26	No	ns	0.65
7574750					
$X_m Y^{*x}$ vs. XX	-35.54	-51.42 to -19.66	Yes	****	< 0.0001
$X_m Y^{*x}$ vs. $X_p Y^{*x}$	-35.64	-50.73 to -20.55	Yes	****	< 0.0001
XX vs. $X_p Y^{*x}$	-0.1	-16.52 to 16.32	No	ns	0.9999
7574752					
$X_m Y^{*x}$ vs. XX	-58.8	-74.68 to -42.92	Yes	****	< 0.0001
$X_m Y^{*x}$ vs. $X_p Y^{*x}$	-62.17	-77.26 to -47.08	Yes	****	< 0.0001
XX vs. $X_p Y^{*x}$	-3.367	-19.79 to 13.06	No	ns	0.8793

7574775					
X _m Y ^{*x} vs. XX	-65.86	-81.74 to -49.98	Yes	****	< 0.0001
X _m Y ^{*x} vs. X _p Y ^{*x}	-65.52	-80.61 to -50.44	Yes	****	< 0.0001
XX vs. X _p Y ^{*x}	0.3333	-16.09 to 16.76	No	ns	0.9987

Table 4: Bisulfite sequencing results demonstrating significant differences between X_mY^{*x} vs. X_pY^{*x} in the methylation of 17 CG sites located in the *Foxp3* upstream enhancer region.

4.7 Expression and methylation status of X chromosome genes *Tlr7* and *Cd40l* in CD4⁺ T cells of SJL XX, XY⁻, X_mY^{*x}, and X_pY^{*x} mice

We next examined the expression and DNA methylation of two other X chromosome gene candidates that are involved in autoimmune responses, *Cluster of differentiation 40 ligand* (*Cd40l*) and *toll-like receptor 7* (*Tlr7*). SJL mice were immunized with PLP 139-151 at day 0, and their lymph nodes harvested on day 12 for *ex vivo* cell culture in the presence of autoantigen. Cells were harvested at 12 hours and 72 hours to examine CD40L and TLR7 expression, respectively. There were no differences in the expression of CD40L (Fig 22A) and TLR7 (Fig 22B), consistent with our earlier findings of no sex chromosome effects on TLR7 expression during adoptive EAE (Fig 10).

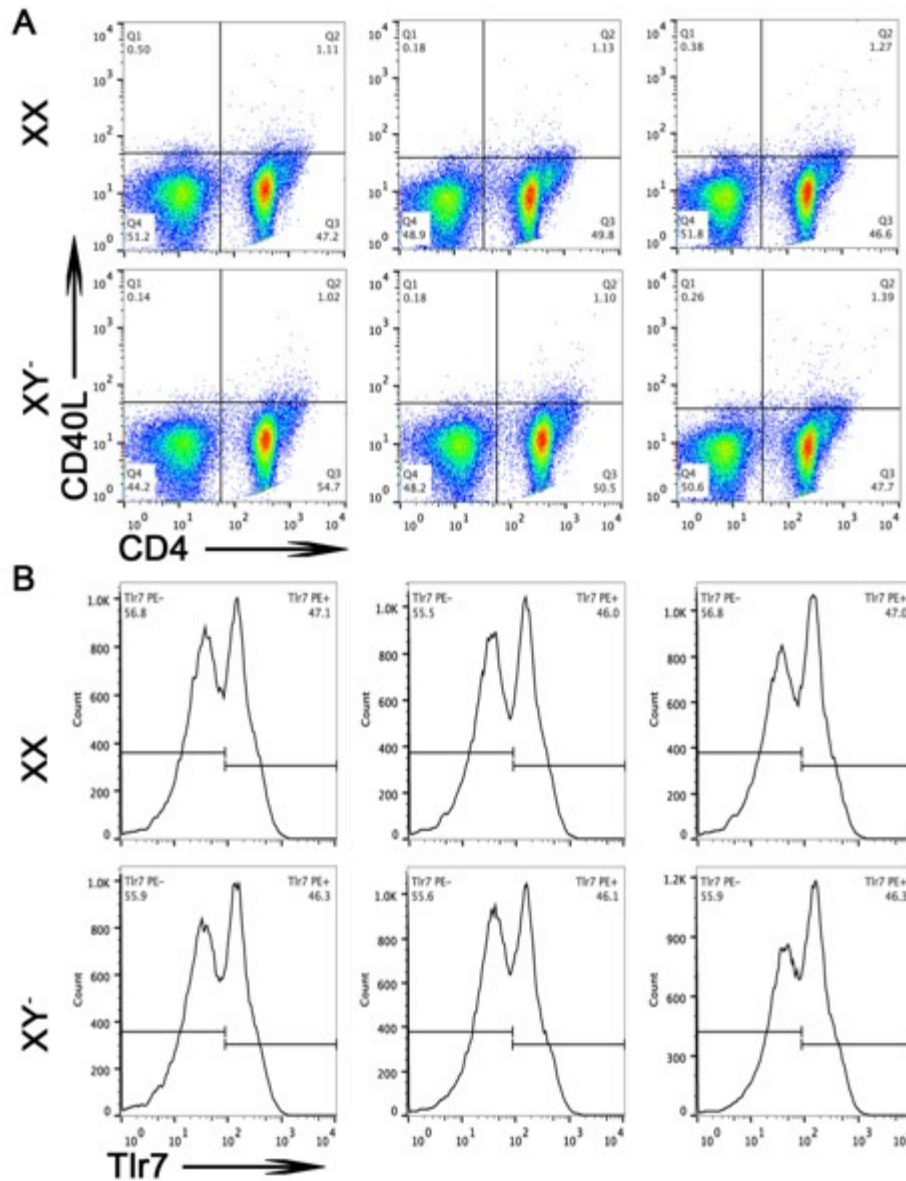


Figure 22: No Differences in CD40L and TLR7 expression during encephalitogenic immune responses. (A) Individual dot plots representing CD40L expression gated on CD4⁺ cells in XX (top) and XY⁻ (bottom) mice. (B) Individual histograms representing TLR7 expression gated on live lymphocytes in XX (top) and XY⁻ (bottom) mice. No differences in CD40L or TLR7 were observed between any groups.

Interestingly, when we examined DNA methylation of the *CD40l* promoter region in CD3/CD4⁺ T cells, we found that the maternal allele had half of the percent methylation than that of the paternal allele (35% vs. 70%, respectively) and the XX littermate controls in nearly half the CG sites that were examined (Fig 23 and Table 5). Similarly, the *Tlr7* promoter region demonstrated less methylation in mice bearing the maternal X as compared to the paternal X in the majority of the CG sites that were examined (Fig 24 and Table 6). Notably, the methylation difference between X_m and X_p in the *Cd40l* and *Tlr7* promoter regions are not as pronounced as that of *Foxp3*, where X_m essentially demonstrated no methylation at these sites (Fig 21). It appears that the paternal allele of the immune genes that we examined, including *Foxp3*, *CD40l*, and *Tlr7*, are preferentially methylated over the maternal allele. It is unclear why CD40L and TLR7 expression at the protein level does not reflect the DNA methylation status during autoimmune responses (Fig 22). Perhaps the particular *CD40l* and *Tlr7* promoter regions we examined were not sensitive to methylation-induced silencing, as promoter methylation does not always lead to silencing (Bird, 1986). By contrast, the *Foxp3* enhancer region we examined has been demonstrated to regulate FOXP3 expression (Lal & Bromberg, 2009; Girdhari Lal et al., 2009).

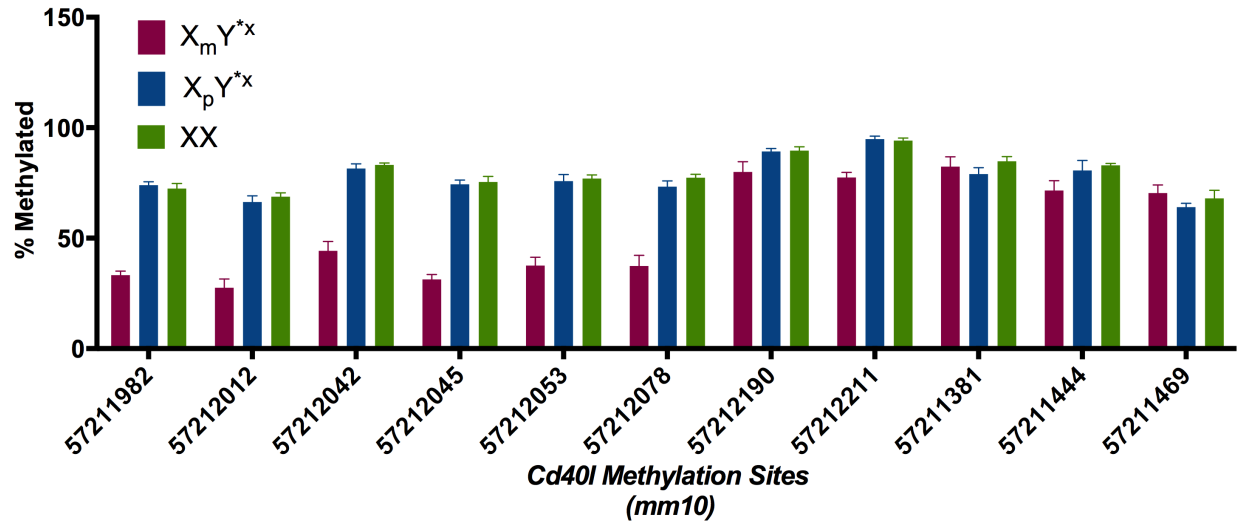


Figure 23. $X_m Y^{*x}$ cells, as compared to $X_p Y^{*x}$, have lower methylation of the *Cd40l* enhancer in $CD4^+$ lymph node cells during induction of immune responses. Percent methylation of *Cd40l* enhancer in $CD3^+CD4^+$ T cells derived from LN of PLP 139-151-immunized $X_m Y^{*x}$ (red), $X_p Y^{*x}$ (blue), and XX (green) mice. $CD3^+CD4^+$ T cells derived from $X_m Y^{*x}$ mice have lower *Cd40l* methylation as compared to $CD3^+CD4^+$ T cells derived from $X_p Y^{*x}$ mice at 7 out of 11 CG sites ($p < 0.0001$, $N=6$ each group, one-way ANOVA). XX littermates to both $X_m Y^{*x}$ and $X_p Y^{*x}$ showed similar levels of DNA methylation and were thus grouped together.

Tukey's multiple comparisons test	Mean Diff.	95% CI of diff.	Significant?	Summary
57211982				
$X_m Y^{*x}$ vs. XX	-39.11	-49.73 to -28.50	Yes	****
$X_m Y^{*x}$ vs. $X_p Y^{*x}$	-40.71	-51.33 to -30.10	Yes	****
XX vs. $X_p Y^{*x}$	-1.6	-13.06 to 9.862	No	ns
57212012				
$X_m Y^{*x}$ vs. XX	-41.23	-51.84 to -30.62	Yes	****
$X_m Y^{*x}$ vs. $X_p Y^{*x}$	-38.76	-48.84 to -28.68	Yes	****
XX vs. $X_p Y^{*x}$	2.467	-8.508 to 13.44	No	ns
57212042				
$X_m Y^{*x}$ vs. XX	-38.91	-49.53 to -28.30	Yes	****
$X_m Y^{*x}$ vs. $X_p Y^{*x}$	-37.21	-47.30 to -27.13	Yes	****
XX vs. $X_p Y^{*x}$	1.7	-9.274 to 12.67	No	ns
57212045				
$X_m Y^{*x}$ vs. XX	-44.11	-54.73 to -33.50	Yes	****
$X_m Y^{*x}$ vs. $X_p Y^{*x}$	-43.05	-53.13 to -32.96	Yes	****
XX vs. $X_p Y^{*x}$	1.067	-9.908 to 12.04	No	ns
57212053				
$X_m Y^{*x}$ vs. XX	-39.43	-50.04 to -28.82	Yes	****
$X_m Y^{*x}$ vs. $X_p Y^{*x}$	-38.26	-48.34 to -28.18	Yes	****
XX vs. $X_p Y^{*x}$	1.167	-9.808 to 12.14	No	ns
57212078				
$X_m Y^{*x}$ vs. XX	-39.97	-50.58 to -29.36	Yes	****
$X_m Y^{*x}$ vs. $X_p Y^{*x}$	-35.9	-45.99 to -25.82	Yes	****
XX vs. $X_p Y^{*x}$	4.067	-6.908 to 15.04	No	ns
57212190				
$X_m Y^{*x}$ vs. XX	-9.6	-20.21 to 1.012	No	ns
$X_m Y^{*x}$ vs. $X_p Y^{*x}$	-9.2	-19.81 to 1.412	No	ns
XX vs. $X_p Y^{*x}$	0.4	-11.06 to 11.86	No	ns
57212211				
$X_m Y^{*x}$ vs. XX	-16.77	-27.38 to -6.159	Yes	***
$X_m Y^{*x}$ vs. $X_p Y^{*x}$	-17.4	-27.49 to -7.322	Yes	***
XX vs. $X_p Y^{*x}$	-0.6333	-11.61 to 10.34	No	ns

57211381				
X_mY^{*x} vs. XX	-2.371	-12.98 to 8.241	No	ns
X_mY^{*x} vs. X_pY^{*x}	3.429	-6.654 to 13.51	No	ns
XX vs. X_pY^{*x}	5.8	-5.174 to 16.77	No	ns
57211444				
X_mY^{*x} vs. XX	-11.43	-22.04 to -0.8165	Yes	*
X_mY^{*x} vs. X_pY^{*x}	-9.095	-19.18 to 0.9878	No	ns
XX vs. X_pY^{*x}	2.333	-8.641 to 13.31	No	ns
57211469				
X_mY^{*x} vs. XX	2.429	-8.183 to 13.04	No	ns
X_mY^{*x} vs. X_pY^{*x}	6.429	-3.654 to 16.51	No	ns
XX vs. X_pY^{*x}	4	-6.974 to 14.97	No	ns

Table 5: Bisulfite sequencing results demonstrating significant differences between X_mY^{*x} vs. X_pY^{*x} in the methylation of 7 out of 11 CG sites located in the *Cd40l* upstream enhancer region.

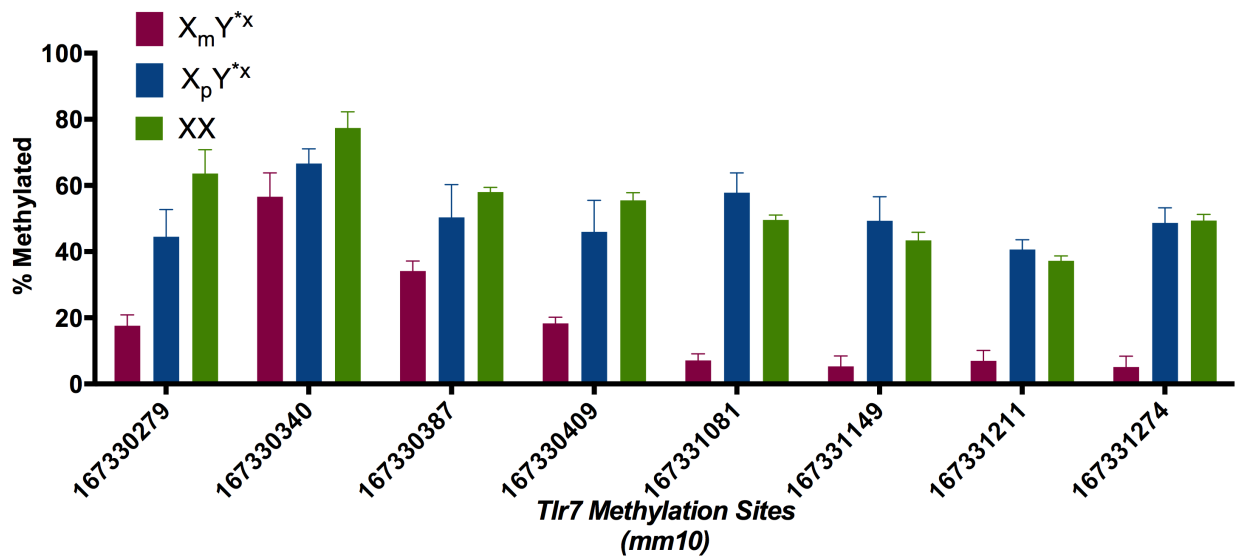


Figure 24. X_mY^{*x} cells, as compared to X_pY^{*x} , have lower methylation of the *Tlr7* enhancer in $CD4^+$ lymph node cells during induction of immune responses. Percent methylation of *Tlr7* enhancer in $CD3^+CD4^+$ T cells derived from LN of PLP 139-151-immunized X_mY^{*x} (red), X_pY^{*x} (blue), and XX (green) mice. $CD3^+CD4^+$ T cells derived from X_mY^{*x} mice

have lower *Tlr7* methylation as compared to CD3⁺CD4⁺ T cells derived from X_pY^{*x} mice at 7 out of 8 CG sites (p<0.0001, N=6 each group, one-way ANOVA). XX littermates to both X_mY^{*x} and X_pY^{*x} showed similar levels of DNA methylation and were thus grouped together.

Tukey's multiple comparisons test	Mean Diff.	95% CI of diff.	Significant?	Summary
167330279				
X _m Y ^{*x} vs. XX	-46.03	-63.05 to -29.01	Yes	****
X _m Y ^{*x} vs. X _p Y ^{*x}	-26.93	-43.10 to -10.76	Yes	***
XX vs. X _p Y ^{*x}	19.1	1.498 to 36.70	Yes	*
167330340				
X _m Y ^{*x} vs. XX	-20.83	-37.85 to -3.808	Yes	*
X _m Y ^{*x} vs. X _p Y ^{*x}	-10.1	-26.27 to 6.077	No	ns
XX vs. X _p Y ^{*x}	10.73	-6.869 to 28.34	No	ns
167330387				
X _m Y ^{*x} vs. XX	-23.86	-42.08 to -5.637	Yes	**
X _m Y ^{*x} vs. X _p Y ^{*x}	-16.19	-32.36 to -0.01806	Yes	*
XX vs. X _p Y ^{*x}	7.667	-11.10 to 26.43	No	ns
167330409				
X _m Y ^{*x} vs. XX	-37.17	-55.93 to -18.40	Yes	****
X _m Y ^{*x} vs. X _p Y ^{*x}	-27.67	-45.27 to -10.06	Yes	***
XX vs. X _p Y ^{*x}	9.5	-10.00 to 29.00	No	ns
167331081				
X _m Y ^{*x} vs. XX	-42.46	-59.48 to -25.44	Yes	****
X _m Y ^{*x} vs. X _p Y ^{*x}	-50.69	-66.86 to -34.52	Yes	****
XX vs. X _p Y ^{*x}	-8.233	-25.84 to 9.369	No	ns
167331149				
X _m Y ^{*x} vs. XX	-38.11	-55.14 to -21.09	Yes	****
X _m Y ^{*x} vs. X _p Y ^{*x}	-44.05	-60.22 to -27.88	Yes	****
XX vs. X _p Y ^{*x}	-5.933	-23.54 to 11.67	No	ns
167331211				
X _m Y ^{*x} vs. XX	-30.2	-47.22 to -13.18	Yes	***

XmY*x vs. XpY*x	-33.67	-49.84 to -17.49	Yes	****
XX vs. XpY*x	-3.467	-21.07 to 14.14	No	ns
167331274				
XmY*x vs. XX	-44.26	-61.28 to -27.24	Yes	****
XmY*x vs. XpY*x	-43.52	-59.70 to -27.35	Yes	****
XX vs. XpY*x	0.7333	-16.87 to 18.34	No	ns

Table 6: Bisulfite sequencing results demonstrating significant differences between X_mY^{*x} vs. X_pY^{*x} in the methylation of 7 out of 8 CG sites located in the *Tlr7* upstream enhancer region.

4.8 Discussion

The growing recognition of the importance of biological sex differences in diseases has recently prompted policy changes at the National Institutes of Health to balance out the sexes in preclinical research (Clayton & Collins, 2014). In the present, it is important to consider research strategies to evaluate the various possible sources of sex differences. There are several classes of sex-related factors that can cause sex differences, all of which ultimately arise from the number and type of sex chromosomes (Arnold, 2012). Possible sources of sex difference include the imbalance of X and Y chromosomes, with females possessing 2X and 0Y chromosome, and males possessing 1X and 1Y chromosome. In fact, there are examples of imbalance of sex chromosomes, either X and Y dosage, affecting disease outcomes, including adiposity and metabolic syndrome, cardiac ischemic/reperfusion injury, and autoimmune disease (Laure K. Case et al., 2015; Chen et al., 2012; Li et al., 2014). Parental imprint of X genes has also been postulated as a source of sex differences in phenotype (Arnold, 2012). However, until now, there has been no example of parental imprinting as an explanation for sex differences. Our study is the first to demonstrate parental X imprinting leading to sex differences in any phenotype.

It has been known for decades that women have more robust humoral and cell-mediated immune responses and higher incidences of autoimmune diseases compared to men (Whitacre, 2001). While the effects of sex hormones leading to this sex difference have been extensively studied, the role of sex chromosomes remains unclear (Bebo et al., 1998; Palaszynski, Liu, Loo, & Voskuhl, 2004; Palaszynski, Loo, et al., 2004). Previous studies have demonstrated a disease promoting effect of autoantigen stimulated immune responses in mice with the XX sex chromosome complement as compared to XY (Palaszynski et al., 2005; Sasidhar et al., 2012;

Smith-Bouvier et al., 2008). *Foxp3* is a transcriptional factor located on the X chromosome that is central to the development of T regulatory cells during autoimmune responses. In this study, we found that mice with XY sex chromosome complement, when compared with XX, had increased FOXP3 expression during autoimmune responses. These data are consistent with prior observations using T_{reg} depletion studies showing a greater ability for males, as compared to females, to regulate effector T cells in PLP 139-151 induced EAE (Reddy et al., 2005). As previously mentioned, sex differences in X chromosome gene expression could theoretically result from differences in X dosage, Y dosage, or parental imprinting. Regarding X dosage, if *Foxp3* escapes X-inactivation in XX mice, we would have expected greater FOXP3 levels in XX as compared XY mice. FOXP3 levels are also unlikely to be influenced by downstream X dosage effects since differences in FOXP3 expression were observed between X_mY^{*x} vs. X_pY^{*x} mice. Thus, differences in FOXP3 are probably not due to X dosage effects. Moreover, our results also excluded the possibility of an indirect Y gene effect on FOXP3 expression since the number of Y chromosomes did not affect outcomes. In contrast, differences in FOXP3 expression were shown to be due to parental imprinting. Specifically, the maternal allele, compared to the paternal imprint, had less *Foxp3* methylation leading to more FOXP3 expression. To our knowledge, this is the first evidence of parental imprinting of an X chromosome gene that offers explanation for sex differences in autoimmunity or any other disease phenotype.

Interestingly, although *FOXP3* dysregulation has been implicated in MS (Fontenot, Gavin, & Rudensky, 2003a; Huan et al., 2005; Venken et al., 2008), evidence from linkage studies examining the X chromosome in MS patients has not demonstrated a role for *FOXP3* or any X locus in MS susceptibility, whether through direct gene products or interactions with autosomal genes (Ebers et al., 1996; Herrera, Coder, et al., 2007). However, linkage studies are

limited to detection of polymorphisms in populations of interest and may not identify epigenetic effects, such as methylation, that may affect the expression level of a given gene, especially if the methylation pattern is similar across all members of one sex. Our findings of a parental imprinting effect on the expression of *Foxp3* underscore the importance of epigenetic factors that can produce sexually dimorphic immune responses which might otherwise undetectable using genome wide association studies (GWAS).

In humans, genetic factors underlying the female preponderance in MS have been attributed to the maternal parent-of-origin (POO) disproportionate transmission of the major histocompatibility complex *HLA-DRB1*15* (chromosome 6) to female offspring (Chao et al., 2010). Other studies have linked maternal POO to higher risk of MS in female offspring based on half-sibling studies, avuncular pair studies, extended pedigree of affected patients, and studies of interracial admixture populations (Ebers et al., 2004; Herrera et al., 2008; Hoppenbrouwers et al., 2008; Ramagopalan et al., 2009). These clinical observations suggest a maternal genetic and female fetal environment interaction during pregnancy that favors the passing of MS susceptibility genes from mother to daughter, as opposed to mother-to-son, and father-to-daughter or -son. Our present findings of maternal imprinting leading to increased FOXP3 expression in an MS model characterized by a female bias in susceptibility suggest a further possibility regarding the female bias in MS (R. R. Voskuhl et al., 1996). Beyond hypothesizing mother-daughter gene-environment interactions, here we provide evidence of a role for epigenetic factors related to parental imprinting of X chromosome genes leading to increased expression of a protective gene (e.g. *FOXP3*) on the X chromosome in the maternal allele relative to the paternal allele. With regard to MS susceptibility, this phenomenon would ultimately benefit males, which inherit and express the protective maternal X allele exclusively,

as compared to the females who express the protective maternal X allele in only half of their cells.

Apart from sex-specific transmission of MS susceptibility genes from unaffected parents, other population-based studies have also found sex differences in the direct parental transmission of MS to offspring. One study found that affected men were more likely to transmit MS to their children than affected women (O. H. Kantarci et al., 2006), although this finding was not replicated in another study (Herrera, Rarnagopalan, et al., 2007). The phenomenon was termed the “Carter effect”. It suggested that men might require more genetic risk factors to develop MS than women, and thus may be more likely to transmit the disease to their children. Why men would have greater physiologic resistance to MS could be due to a variety of non-genetic factors including a protective effect of testosterone or environmental factors. Our findings of increased FOXP3 expression in X_mY^- mice compared to X_mX_p are consistent with the idea of a compensatory mechanism in males that attempts to counter the increased autosomal genetic risk for MS in men.

It has been well established that exogenous and supraphysiological levels of sex hormones play a role in *Foxp3* regulation. Indeed, some groups have previously shown that FOXP3 expression is influenced at least in part by estrogens, as supported by expansion of $CD4^+CD25^+FoxP3^+$ T_{reg} cells during pregnancy when estrogen levels are highly elevated (Polanczyk et al., 2005; Tai et al., 2008). This increased T_{reg} activity is hypothesized to aid maternal tolerance to the half foreign fetus during pregnancy. Moreover, during autoimmunity, mice treated with estrogens had an expansion of $CD4^+CD25^+FoxP3^+$ T_{reg} cells (Polanczyk et al., 2004). Our results provide evidence for a role of another sex related factor, X chromosome imprinting, in regulating FOXP3 expression. While a protective effect of high levels of

estrogens at high levels on increasing CD4⁺CD25⁺FoxP3⁺ T_{reg} cells may contribute to mechanisms of amelioration of cell mediated autoimmune diseases such as multiple sclerosis and rheumatoid arthritis during pregnancy (Haghmorad et al., 2014; Polanczyk et al., 2005), an effect of estrogens at lower physiologic cycling levels could not explain the sex difference in susceptibility since it runs counter to the clinical observation of females being more susceptible than males (Whitacre, 2001). In contrast, the finding here of an X chromosome imprinting effect is consistent with sex differences in susceptibility to autoimmune disease, where the maternal allele is expressed in all cells of XY males which have less *Foxp3* methylation and higher numbers of CD4⁺CD25⁺FoxP3⁺ T_{reg} cells. Notably, our data demonstrating a role of X gene imprinting in sex differences in autoimmunity are not mutually exclusive of additional immunomodulatory role of endogenous physiologic testosterone in males (Rhonda R. Voskuhl & Gold, 2012). In conclusion, both sex hormones and sex chromosomes must be considered for their roles in the female bias in autoimmunity.

Chapter 5: Conclusions

5.1 The maternal X allele leads to a more neurodegenerative response to injury

The first goal of my dissertation was to examine why men would have worse neurodegeneration during immune mediated injury. This was based on the clinical observation of more rapid disease progression in men with MS, even though this disease is more prevalent in women. In Chapters 2 and 3, I used bone marrow chimeras in the MS model, EAE, and showed that mice possessing CNS cells with the XY sex chromosomes, as compared to XX, resulted in greater neurodegeneration and higher Tlr7 expression in cerebral cortical neurons. To further examine the nature of the sex chromosome differences, I next demonstrated that greater neurodegeneration in the XY CNS were not due to the presence of absence of the Y chromosome. Finally, using parentally imprinted transgenic mice I showed that mice bearing the maternal X chromosome resulted in greater clinical disease severity than the paternal X. Together, these experiments demonstrated that the parent-of-origin of the X chromosome leads to sex differences in the neurodegenerative response to injury during EAE.

Parent-of-origin effects have been documented in other diseases, namely Angelman syndrome and Prader-Willi syndrome. Both diseases result from deletion of genes on one allele on chromosome 15 of maternal or paternal origin, respectively, while the other copy of normal sequence is silenced due to imprinting. The studies herein expand the catalog of parent-of-origin effects on diseases to encompass sex differences in the neurodegenerative response to injury that do not involve DNA mutation or aneuploidy. Notably, in the MS model, deleterious effects of the maternal X imprint, which are unopposed in males, are consistent with males having faster disability progression as compared to females in MS. Further studies examining epigenetic

effects on X genes as well as autosomal genes in MS may reveal novel therapeutic targets to prevent disability progression.

5.2 Parental imprinting of *Foxp3* on the X chromosome affects T regulatory cells during autoimmunity

The second goal of my dissertation was to examine the role of sex chromosomes in the increased susceptibility of females to autoimmune diseases. This work built upon previous findings in the lab using mouse models of MS and systemic lupus erythematosus that mice with XX immune systems have greater autoimmune response than XY (Sasidhar et al., 2012; Smith-Bouvier et al., 2008). In Chapter 4, I used XX, XY⁻, X_mY^{*x} and X_pY^{*x} mice to demonstrate that maternal X allele of the *Foxp3* gene, compared with the paternal X allele, resulted in increased the number of FoxP3⁺ T_{regs} in XY⁻ mice relative to XX and reduced autoimmune responses. It has been demonstrated that FoxP3⁺ T_{regs} are reduced with estrogen treatment and during pregnancy in mouse and humans (Polanczyk et al., 2004; Polanczyk et al., 2005). Together, the findings herein as well as previous work suggest that FoxP3⁺ Treg development is affected by a multitude of sex-related factors that includes sex hormones and sex chromosomes. Importantly, this is the first evidence demonstrating that parental imprinting of an X chromosome gene leading to sex differences in autoimmunity.

5.3 Preferential expression of maternal X chromosome genes in the CNS and immune system in the adult mouse during EAE

I have now examined the parent-of-origin of the X chromosome effect in the CNS and immune system during EAE. The maternal X chromosome protected XY⁻ mice from increased

autoimmune responses by increasing FoxP3⁺T_{reg} in the immune compartment, but also greater risk for neurodegeneration by increasing TLR7 expression in cerebral cortical neurons in the CNS compartment. While the effects on EAE were opposite in the CNS and immune system, a common theme has emerged of a preferential expression of the maternal X chromosome genes in several tissues. These studies have been focused on the EAE disease model, but it is conceivable that X chromosome imprinting in some tissues or cell types preferentially skews toward X_p repression or silencing, at least during disease state. It is unlikely that there is a preference for X_p inactivation in the adult mouse.

Preferential, albeit incomplete, X_p inactivation has been described in metatherian marsupials (Vandeberg, Robinson, Samollow, & Johnston, 1987), but this phenomenon ensues for only a brief period in eutherian mammals. In the female mouse, evidences for non-random X inactivation with preferential inactivation of X_p have been described in early developmental events (Frels & Chapman, 1980; Frels, Rossant, & Chapman, 1979; Harper, Fosten, & Monk, 1982; Takagi & Sasaki, 1975; Takagi, Sugawara, & Sasaki, 1982). If X inactivation in adult females were not entirely random but exhibits preferential X_p inactivation in some tissues, then this would imply that X inactivation evolutionarily regulates the dosage of the X chromosome gene expression between males and females to a narrow range, providing an even higher order of regulation of allelic gene expression than in autosomes.

Currently, there is no literature supporting complete non-random X inactivation in the adult mouse, but a cluster of imprinted X genes has been identified in Turner's syndrome (Skuse et al., 1997), with further studies revealing preferential paternal repression of this X gene cluster in the brains of karyotypically normal (40, XX, and 40, XY) and Turner-like mice (39, X_m, and 39, X_p) (Raefski & O'Neill, 2005). Specifically, transcriptome analysis during late embryonic

development, neonatal period, and adulthood showed preferential paternal repression in several X-linked lymphocyte regulated (*Xlr*) genes, *Xlr3b*, *Xlr4b*, and *Xlr4c* (Raefski & O'Neill, 2005). The *Xlr* gene family maps in humans near the pseudoautosomal region at the terminus of the long arm of the X in Xq28, a region with high concentration of loci involved in neurodevelopmental pathologies. First discovered in lymphocytes and linked to X-linked immunodeficiency disorder (Bergsagel, Timblin, Kozak, & Kuehl, 1994; Cohen et al., 1985), *Xlr3b* has now also been linked to cognitive function in mice (W. Davies et al., 2005). Taken together, it appears that the maternal X weighs in much more than the paternal X on immune function and neurodevelopment, even if not by a large enough a margin to abolish parental imprinting effects on the immune system and CNS during an autoimmune attack. Further investigation into the X-linked parental imprinting landscape with respect to CNS development and pathology may be a potentially exciting avenue of future research.

Chapter 6: Methods

6.1 Animals

Four-Core Genotypes. MF1 XY⁻ (*Sry*⁺) males (Y⁻ chromosome of 129 origin) were backcrossed with WT SJL and C57BL/6 females for over 20 generations to obtain litters consisting of the following “four-core genotypes” (FCG): gonadal female XX and XY⁻, gonadal male XX (+*Sry*), and XY⁻ (+*Sry*).

*X_mY^{*x} mice.* XY^{*} mice on an SJL background were generated by backcrossing B6Ei.LT-Y^{*}/EiJ X_mY^{*x} males (Jackson Laboratory) with WT SJL/J females for 10 generations. Other possible gonadal female genotypes include X_mX_p and X_mO. However, this breeding scheme has never produced a viable X_mO mouse. Breeding females are reproductive from 6 weeks to 1 year age, with average litter size of 6-8 pups. The ratio of X_mX_p to X_mY^{*x} is about 50:50. Possible gonadal male genotypes include X_mY^{*}, X_mX_pY^{*}, however, since all gonadal males are euthanized at weaning, we do not have data on the probability of either genotypes.

*X_pY^{*x} mice.* X_pY^{*x} mice were generated by crossing SJL or C57BL/6 X_mY^{*x} females with same strain WT XY males for F1 generation. X_mY^{*x} females are reproductive from 6 weeks to 6 months age, and the frequency of pregnancy in breeding females is comparable to that of WT females. The pups are viable with no noticeable difference from WT mice in physical appearance or social behavior. Although productive, X_mY^{*x} females produce small litter sizes of only 3-4 pups each pregnancy. The X_pY^{*x} genotype occurs only about 12% of the time or even less. In the other 88% of the time, the genotypes are equally divided between X_mX_p and X_mX_pY^{*x}. Since all gonadal males are euthanized at weaning, no data is available on the

frequency of the other possible genotypes, such as X_mY and X_mYY^{*x} . This breeding scheme has never resulted in the X_pO females.

Only XX , XY , X_mY^{*x} and X_pY^{*x} genotypes, all gonadal females, were used in these studies. XX littermates from FCG, X_mY^{*x} , and X_pY^{*x} breeding were used as controls for cross-litter comparison. All procedures were done in accordance with the guidelines of the National Institutes of Health and the Chancellor's Animal Research Committee of the University of California, Los Angeles Office for the Protection of Research Subjects.

6.2 Karyotyping

The sex chromosome karyotype of progeny of XY^* fathers and XY^{*x} mothers were determined based on metaphase spreads obtained from 72-96-hour fibroblast cultures. Only gonadal females were karyotyped. Ear tissues were collected in 70% ethanol, then immersed in 30% betadine for 30 sec. Tissues were then incubated in 0.5% collagenase/HBSS solution at 37°C in 5% CO_2 for 3-5 hrs, followed by mechanical dissociation in DMEM supplemented with 10% FBS and 10 U/ml penicillin-streptomycin. Cells were then transferred to a 60 mm culture dish in 5 ml supplemented DMEM and incubated at 37°C in 5% CO_2 for 72-96 hrs. Next, 2 μ l/ml of colcemid was added to the media and incubated at 37°C in 5% CO_2 for 2 hrs, followed by incubation in 0.25% trypsin-1mM EDTA at 37°C in 5% CO_2 for 5 mins before being deactivated by dilution with supplemented DMEM.

To prepare metaphase spreads, cells, were collected and centrifuged at 1100 rpm for 5 min, resuspended in 0.075 M KCl for 5-10 min at RT, followed by dropwise fresh ice-cold 3:1 methanol: acetic acid fixative. The fixative step is repeated several times and then cells are dropped onto superfrost slides.

To visualize the chromosomes, slides are stained with 2% Giemsa solution in 50 mM PBS solution, pH 6.8, for 2-4 minutes, washed with tap water, and then air dried.

6.3 Ovariectomy

All mice used in experiments were ovariectomized at 5-weeks age. Animals were anesthetized with 2.5% isoflurane/oxygen (Butler Schein), administered using an anesthesia inhalation system (Kent Scientific), and body temperature was maintained with a heat pad. Surgeries were performed on sterilized preparation area. Bilateral incisions were made in the inguinal area and ovaries were identified by a gonadal fat mass below the incision site and verified by its connection to the uterus. A hemostat was applied and the ovaries were excised and the fascia was sutured with Vicryl. The skin was stapled and triple antibiotic ointment applied following wound closure. Animals were also post-operatively treated with LRS injections and 5 units carprofen twice over 48 hours to relieve pain. Their drinking water was supplemented with the antibiotic Amoxil (Butler Schein) for 5 days and mice were monitored daily until complete recovery.

6.4 Bone Marrow Chimera

Bone marrow cells were isolated from both femurs and tibias of age-matched, 5-week old, ovariectomized donors and depleted of T and B cells using anti-Thy1.2 and anti-CD19 microbeads, respectively, and AutoMACS Magnetic Cell Separator (Miltenyi Biotec) according to the manufacturer's instruction. Anti-Thy1.2 and -CD19 microbeads were applied at a 1:10 dilutions in 1x PBS/0.05% BSA/0.09% sodium azide buffer for a total of 100 μ l solution per 10^7 cells for 15 min at 4°C. Cells were washed with ice-cold buffer, resuspended at the

concentration of 10^8 cells/500 μ l buffer and passed through the AutoMACS “Deplete” program. Thy1.2⁺ and CD19⁺ cells were washed twice with ice-cold PBS and then transferred intravenously into 4-week old irradiated recipients by tail vein injection at the concentration of 1.5×10^7 cells/0.2 ml injectable grade PBS per animal. Host recipients were irradiated with a total dose of 850 RADS from a ¹³⁷Cesium source irradiator (Model MKI-68A, JL Shepherd) over two days (425 RADS/day) with the last dose given within 2 h of receiving bone marrow cell injection. Animals were given antibiotic water since ovariectomy at age 4 weeks and continued with medicated water for at least two weeks after reconstitution.

6.5 EAE Induction and Scoring

Seven weeks after reconstitution, at age 12 weeks, active EAE ensued with a single injection of 200 μ g Proteolipid Protein, amino acids 139-151 (PLP 139-151) in SJL mice, 200 μ g Myelin Oligodendrocyte Glycoprotein 35-55 (MOG 35-55) in C57BL/6 mice, supplemented with complete Freund’s adjuvant and *Mycobacterium tuberculosis H37Ra*. While C57BL/6 mice would normally receive two antigen immunizations seven days apart, bone marrow chimera mice were spared from the second dose injection, as well as pertussis toxin (PTX). Irradiated mice were observed to display greater vulnerability to EAE with the original protocol of two immunizations and two PTX injections, with many reaching the moribund state and earlier onset of symptoms (around days 5-7). This is possibly due to irradiation-induced damage of the blood brain barrier.

Animals were monitored daily for EAE signs based on a standard EAE 0–5 scale scoring system: 0—healthy, 1—complete loss of tail tonicity, 2—loss of righting reflex, 3—partial paralysis, 4—complete paralysis of one or both hind limbs, and 5—moribund.

6.6 Adoptive Transfer and Tlr7 Immune Studies

Donor lymph node cells were cultured in the presence of PLP 139-151 for 72 hours, and then harvested and adoptively transferred into ovariectomized naïve recipients at the concentration of 1×10^7 cells/0.3 ml injectable grade PBS. Remaining lymph node cells were stained with surface antigens with the following antibodies at 1:100 dilutions on ice: CD45, CD4, CD19 and CD11b (Biolegend). Cells were then fixed and permeabilized in 2% Tween 20 solution and 4% paraformaldehyde for 30 minutes, and then stained with intracellular antigen anti-Tlr7 (Imgenex) for 30 minutes at 4°C at 1:100 dilution, followed by 30 minutes in secondary PE-conjugated antibody in the dark at 1:100 dilution and 4°C. Finally, cells were washed 3 times in FACS buffer (5% FBS in PBS), and then harvested on a FACS Calibur (Becton Dickinson). Flow cytometry data were analyzed with the FlowJo v10.0.6 software (Tree Star, Inc.). All samples were gated based on isotype antibody staining controls.

6.7 Histological Preparation

Mice were deeply anesthetized in 2.5% isoflurane-oxygen mixture and perfused transcardially with ice-cold 1x PBS for 20-30 min, followed by 10% formalin for 10-15 min. Spinal cords were dissected and submerged in 10% formalin overnight at 4°C, followed by 30% sucrose for 24 h. Spinal cords were cut in thirds and embedded in a 75% gelatin/15% sucrose solution. Forty-micrometer thick free-floating spinal cord cross-sections and cerebellar sagittal sections were obtained with a microtome cryostat (Model HM505E, Microm) at -20°C. Tissue sections were collected serially and stored in 1x PBS with 0.1% sodium azide in 4°C until immunohistochemistry.

6.8 Fluorescence Immunohistochemistry

Tissue sections were thoroughly washed with 1x PBS. In the case of anti-MBP labeling, tissue sections undergo additional 30 min incubation with 5% glacial acetic acid in 100-proof ethanol at room temperature, followed by 30 min incubation in 3% hydrogen peroxide in PBS. All tissue sections were permeabilized with 0.3% Triton X-100 in 1x PBS and 2% normal goat serum (NGS) for 30 min at room temperature (RT) and blocked with 10-15% NGS in 1x PBS for 2 h or overnight at 4°C. The following primary antibody (Ab) were used: anti-MBP at 1:1000 dilutions, anti-NF200 at 1:750 dilutions, anti-CD68 at 1:200 dilutions (Sigma-Aldrich), anti-Tlr7 at 1:500 dilutions (Imgenex), and anti-Iba1 at 1:4000 dilutions (Wako Chemicals). All tissue sections followed with secondary Ab conjugated to FITC or Cy5 (Vector Labs and Chemicon) for 1.5 h. A nuclear stain DAPI (2 ng/mL; Molecular Probes) was added 10 min prior to final washes after secondary Ab incubation. Sections were mounted on slides, allowed to semi-dry, and cover slipped in fluoromount G (Fisher Scientific). IgG-control experiments were performed for all primary Ab, and only non-immunoreactive tissues under these conditions were analyzed.

6.9 Chromagen Immunohistochemistry

Tissue sections were thoroughly washed with 1x PBS and treated with 3% hydrogen peroxide for 30 min at RT and then simultaneously blocked with 10% NGS and permeabilized with 0.3% Triton X-100 in 1x PBS for 1 h at room temperature. Primary antibodies: anti-CD3 at 1:2000 dilutions (Sigma), anti-Iba1 at 1:10,000 dilutions (Wako), anti-Calbindin D28K at 1:1000 dilutions (Millipore), and anti-Tlr7 at 1:5000 dilutions (Imgenex), were added for 2 h at RT, and

then placed in 4°C overnight. Tissue sections then followed with secondary Ab labeling at 1:1000 dilutions for 1 h at room temperature and then with Avidin-Biotin Conjugation solution (Vector Labs) for 1 h at RT. Tissue sections were treated with DAB peroxidase substrate (Vector labs) according to manufacturer instructions. IgG-control experiments were performed for all primary Ab, and only non-immunoreactive tissues under these conditions were analyzed.

6.10 Fluorescence *in-situ* Hybridization

Splenocytes were collected in a single cell suspension and treated with 0.075 M KCl hypotonic solution for 7 min at RT prior to being fixed with five rounds of ice-cold 3:1 methanol/acetic acid. A droplet of cells suspended in methanol/acetic acid fixative was released onto a microscope slide from 10-12 inches height, air-dried, and stored in -80°C. Slides were treated with 2x SSC, 0.5% Igepal pH 7.0 (Sigma-Aldrich), at 37°C for 15 min, dehydrated in 70%, 85% and 100% ethanol consecutively for 1 min each. Cells were denatured in 70% formamide/2x SSC pH 7.0 (Fisher Scientific) at 72°C for 2 min, dehydrated and air-dried. The probe mix RAB9B (XqF1)/WC Y probe (Kreatech Diagnostics) was denatured at 90°C for 10 min, applied to air-dry slides and slides were placed in a humidified chamber at 37°C overnight. Slides were washed in 2x SSC/0.1% Igepal for 2 min at RT, followed by 0.4x SSC/0.3% Igepal for 2 min at 72°C, and 2x SSC/0.1% Igepal for 1 min at RT, and then dehydrated and air dried. DAPI, 15 µl at 1:1000 dilutions, and Vectashield (10 µl, Vector Labs) were applied and slides were cover-slipped before proceeding with microscopy. Under a 40x objective, a single color red under the Cy5 channel and a single color green under the FITC channel within a DAPI⁺ cell identified XY, while two red signals identified XX.

6.11 Reconstitution Efficiency

To assess reconstitution efficiency, 150 or more splenocytes taken from XX \rightarrow XY \bar{c} and XY \bar{c} \rightarrow XX chimeras were identified under a 40x objective as either XX or XY according to fluorescence *in situ* hybridization labeled for the presence of the Y chromosome using RAB9B (XqF1)/WC Y probe (Kreatech Diagnostics). The percentage reconstitution was calculated based on the number of donor cells present in the total cells counted, normalized to the efficiency of the Y probe stain.

6.12 Microscopy

Stained sections were examined and photographed using a confocal microscope (Leica TCS-SP, Mannheim, Germany) or a fluorescence microscope (BX51WI; Olympus, Tokyo, Japan) equipped with Plan Fluor objectives connected to a camera (DP70; Olympus). Digital images were collected and analyzed using Leica confocal and DP70 camera software. Images were assembled using Adobe Photoshop (Adobe Systems, San Jose, CA, USA).

6.13 Quantification of Microscopy

To quantify immunohistochemical staining results, three spinal cord cross-sections at the T1–T5 level from each mouse (n=5) were captured under microscope at 10x magnification using the DP70 Image software and a DP70 camera (both from Olympus). All images in each experimental set were captured under the same light intensity and exposure limits. Image analysis was performed using ImageJ Software v1.30 from the NIH website (<http://rsb.info.nih.gov/ij>). Confocal stacks of immunolabeled images were processed first by

splitting the RGB channels of the images and then converting to eight-bit gray images in Image J. All images of the same antibody stain were set to the same threshold.

To quantify demyelination in the spinal cord and cerebellum, gray and white matter were manually delineated on the basis of DAPI staining, and white matter density was calculated and reported as a percentage of total area. Axonal densities were calculated by counting the number of NF200⁺ cells in a 40x image over the area of the captured tissue section. Cerebellar Purkinje cells were manually quantified using a brightfield 10x microscope over the entire sagittal cerebellum, and results were reported as number of Purkinje cells per area in mm². Only healthy Purkinje cells were counted, as indicated by full-bodied balloon-like soma with dendritic branching. PSD-95 and Synapsin1 density was measured and reported as a percentage of the sampled area. Activated microglia were manually counted on the basis of Iba1⁺ staining in a 10x brightfield image over the captured entire tissue cross-section. CD68⁺ macrophages in whole cervical spinal cord cross-sections were manually quantified under a confocal 10x microscope.

To quantify Tlr7 expression in the cerebral cortex, three coronal sections from each mouse (n=5) of the frontal lobe cortical layers I-VI were captured under microscope at 10x magnification under the same light intensity and exposure limits. Confocal stacks of immunolabeled RGB images were held to the same threshold on ImageJ and Tlr7 and NeuN colocalization were manually assessed based on green and red overlay (appearing yellow), and results were reported as percentages of Tlr7 positive NeuN cells per area in mm².

6.14 Cell Culture

Single cell suspension from PLP 139-151 immunized mice were obtained by passing LN successively through 70 μm and 35 μm cell strainers and cultured at a concentration of 4×10^6

cells/ml RPMI 1640 media (Life Technologies) supplemented with 10% v/v heat-inactivated fetal bovine serum (Gibco), 10 U/ml penicillin/streptomycin, 5 mM L-glutamine, 20 mM HEPES buffer, 0.1 mM non-essential amino acids, 1 mM sodium pyruvate (Lonza), and 0.5 mM 2 β -mercaptoethanol (Sigma-Aldrich) in a 24-well plate in the presence of 25 μ g/ml PLP 139-151 in 37°C and 5% CO₂ for 12 hours if examining CD40L expression, and 72 hours if examining FoxP3 and Tlr7 expression by flow cytometry.

6.15 Flow Cytometry

Mouse LNCs were collected on a 96 v-shaped plate (Titertek) for flow cytometric analysis. Single cell suspensions in FACS buffer (2% FBS in PBS) were incubated with anti-CD16/32 (Biolegend) at 1:100 dilutions for 20 min at 4°C to block Fc receptors, centrifuged, and resuspended in FACS buffer with the following Ab added at 1:100 dilutions for 30 min at 4°C: anti-CD4, anti-CD25, anti-FoxP3, anti-CD40L (CD154) (Biolegend), anti-Tlr7 (Imgenex), and Rat-IgG1, -IgG2a, and -IgG2b or Hamster-IgG isotype controls (Biolegend). Cells were subsequently washed twice in FACS buffer and then acquired on a FACSCalibur (BD Biosciences) and analyzed by FlowJo software (Treestar). Quadrants were determined using cells labeled with appropriate isotype control Ab. All flow cytometry figures are representative of three repeated experiments.

6.16 Cell Sorting and DNA Isolation

All cell-sorting for *FoxP3 promoter methylation* was performed in the UCLA Jonsson Comprehensive Cancer Center (JCCC) and Center for AIDS Research Flow Cytometry Core Facility that is supported by National Institutes of Health awards CA-16042 and AI-28697, and

by the JCCC, the UCLA AIDS Institute, the David Geffen School of Medicine at UCLA, and the UCLA Chancellor's Office. Mice were immunized with PLP 139-151 auto-antigen over axillary and inguinal draining lymph nodes, and LNCs were harvested 10 days later. Single cells were cultured *in vitro* with 25 µg/ml PLP 139-151 at a concentration of 4×10^6 cells/ml complete RPMI media in a 24-well plate, at 37°C and 5% CO₂. After 18 hours, LNCs were surface collected and centrifuged in Ficoll to remove dead cells, and then labeled with CD3-FITC and CD4-PE (Biolegend). CD3⁺CD4⁺ T cells were sorted with FACSAria II cytometer and FACSDiva software, version 6.1 (BD Biosciences) and DNA was isolated with Qiagen All Prep DNA/RNA Mini Kit according to manufacturer's instructions. DNA concentration and quality were assessed using a NanoDrop 3300. All DNA used in subsequent methylation experiments had A₂₆₀₋₂₈₀ value between 1.8-2.0.

6.17 T_{reg} Suppression Assay

Mice were immunized with PLP 139-151 and LNCs were harvested on day 12 after immunization. LNs were passed through a 70 µm and 35 µm to obtain single cell suspension, and then LNCs were incubated with ACK lysis buffer for 3 mins at room temperature (RT) to remove red blood cells. LNCs were stained with the following antibodies at 1:100 dilutions in 4°C for 30 mins in FACS buffer supplemented with 5% FCS: anti-CD4-APC, anti-CD25-PE, anti-CD45RB-FITC and anti-FoxP3-APC (Biolegend). Cells were washed and sorted for CD45RB⁺CD25⁻ T_{conv} and CD45RB⁻CD25⁺FoxP3⁺ T_{regs}. T_{conv} and T_{regs} were plated in 96-well round bottom plates with LEAF anti-CD3 at 1 µg/ml and 5×10^5 irradiated splenocytes (with 3000 RADS). Final concentrations of reagents were as follows: T_{conv} = 2.5×10^4 cells/well; T_{regs} = 1.25×10^4 cells at 2:1 ratio. Control wells included: 1) APC only + antigen, and 2) T_{regs} +

antigen. Cells were incubated at 37°C, 5% CO₂ for 72 hours. Eight hours prior to completion of incubation, cells were pulsed with 0.1 µCi [³H]-Thymidine (MP Biomedical). Cells were harvested with a Harvester 96 Mach 2 (Tomtec) and proliferation was determined by assessing [³H]-Thymidine incorporation using beta-plate counter (Perkin-Elmer).

6.18 DNA Methylation

DNA methylation was quantified in a CG-rich *Foxp3* upstream enhancer region using bisulfite sequencing as previously described (Coit, Yalavarthi, Zhao, Kaplan, & Sawalha, 2014). Briefly, genomic DNA was first bisulfite treated using the EZ DNA Methylation kit (Zymo Research, Irvine, CA). Primers were designed using EpiDesigner (Sequenom, San Diego, CA), and primer quality was verified using Premier Biosoft's Netprimer online tool. The following primers were used: Forward 5'-TAGGTGATTGATAAGTAGGAGAAGTT-3', reverse 5'-AAACTCCTCCATTA ACTCATTACAA-3'. PCR reactions were performed using a Bio-Rad T100 (Bio-Rad, Hercules, CA) and ZymoTaq one-step master mix (Zymo, Orange, CA). The following PCR reaction conditions were used: 95°C for 10 min followed by 40 cycles of 95°C for 30 seconds, then 58.3°C for 40 seconds, then 72°C for 1 min, followed by 72°C for 7 min. PCR products were sequenced using an Applied Biosystems 3730 XL sequencer, and the methylation status on each CG site in each sample was quantified using ESME software package (Epigenomics AG, Berlin).

6.19 RNA Isolation

Lymph node tissues were collected from XX, XY⁻, and XY^{*x} mice at day 10 after immunization with PLP 139-151, flash frozen in liquid nitrogen, and stored in -80°C until use.

Tissues were homogenized with a power homogenizer in 1 ml Trizol (Ambion) for 30 secs. Homogenates in Trizol were incubated for 5 mins at room temperature (RT), then 0.2 ml chloroform (Sigma-Aldrich) was added to the suspension. The solution was vigorously vortexed and then centrifuged at 12,000 g for 15 mins at 4°C. The aqueous top layer was collected to a new tube and precipitated with 100% 2-propanol (Fisher Scientific) for 10 minutes RT, and then centrifuged again at 12,000 g for 10 mins at 4°C. The pellet was then washed with 75% ethanol (EM Sciences) and centrifuged at 7,500 g for 5 mins at 4°C. The pellet was allowed to dry for 5-7 mins and then dissolved in nuclease-free DEPC-treated water (Ambion). RNA quality and concentration were assessed using NanoDrop 3300 (Thermo Scientific), and RNA with $A_{260/280}$ ranging between 1.8-2.0 was used for subsequent qRT-PCR reactions.

6.20 Quantitative Real-Time Polymerase Chain Reaction

qRT-PCR was performed with ABI 7300 Real-Time PCR System (Applied Biosystems) on genomic DNA isolated from the lymph nodes of XX, XY⁻ and XY^{*x} mice day 10 after PLP 139-151 immunization. The 2x Sensi SYBR green master mix was used according to manufacturer's instructions using 25 ng of genomic DNA (Bioline). Primers used include: *Foxp3* Forward- AGAAGACAGACCCATGCTGTG, and Reverse- CAGAGGCAGGCTGGATAACG, yielding a product size of 109 base pairs, and housekeeping gene *B2m* Forward-TGCTATCCAGAAAACCCCTCA, and Reverse- TTTC AATGTGAGGCGGGTGG, yielding a product size of 113 base pairs. The following parameters were used: 50°C for 2 min; 95°C for 10 min; 40 cycles at 95°C for 15 sec; 60°C for 1 min; followed by a dissociation stage at 95°C for 15 sec, 60°C for 1 min, 95°C for 15 sec, 60°C

for 15 sec. Fold differences were calculated pair-wise against the XX genotype and were obtained by the delta-delta-Ct method using *B2m* and as a housekeeping gene.

6.21 Statistical Analysis

Clinical EAE and rotarod behavioral tests were analyzed using repeated measures one-way ANOVA with Bonferroni post-hoc test to correct for multiple comparisons.

Immunohistochemical, cytokine, and *Foxp3* methylation data were analyzed by one-way ANOVA with Tukey's post-hoc test to correct for multiple comparisons. mRNA fold differences were evaluated using paired Student's t-test. Flow cytometry results, T_{reg} suppression activity, and *Foxp3* methylation were analyzed using one-way ANOVA with Tukey's post-hoc test to correct for multiple comparisons. All statistical analyses were performed with Prism GraphPad v6.0d.

Chapter 7: Limitations

7.1 Lack of mouse models to evaluate X dosage effects without confounding effects of parental imprinting

This dissertation combined two transgenic mouse models to evaluate the effect of Y dosage and parental imprinting effects. However, there are currently no mouse models that can differentiate between effects of X dosage vs. parental imprinting. The four-core genotypes allowed for the comparison between effects of XY and XX sex chromosome complement in our animal disease models without confounding effects of sex hormones. Since XY and XX animals have varying non-pseudoautosomal X (NPX) and non-pseudoautosomal Y (NPY), this comparison alone cannot distinguish between effects of X dosage, Y dosage, or parental imprinting, thus requiring an additional genotype.

As demonstrated in Chapters 2-4, the evaluation of Y dosage can be achieved with the addition of the XY^{*x} mouse that results from a separate breeding scheme using XY^* males to breed with WT XX females (Table 1). The Y^{*x} contains no NPY, and both XY^- and XY^{*x} mice possess a maternal X chromosome, thus eliminating possible confounding effects of X imprinting when examining effects of Y dosage. Cross litter comparison could theoretically be justified if the common genotype between these two transgenic models (e.g. XX), demonstrate similarities in a given outcome measure (e.g. EAE disease severity).

The evaluation of X dosage effects is more complicated. The breeding of X_mY^{*x} with WT X_pY commonly produces $X_mX_pY^{*x}$ offspring that could theoretically be compared to X_pY^{*x} mice. However, if there are any differences between X_pY^{*x} and $X_mX_pY^{*x}$, one would still be unable to eliminate the possibility of parental imprinting effects because of the additional

variable of the parent-of-origin of the second X chromosome in $X_mX_pY^{*x}$ (Table 7). In conclusion, while parental imprinting effects have been observed in our disease model using four-core genotype and XY^{*x} mice, in some cases there remains the possibility of additional effects of X dosage.

Parents	Progeny Genotype	NPX	NPY	X_m	X_p	Y^{*x}
$XY^{*x} \times XY$	X_pY^{*x}	1+	0	0	1	1
$XY^{*x} \times XY$	$X_mX_pY^{*x}$	2+	0	1	1	1

Table 7. Breeding schematic to examine X dosage in immune responses and neurodegeneration is confounded by parental X imprinting. Mating X_mY^{*x} females with WT XY males produces X_pY^{*x} and $X_mX_pY^{*x}$ progenies, among several others. The Y^{*x} contains a minute segment of X genes adjacent to the pseudoautosomal region, hence the “+” notation in NPX dosage. Comparison between X_pY^{*x} and $X_mX_pY^{*x}$ (green) does not reveal effects of X dosage because it is confounded by parental X imprinting (red). All progenies in this table are ovary-bearing. X_m , maternal X; X_p , paternal X.

7.2 The Y^{*x} chromosome in the XY^{*x} mouse model may carry some NPX genes adjacent to the X PAR boundary

The XY^{*x} mouse was useful in determining the effect of the Y chromosome in our sex chromosome studies when compared with XY^- mice. One advantage of this comparison is that the Y^{*x} chromosome is composed mostly of PAR, thus balancing the number of PARs when assessing the effect of Y dosage. However, the Y^{*x} chromosome also carries a small segment of NPX genes that may include some genes in the X PAR boundary. Since XY^{*x} mice are monosomic for X, these mice would not undergo X-inactivation, assuring that NPX genes on the

Y^{*x} chromosome are expressed. Combined with the expression from the X chromosome, NPX genes on the Y^{*x} are expressed in double doses. This is a possible confound when comparing XY^{*x} with XY^- because any differences in outcome measures between the two sex chromosome complement could be due to the presence or absence of Y, or differences in dosage of NPX genes on the Y^{*x} chromosome. However, in the case of similar outcomes between XY^{*x} and XY^- , it would eliminate the involvement of NPX genes on the Y^{*x} chromosome. For instance, since mice with XY^{*x} and XY^- and mice have similar EAE disease severity (Fig 11), this eliminates the possibility of X dosage effects with respect to the NPX genes located on the Y chromosome on neurodegeneration.

Bibliography

- Agulnik, A. I., Mitchell, M. J., Mattei, M. G., Borsani, G., Avner, P. A., Lerner, J. L., & Bishop, C. E. (1994). A NOVEL X-GENE WITH A WIDELY TRANSCRIBED Y-LINKED HOMOLOG ESCAPES X-INACTIVATION IN MOUSE AND HUMAN. *Human Molecular Genetics*, 3(6), 879-884. doi: 10.1093/hmg/3.6.879
- Antulov, R., Weinstock-Guttman, B., Cox, J. L., Hussein, S., Durfee, J., Caiola, C., . . . Zivadinov, R. (2009). Gender-related differences in MS: a study of conventional and nonconventional MRI measures. *Multiple Sclerosis*, 15(3). doi: 10.1177/1352458508099479
- AP, A., X, C., JC, L., Y, I., & K., R. (2013, April). *Cell-autonomous sex determination outside of the gonad* (242, 4). *Developmental Dynamics*.
- Arnold, A. P. (2009). Mouse Models for Evaluating Sex Chromosome Effects that Cause Sex Differences in Non-Gonadal Tissues. *Journal of Neuroendocrinology*, 21(4). doi: 10.1111/j.1365-2826.2009.01831.x
- Arnold, A. P. (2012). The end of gonad-centric sex determination in mammals. *Trends in Genetics*, 28(2), 55-61. doi: 10.1016/j.tig.2011.10.004
- Arnold, A. P., & Chen, X. (2009). What does the "four core genotypes" mouse model tell us about sex differences in the brain and other tissues? *Frontiers in Neuroendocrinology*, 30(1), 1-9. doi: 10.1016/j.yfrne.2008.11.001
- Arnold, A. P., & Chen, X. Q. (2009). What does the "four core genotypes" mouse model tell us about sex differences in the brain and other tissues? *Frontiers in Neuroendocrinology*, 30(1), 1-9. doi: 10.1016/j.yfrne.2008.11.001
- Baranzini, S. E., Wang, J., Gibson, R. A., Galwey, N., Naegelin, Y., Barkhof, F., . . . Oksenberg, J. R. (2009). Genome-wide association analysis of susceptibility and clinical phenotype in multiple sclerosis. *Human Molecular Genetics*, 18(4), 767-778. doi: Doi 10.1093/Hmg/Ddn388
- Bebo, B. F., Zelinka-Vincent, E., Adamus, G., Amundson, D., Vandenbark, A. A., & Offner, H. (1998). Gonadal hormones influence the immune response to PLP 139-151 and the

- clinical course of relapsing experimental autoimmune encephalomyelitis. *Journal of Neuroimmunology*, 84(2), 122-130. doi: 10.1016/s0165-5728(97)00214-2
- Beecham, A. H., Patsopoulos, N. A., Xifara, D. K., Davis, M. F., Kempainen, A., Cotsapas, C., . . . IIBDGC, I. I. G. C. (2013). Analysis of immune-related loci identifies 48 new susceptibility variants for multiple sclerosis. *Nature Genetics*, 45(11), 1353-+. doi: 10.1038/Ng.2770
- Bergsagel, P. L., Timblin, C. R., Kozak, C. A., & Kuehl, W. M. (1994). SEQUENCE AND EXPRESSION OF MURINE CDNAS ENCODING XLR3 A AND XLR3B, DEFINING A NEW X-LINKED LYMPHOCYTE-REGULATED XLR GENE SUBFAMILY. *Gene*, 150(2), 345-350. doi: 10.1016/0378-1119(94)90450-2
- Berletch, J. B., Yang, F., Xu, J., Carrel, L., & Disteche, C. M. (2011). Genes that escape from X inactivation. *Human Genetics*, 130(2), 237-245. doi: 10.1007/s00439-011-1011-z
- Bird, A. P. (1986). CPG-RICH ISLANDS AND THE FUNCTION OF DNA METHYLATION. *Nature*, 321(6067), 209-213. doi: 10.1038/321209a0
- Bourque, M., Dluzen, D. E., & Di Paolo, T. (2009). Neuroprotective actions of sex steroids in Parkinson's disease. *Frontiers in Neuroendocrinology*, 30(2), 142-157. doi: 10.1016/j.yfrne.2009.04.014
- Burgoyne, P. S. (1998). The role of Y-encoded genes in mammalian spermatogenesis. *Seminars in Cell & Developmental Biology*, 9(4), 423-432.
- Burgoyne, P. S., Mahadevaiah, S. K., Perry, J., Palmer, S. J., & Ashworth, A. (1998). The Y* rearrangement in mice: new insights into a perplexing PAR. *Cytogenetics and Cell Genetics*, 80(1-4), 37-40. doi: 10.1159/000014954
- Cahill, L. (2006). Why sex matters for neuroscience. *Nature Reviews Neuroscience*, 7(6). doi: 10.1038/nrn1909
- Carruth, L. L., Reisert, I., & Arnold, A. P. (2002). Sex chromosome genes directly affect brain sexual differentiation. *Nature Neuroscience*, 5(10), 933-934. doi: 10.1038/nn922
- Case, L. K., Wall, E. H., Dragon, J. A., Saligrama, N., Kremmentsov, D. N., Moussawi, M., . . . Teuscher, C. (2013). The Y chromosome as a regulatory element shaping Immune cell

- transcriptomes and susceptibility to autoimmune disease. *Genome Research*, 23(9), 1474-1485. doi: 10.1101/gr.156703.113
- Case, L. K., Wall, E. H., Osmanski, E. E., Dragon, J. A., Saligrama, N., Zachary, J. F., . . . Teuscher, C. (2015). Copy number variation in Y chromosome multicopy genes is linked to a paternal parent-of-origin effect on CNS autoimmune disease in female offspring. *Genome biology*, 16, 28-28. doi: 10.1186/s13059-015-0591-7
- Chao, M. J., Herrera, B. M., Ramagopalan, S. V., Deluca, G., Handunnetthi, L., Orton, S. M., . . . Ebers, G. C. (2010). Parent-of-origin effects at the major histocompatibility complex in multiple sclerosis. *Human Molecular Genetics*, 19(18), 3679-3689. doi: 10.1093/hmg/ddq282
- Chen, X., McClusky, R., Chen, J., Beaven, S. W., Tontonoz, P., Arnold, A. P., & Reue, K. (2012). The Number of X Chromosomes Causes Sex Differences in Adiposity in Mice. *Plos Genetics*, 8(5). doi: 10.1371/journal.pgen.1002709
- Chen, X., McClusky, R., Itoh, Y., Reue, K., & Arnold, A. P. (2013). X and Y Chromosome Complement Influence Adiposity and Metabolism in Mice. *Endocrinology*, 154(3), 1092-1104. doi: 10.1210/en.2012-2098
- Chen, X., Watkins, R., Delot, E., Reliene, R., Schiesti, R. H., Burgoyne, P. S., & Arnold, A. P. (2008). Sex difference in neural tube defects in p53-null mice is caused by differences in the complement of X not Y genes. *Developmental Neurobiology*, 68(2), 265-273. doi: 10.1002/dneu.20581
- Chen, X., Watkins, R., Delot, E., Reliene, R., Schiestl, R. H., Burgoyne, P. S., & Arnold, A. P. (2008). Sex difference in neural tube defects in p53-null mice is caused by differences in the complement of X not Y genes. *Dev Neurobiol*, 68(2), 265-273. doi: 10.1002/dneu.20581
- Chestnut, B. A., Chang, Q., Price, A., Lesuisse, C., Wong, M., & Martin, L. J. (2011). Epigenetic Regulation of Motor Neuron Cell Death through DNA Methylation. *Journal of Neuroscience*, 31(46), 16619-16636. doi: 10.1523/jneurosci.1639-11.2011
- Clayton, J. A., & Collins, F. S. (2014). NIH to balance sex in cell and animal studies. *Nature*, 509(7500), 282-283.
- Cohen, D. I., Hedrick, S. M., Nielsen, E. A., Deustachio, P., Ruddle, F., Steinberg, A. D., . . . Davis, M. M. (1985). ISOLATION OF A CDNA CLONE CORRESPONDING TO AN

X-LINKED GENE FAMILY (XLR) CLOSELY LINKED TO THE MURINE IMMUNODEFICIENCY DISORDER XID. *Nature*, 314(6009), 369-372. doi: 10.1038/314369a0

Coit, P., Yalavarthi, S., Zhao, W. P., Kaplan, M. J., & Sawalha, A. H. (2014). Epigenome Profiling Reveals Robust Hypomethylation of Interferon Signature Genes in Lupus Neutrophils. *Arthritis & Rheumatology*, 66, S32-S33.

Confavreux, C., Vukusic, S., & Adeleine, P. (2003). Early clinical predictors and progression of irreversible disability in multiple sclerosis: an amnesic process. *Brain*, 126. doi: 10.1093/brain/awg081

Davies, W., Isles, A., Smith, R., Karunadasa, D., Burrmann, D., Humby, T., . . . Wilkinson, L. (2005). Xlr3b is a new imprinted candidate for X-linked parent-of-origin effects on cognitive function in mice. *Nature Genetics*, 37(6). doi: 10.1038/ng1577

Davies, W., Isles, A. R., Humby, T., & Wilkinson, L. S. (2007). What are imprinted genes doing in the brain? *Epigenetics*, 2(4).

De Vries, G. J. (2004). Minireview: Sex differences in adult and developing brains: Compensation, compensation, compensation. *Endocrinology*, 145(3), 1063-1068. doi: 10.1210/en.2003-1504

Dorr, A. E., Lerch, J. P., Spring, S., Kabani, N., & Henkelman, R. M. (2008). High resolution three-dimensional brain atlas using an average magnetic resonance image of 40 adult C57Bl/6J mice. *Neuroimage*, 42(1). doi: 10.1016/j.neuroimage.2008.03.037

Du, S., Itoh, N., Askarinam, S., Hill, H., Arnold, A. P., & Voskuhl, R. R. (2014). XY sex chromosome complement, compared with XX, in the CNS confers greater neurodegeneration during experimental autoimmune encephalomyelitis. *Proceedings of the National Academy of Sciences of the United States of America*, 111(7), 2806-2811. doi: Doi 10.1073/Pnas.1307091111

Ebers, G. C., Kukay, K., Bulman, D. E., Sadovnick, A. D., Rice, G., Anderson, C., . . . Risch, N. (1996). A full genome search in multiple sclerosis. *Nature Genetics*, 13(4), 472-476. doi: Doi 10.1038/Ng0896-472

Ebers, G. C., Sadovnick, A. D., Dyment, D. A., Yee, I. M. L., Willer, C. J., & Risch, N. (2004). Parent-of-origin effect in multiple sclerosis: observations in half-siblings. *Lancet*, 363(9423), 1773-1774. doi: 10.1016/s0140-6736(04)16304-6

- Ehrmann, I. E., Ellis, P. S., Mazeyrat, S., Duthie, S., Brockdorff, N., Mattei, M. G., . . . Scott, D. M. (1998). Characterization of genes encoding translation initiation factor eIF-2 gamma in mouse and human: sex chromosome localization, escape from X-inactivation and evolution. *Human Molecular Genetics*, 7(11), 1725-1737. doi: 10.1093/hmg/7.11.1725
- Floess, S., Freyer, J., Siewert, C., Baron, U., Olek, S., Polansky, J., . . . Huehn, J. (2007). Epigenetic control of the foxp3 locus in regulatory T cells. *Plos Biology*, 5(2), 169-178. doi: 10.1371/journal.pbio.0050038
- Fontenot, J. D., Gavin, M. A., & Rudensky, A. Y. (2003a). Foxp3 programs the development and function of CD4(+)CD25(+) regulatory T cells. *Nature Immunology*, 4(4), 330-336. doi: Doi 10.1038/Ni904
- Fontenot, J. D., Gavin, M. A., & Rudensky, A. Y. (2003b). Foxp3 programs the development and function of CD4+CD25+ regulatory T cells. *Nat Immunol*, 4(4), 330-336. doi: 10.1038/ni904
- Frels, W. I., & Chapman, V. M. (1980). EXPRESSION OF THE MATERNALLY DERIVED X-CHROMOSOME IN THE MURAL TROPHOBLAST OF THE MOUSE. *Journal of Embryology and Experimental Morphology*, 56(APR), 179-190.
- Frels, W. I., Rossant, J., & Chapman, V. M. (1979). MATERNAL X-CHROMOSOME EXPRESSION IN MOUSE CHORIONIC ECTODERM. *Developmental Genetics*, 1(2), 123-132. doi: 10.1002/dvg.1020010202
- Geetz, J., Shoubridge, C., & Corbett, M. (2009). The genetic landscape of intellectual disability arising from chromosome X. *Trends in Genetics*, 25(7), 308-316. doi: 10.1016/j.tig.2009.05.002
- Gonzales, M. L., & LaSalle, J. M. (2010). The Role of MeCP2 in Brain Development and Neurodevelopmental Disorders. *Current Psychiatry Reports*, 12(2), 127-134. doi: 10.1007/s11920-010-0097-7
- Greenfield, A., Carrel, L., Pennisi, D., Philippe, C., Quaderi, N., Siggers, P., . . . Koopman, P. (1998). The UTX gene escapes X inactivation in mice and humans. *Human Molecular Genetics*, 7(4), 737-742. doi: 10.1093/hmg/7.4.737
- Gregg, C., Zhang, J., Butler, J. E., Haig, D., & Dulac, C. (2010). Sex-Specific Parent-of-Origin Allelic Expression in the Mouse Brain. *Science*, 329(5992), 682-685. doi: 10.1126/science.1190831

- Gregg, C., Zhang, J., Weissbourd, B., Luo, S., Schroth, G. P., Haig, D., & Dulac, C. (2010). High-Resolution Analysis of Parent-of-Origin Allelic Expression in the Mouse Brain. *Science*, 329(5992), 643-648. doi: 10.1126/science.1190830
- Guan, H., Nagarkatti, P. S., & Nagarkatti, M. (2011). CD44 Reciprocally Regulates the Differentiation of Encephalitogenic Th1/Th17 and Th2/Regulatory T Cells through Epigenetic Modulation Involving DNA Methylation of Cytokine Gene Promoters, Thereby Controlling the Development of Experimental Autoimmune Encephalomyelitis. *Journal of Immunology*, 186(12), 6955-6964. doi: 10.4049/jimmunol.1004043
- Haghmorad, D., Amini, A. A., Mahmoudi, M. B., Rastin, M., Hosseini, M., & Mahmoudi, M. (2014). Pregnancy level of estrogen attenuates experimental autoimmune encephalomyelitis in both ovariectomized and pregnant C57BL/6 mice through expansion of Treg and Th2 cells. *J Neuroimmunol*, 277(1-2), 85-95. doi: 10.1016/j.jneuroim.2014.10.004
- Harper, M. I., Fosten, M., & Monk, M. (1982). PREFERENTIAL PATERNAL X-INACTIVATION IN EXTRA-EMBRYONIC TISSUES OF EARLY MOUSE EMBRYOS. *Journal of Embryology and Experimental Morphology*, 67(FEB), 127-135.
- Herrera, B. M., Coder, M. Z., Dymen, D. A., Bell, J. T., DeLuca, G. C., Willer, C. J., . . . Ebers, G. C. (2007). Multiple sclerosis susceptibility and the X chromosome. *Multiple Sclerosis*, 13(7), 856-864. doi: 10.1177/352458507076961
- Herrera, B. M., Ramagopalan, S. V., Lincoln, M. R., Orton, S. M., Chao, M. J., Sadovnick, A. D., & Ebers, G. C. (2008). Parent-of-origin effects in MS: Observations from avuncular pairs. *Neurology*, 71(11), 799-803. doi: 10.1212/01.wnl.0000312377.50395.00
- Herrera, B. M., Ramagopalan, S. V., Orton, S., Chao, M., Yee, I. M., Sadovnick, A. D., & Ebers, G. C. (2007). Parental transmission of MS in a population-based Canadian cohort. *Neurology*, 69(12), 1208-1212. doi: Doi 10.1212/01.Wnl.0000268486.40851.D6
- Hong, D. S., & Reiss, A. L. (2014). Cognitive and neurological aspects of sex chromosome aneuploidies. *Lancet Neurology*, 13(3), 306-318.
- Hoppenbrouwers, I. A., Liu, F., Aulchenko, Y. S., Ebers, G. C., Oostra, B. A., van Duijn, C. M., & Hintzen, R. Q. (2008). Maternal transmission of multiple sclerosis in a Dutch population. *Archives of Neurology*, 65(3), 345-348. doi: Doi 10.1001/Archneurol.2007.63

- Hori, S., Nomura, T., & Sakaguchi, S. (2003). Control of regulatory T cell development by the transcription factor Foxp3. *Science*, 299(5609), 1057-1061. doi: 10.1126/science.1079490
- Huan, J., Culbertson, N., Spencer, L., Bartholomew, R., Burrows, G. G., Chou, Y. K., . . . Vandenberg, A. A. (2005). Decreased FOXP3 levels in multiple sclerosis patients. *Journal of Neuroscience Research*, 81(1), 45-52. doi: Doi 10.1002/Jnr.20522
- Hussain, R., Ghomari, A. M., Bielecki, B., Steibel, J., Boehm, N., Liere, P., . . . Ghandour, M. S. (2013). The neural androgen receptor: a therapeutic target for myelin repair in chronic demyelination. *Brain*, 136, 132-146. doi: 10.1093/brain/aws284
- Isles, A. R., Davies, W., Burrmann, D., Burgoyne, P. S., & Wilkinson, L. S. (2004). Effects on fear reactivity in XO mice are due to haploinsufficiency of a non-PAR X gene: implications for emotional function in Turner's syndrome. *Human Molecular Genetics*, 13(17), 1849-1855. doi: 10.1093/hmg/ddh203
- Itoh, Y., Mackie, R., Kampf, K., Domadia, S., Brown, J. D., O'Neill, R., & Arnold, A. P. (2015). Four Core Genotypes mouse model: localization of the Sry transgene and bioassay for testicular hormone levels. *BMC research notes*, 8(1), 986. doi: 10.1186/s13104-015-0986-2
- Jansson, L., Olsson, T., & Holmdahl, R. (1994). ESTROGEN INDUCES A POTENT SUPPRESSION OF EXPERIMENTAL AUTOIMMUNE ENCEPHALOMYELITIS AND COLLAGEN-INDUCED ARTHRITIS IN MICE. *Journal of Neuroimmunology*, 53(2), 203-207. doi: 10.1016/0165-5728(94)90030-2
- Junker, A., Krumbholz, M., Eisele, S., Mohan, H., Augstein, F., Bittner, R., . . . Meinel, E. (2009). MicroRNA profiling of multiple sclerosis lesions identifies modulators of the regulatory protein CD47. *Brain*, 132, 3342-3352. doi: 10.1093/brain/awp300
- Kantarci, O. H., Barcellos, L. F., Atkinson, E. J., Ramsay, P. P., Lincoln, R., Achenbach, S. J., . . . Weinshenker, B. G. (2006). Men transmit MS more often to their children vs women - The Carter effect. *Neurology*, 67(2), 305-310. doi: 10.1212/01.wnl.0000225070.13682.11
- Kantarci, O. H., Hebrink, D. D., Schaefer-Klein, J., Sun, Y., Achenbach, S., Atkinson, E. J., . . . Weinshenker, B. G. (2008). Interferon gamma allelic variants - Sex-biased multiple sclerosis susceptibility and gene expression. *Archives of Neurology*, 65(3), 349-357. doi: 10.1001/archneurol.2007.66

- Kim, S., Dalal, M., & Voskuhl, R. (1998). Estriol ameliorates EAE: Mechanisms in the shift toward Th2 during pregnancy. *Neurology*, *50*(4), A424-A425.
- Koch, M., Kingwell, E., Rieckmann, P., Tremlett, H., & Neurologists, U. M. C. (2010). The natural history of secondary progressive multiple sclerosis. *Journal of Neurology Neurosurgery and Psychiatry*, *81*(9). doi: 10.1136/jnnp.2010.208173
- Lal, G., & Bromberg, J. S. (2009). Epigenetic mechanisms of regulation of Foxp3 expression. *Blood*, *114*(18), 3727-3735. doi: 10.1182/blood-2009-05-219584
- Lal, G., Zhang, N., van der Touw, W., Ding, Y., Ju, W., Bottinger, E. P., . . . Bromberg, J. S. (2009). Epigenetic Regulation of Foxp3 Expression in Regulatory T Cells by DNA Methylation. *Journal of Immunology*, *182*(1), 259-273.
- Lal, G., Zhang, N., van der Touw, W., Ding, Y. Z., Ju, W. J., Bottinger, E. P., . . . Bromberg, J. S. (2009). Epigenetic Regulation of Foxp3 Expression in Regulatory T Cells by DNA Methylation. *Journal of Immunology*, *182*(1), 259-273.
- Lalivé, P. H., Benkhoucha, M., Tran, N. L., Kreutzfeldt, M., Merkler, D., & Santiago-Raber, M. L. (2014). TLR7 signaling exacerbates CNS autoimmunity through downregulation of Foxp3(+) Treg cells. *European Journal of Immunology*, *44*(1), 46-57.
- Lehmann, S. M., Krueger, C., Park, B., Derkow, K., Rosenberger, K., Baumgart, J., . . . Lehnardt, S. (2012). An unconventional role for miRNA: let-7 activates Toll-like receptor 7 and causes neurodegeneration. *Nature Neuroscience*, *15*(6). doi: 10.1038/nn.3113
- Lehmann, S. M., Krueger, C., Park, B., Derkow, K., Rosenberger, K., Baumgart, J., . . . Lehnardt, S. (2012). An unconventional role for miRNA: let-7 activates Toll-like receptor 7 and causes neurodegeneration. *Nat Neurosci*, *15*(6), 827-835. doi: nn.3113 [pii] 10.1038/nn.3113
- Lepage, J.-F., Hong, D. S., Mazaika, P. K., Raman, M., Sheau, K., Marzelli, M. J., . . . Reiss, A. L. (2013). Genomic Imprinting Effects of the X Chromosome on Brain Morphology. *Journal of Neuroscience*, *33*(19), 8567-8574. doi: 10.1523/jneurosci.5810-12.2013
- Li, J., Chen, X., McClusky, R., Ruiz-Sundstrom, M., Itoh, Y., Umar, S., . . . Eghbali, M. (2014). The number of X chromosomes influences protection from cardiac ischaemia/reperfusion injury in mice: one X is better than two. *Cardiovascular Research*, *102*(3). doi: 10.1093/cvr/cvu064

- Luders, E., Gaser, C., Narr, K. L., & Toga, A. W. (2009). Why Sex Matters: Brain Size Independent Differences in Gray Matter Distributions between Men and Women. *Journal of Neuroscience*, 29(45). doi: 10.1523/jneurosci.2261-09.2009
- MacKenzie-Graham, A., Rinek, G. A., Avedisian, A., Gold, S. M., Frew, A. J., Aguilar, C., . . . Alger, J. R. (2012). Cortical atrophy in experimental autoimmune encephalomyelitis: In vivo imaging. *Neuroimage*, 60(1), 95-104. doi: 10.1016/j.neuroimage.2011.11.099
- Masliah, E., Mallory, M., Alford, M., DeTeresa, R., Hansen, L. A., McKeel, D. W., & Morris, J. C. (2001). Altered expression of synaptic proteins occurs early during progression of Alzheimer's disease. *Neurology*, 56(1), 127-129.
- Mastronardi, F. G., Noor, A., Wood, D. D., Paton, T., & Moscarello, M. A. (2007). Peptidyl argininedeiminase 2 CpG island in multiple sclerosis white matter is hypomethylated. *Journal of Neuroscience Research*, 85(9), 2006-2016. doi: 10.1002/jnr.21329
- Matejuk, A., Adlard, K., Zamora, A., Silverman, M., Vandembark, A. A., & Offner, H. (2001). 17 beta-Estradiol inhibits cytokine, chemokine, and chemokine receptor mRNA expression in the central nervous system of female mice with experimental autoimmune encephalomyelitis. *Journal of Neuroscience Research*, 65(6), 529-542. doi: 10.1002/jnr.1183
- McGeachy, M. J., Stephens, L. A., & Anderton, S. M. (2005). Natural recovery and protection from autoimmune encephalomyelitis: Contribution of CD4(+)CD25(+) regulatory cells within the central nervous system. *Journal of Immunology*, 175(5), 3025-3032.
- Moldovan, I. R., Cotleur, A. C., Zamor, N., Butler, R. S., & Pelfrey, C. M. (2008). Multiple sclerosis patients show sexual dimorphism in cytokine responses to myelin antigens. *Journal of Neuroimmunology*, 193(1-2). doi: 10.1016/j.jneuroim.2007.10.010
- Nguyen, D. K., & Disteché, C. M. (2006). High expression of the mammalian X chromosome in brain. *Brain Research*, 1126, 46-49. doi: 10.1016/j.brainres.2006.08.053
- Okuda, Y., Okuda, M., & Bernard, C. C. A. (2002). Gender does not influence the susceptibility of C57BL/6 mice to develop chronic experimental autoimmune encephalomyelitis induced by myelin oligodendrocyte glycoprotein. *Immunology Letters*, 81(1), 25-29. doi: 10.1016/s0165-2478(01)00339-x
- Palaszynski, K. M., Liu, H. B., Loo, K. K., & Voskuhl, R. R. (2004). Estriol treatment ameliorates disease in males with experimental autoimmune encephalomyelitis:

- implications for multiple sclerosis. *Journal of Neuroimmunology*, 149(1-2), 84-89. doi: 10.1016/j.jneuroim.2003.12.015
- Palaszynski, K. M., Loo, K. K., Ashouri, J. F., Liu, H. B., & Voskuhl, R. R. (2004). Androgens are protective in experimental autoimmune encephalomyelitis: implications for multiple sclerosis. *Journal of Neuroimmunology*, 146(1-2), 144-152. doi: 10.1016/j.jneuroim.2003.11.004
- Palaszynski, K. M., Smith, D. L., Kamrava, S., Burgoyne, P. S., Arnold, A. P., & Voskuhl, R. R. (2005). A Yin-Yang effect between sex chromosome complement and sex hormones on the immune response. *Endocrinology*, 146(8), 3280-3285. doi: 10.1210/en.2005-0284
- Papenfuss, T. L., Rogers, C., Gienapp, I., Valo, J., McClain, M., Damico, N., & Whitacre, C. C. (2003). Sex differences in experimental autoimmune encephalomyelitis (EAE) are murine strain and neuroantigen dependent. *Faseb Journal*, 17(7).
- Pedre, X., Mastronardi, F., Bruck, W., Lopez-Rodas, G., Kuhlmann, T., & Casaccia, P. (2011). Changed Histone Acetylation Patterns in Normal-Appearing White Matter and Early Multiple Sclerosis Lesions. *Journal of Neuroscience*, 31(9), 3435-3445. doi: 10.1523/jneurosci.4507-10.2011
- Pelfrey, C. M., Cotleur, A. C., Lee, J. C., & Rudick, R. A. (2002). Sex differences in cytokine responses to myelin peptides in multiple sclerosis. *Journal of Neuroimmunology*, 130(1-2). doi: 10.1016/s0165-5728(02)00224-2
- Pike, C. J., Carroll, J. C., Rosario, E. R., & Barron, A. M. (2009). Protective actions of sex steroid hormones in Alzheimer's disease. *Frontiers in Neuroendocrinology*, 30(2), 239-258. doi: 10.1016/j.yfrne.2009.04.015
- Pisitkun, P., Deane, J., Difilippantonio, M. J., Tarasenko, T., Satterthwaite, A., & Bolland, S. (2006). TLR7 gene duplication accelerates autoimmunity and promotes nucleolar-specific B cells. *Journal of Immunology*, 176, S154-S154.
- Polanczyk, M. J., Carson, B. D., Subramanian, S., Afentoulis, M., Vandenbark, A. A., Ziegler, S. F., & Offner, H. (2004). Cutting edge: Estrogen drives expansion of the CD4(+) CD25(+) regulatory T cell compartment. *Journal of Immunology*, 173(4), 2227-2230.
- Polanczyk, M. J., Hopke, C., Huan, J. Y., Vandenbark, A. A., & Offner, H. (2005). Enhanced FoxP3 expression and Treg cell function in pregnant and estrogen-treated mice. *Journal of Neuroimmunology*, 170(1-2), 85-92. doi: 10.1016/j.jneuroim.2005.08.023

- Polansky, J. K., Kretschmer, K., Freyer, J., Floess, S., Garbe, A., Baron, U., . . . Huehn, J. (2008). DNA methylation controls Foxp3 gene expression. *European Journal of Immunology*, 38(6), 1654-1663. doi: 10.1002/eji.200838105
- Pozzilli, C., Tomassini, V., Marinelli, F., Paolillo, A., Gasperini, C., & Bastianello, S. (2003). 'Gender gap' in multiple sclerosis: magnetic resonance imaging evidence. *European Journal of Neurology*, 10(1). doi: 10.1046/j.1468-1331.2003.00519.x
- Raefski, A. S., & O'Neill, M. J. (2005). Identification of a cluster of X-linked imprinted genes in mice. *Nature Genetics*, 37(6), 620-624. doi: 10.1038/ng1567
- Ramagopalan, S. V., Yee, I. M., Dyment, D. A., Orton, S. M., Marrie, R. A., Sadovnick, A. D., . . . Canadian Collaborative Study, G. (2009). Parent-of-origin effect in multiple sclerosis Observations from interracial matings. *Neurology*, 73(8), 602-605. doi: 10.1212/WNL.0b013e3181af33cf
- Rasmussen, S., Wang, Y., Kivisaekk, P., Bronson, R. T., Meyer, M., Imitola, J., & Khoury, S. J. (2007). Persistent activation of microglia is associated with neuronal dysfunction of callosal projecting pathways and multiple sclerosis-like lesions in relapsing - remitting experimental autoimmune encephalomyelitis. *Brain*, 130, 2816-2829. doi: 10.1093/brain/awm219
- Reddy, J., Waldner, H., Zhang, X. M., Illes, Z., Wucherpfennig, K. W., Sobel, R. A., & Kuchroo, V. K. (2005). Cutting edge: CD4(+)CD25(+) regulatory T cells contribute to gender differences in susceptibility to experimental autoimmune encephalomyelitis. *Journal of Immunology*, 175(9), 5591-5595.
- Sasidhar, M. V., Itoh, N., Gold, S. M., Lawson, G. W., & Voskuhl, R. R. (2012). The XX sex chromosome complement in mice is associated with increased spontaneous lupus compared with XY. *Annals of the Rheumatic Diseases*, 71(8), 1418-1422. doi: 10.1136/annrheumdis-2011-201246
- Savettieri, G., Messina, D., Andreoli, V., Bonavita, S., Caltagirone, C., Cittadella, R., . . . Quattrone, A. (2004). Gender-related effect of clinical and genetic variables on the cognitive impairment in multiple sclerosis. *Journal of Neurology*, 251(10). doi: 10.1007/s00415-004-0508-y
- Sawcer, S., Hellenthal, G., Pirinen, M., Spencer, C. C. A., Patsopoulos, N. A., Moutsianas, L., . . . Consor, W. T. C. C. (2011). Genetic risk and a primary role for cell-mediated immune mechanisms in multiple sclerosis. *Nature*, 476(7359), 214-219. doi: Doi 10.1038/Nature10251

- Shin, D., Shin, J.-Y., McManus, M. T., Ptacek, L. J., & Fu, Y.-H. (2009). Dicer Ablation in Oligodendrocytes Provokes Neuronal Impairment in Mice. *Annals of Neurology*, *66*(6), 843-857. doi: 10.1002/ana.21927
- Skuse, D. H., James, R. S., Bishop, D. V. M., Coppin, B., Dalton, P., AamodtLeeper, G., . . . Jacobs, P. A. (1997). Evidence from Turner's syndrome of an imprinted X-linked locus affecting cognitive function. *Nature*, *387*(6634), 705-708. doi: 10.1038/42706
- Smith-Bouvier, D. L., Divekar, A. A., Sasidhar, M., Du, S., Tiwari-Woodruff, S. K., King, J. K., . . . Voskuhl, R. R. (2008). A role for sex chromosome complement in the female bias in autoimmune disease. *Journal of Experimental Medicine*, *205*(5), 1099-1108. doi: 10.1084/jem.20070850
- Spence, R. D., & Voskuhl, R. R. (2012). Neuroprotective effects of estrogens and androgens in CNS inflammation and neurodegeneration. *Frontiers in Neuroendocrinology*, *33*(1), 105-115. doi: 10.1016/j.yfrne.2011.12.001
- Spring, S., Lerch, J. P., & Henkelman, R. M. (2007). Sexual dimorphism revealed in the structure of the mouse brain using three-dimensional magnetic resonance imaging. *Neuroimage*, *35*(4), 1424-1433. doi: 10.1016/j.neuroimage.2007.02.023
- Stridh, P., Ruhrmann, S., Bergman, P., Hedreul, M. T., Flytzani, S., Beyeen, A. D., . . . Jagodic, M. (2014). Parent-of-Origin Effects Implicate Epigenetic Regulation of Experimental Autoimmune Encephalomyelitis and Identify Imprinted Dlk1 as a Novel Risk Gene. *PLoS Genetics*, *10*(3). doi: 10.1371/journal.pgen.1004265
- Subramanian, S., Tus, K., Li, Q.-Z., Wang, A., Tian, X.-H., Zhou, J., . . . Wakeland, E. K. (2006). A Tlr7 translocation accelerates systemic autoimmunity in murine lupus. *Proceedings of the National Academy of Sciences of the United States of America*, *103*(26), 9970-9975. doi: 10.1073/pnas.0603912103
- Tai, P., Wang, J. P., Jin, H. L., Song, X. M., Yan, J., Kang, Y. M., . . . Wang, B. (2008). Induction of regulatory T cells by physiological level estrogen. *Journal of Cellular Physiology*, *214*(2), 456-464. doi: 10.1002/jcp.21221
- Takagi, N., & Sasaki, M. (1975). PREFERENTIAL INACTIVATION OF PATERNALLY DERIVED X-CHROMOSOME IN EXTRAEMBRYONIC MEMBRANES OF MOUSE. *Nature*, *256*(5519), 640-642. doi: 10.1038/256640a0

- Takagi, N., Sugawara, O., & Sasaki, M. (1982). REGIONAL AND TEMPORAL CHANGES IN THE PATTERN OF X-CHROMOSOME REPLICATION DURING THE EARLY POST-IMPLANTATION DEVELOPMENT OF THE FEMALE MOUSE. *Chromosoma*, 85(2), 275-286. doi: 10.1007/bf00294971
- Usdin, M. T., Shelbourne, P. F., Myers, R. M., & Madison, D. V. (1999). Impaired synaptic plasticity in mice carrying the Huntington's disease mutation. *Human Molecular Genetics*, 8(5), 839-846. doi: 10.1093/hmg/8.5.839
- Vandeberg, J. L., Robinson, E. S., Samollow, P. B., & Johnston, P. G. (1987). X-LINKED GENE-EXPRESSION AND X-CHROMOSOME INACTIVATION - MARSUPIALS, MOUSE, AND MAN COMPARED. *Isozymes-Current Topics in Biological and Medical Research*, 15, 225-253.
- Venken, K., Hellings, N., Thewissen, M., Somers, V., Hensen, K., Rummens, J. L., . . . Stinissen, P. (2008). Compromised CD4(+) CD25(high) regulatory T-cell function in patients with relapsing-remitting multiple sclerosis is correlated with a reduced frequency of FOXP3-positive cells and reduced FOXP3 expression at the single-cell level. *Immunology*, 123(1), 79-89. doi: Doi 10.1111/J.1365-2567.2007.02690.X
- Voskuhl, R. R., & Gold, S. M. (2012). Sex-related factors in multiple sclerosis susceptibility and progression. *Nature Reviews Neurology*, 8(5), 255-263. doi: 10.1038/nrneurol.2012.43
- Voskuhl, R. R., & Palaszynski, K. (2001). Sex hormones in experimental autoimmune encephalomyelitis: Implications for multiple sclerosis. *Neuroscientist*, 7(3), 258-270.
- Voskuhl, R. R., PitchejianHalabi, H., MacKenzieGraham, A., McFarland, H. F., & Raine, C. S. (1996). Gender differences in autoimmune demyelination in the mouse: Implications for multiple sclerosis. *Annals of Neurology*, 39(6), 724-733. doi: 10.1002/ana.410390608
- Weinshenker, B. G. (1994). NATURAL-HISTORY OF MULTIPLE-SCLEROSIS. *Annals of Neurology*, 36. doi: 10.1002/ana.410360704
- Weinshenker, B. G., Rice, G. P. A., Noseworthy, J. H., Carriere, W., Baskerville, J., & Ebers, G. C. (1991). THE NATURAL-HISTORY OF MULTIPLE-SCLEROSIS - A GEOGRAPHICALLY BASED STUDY .3. MULTIVARIATE-ANALYSIS OF PREDICTIVE FACTORS AND MODELS OF OUTCOME. *Brain*, 114. doi: 10.1093/brain/114.2.1045

- Whitacre, C. C. (2001). Sex differences in autoimmune disease. *Nat Immunol*, 2(9), 777-780. doi: 10.1038/ni0901-777
- Whitacre, C. C., Reingold, S. C., O'Looney, P. A., & Task Force Gender Multiple Sclerosis, A. (1999). Biomedicine - A gender gap in autoimmunity. *Science*, 283(5406), 1277-1278. doi: 10.1126/science.283.5406.1277
- Wise, P. M. (2002). Estrogens and neuroprotection. *Trends in Endocrinology and Metabolism*, 13(6), 229-230. doi: 10.1016/s1043-2760(02)00611-2
- Wolinsky, J. S., Shochat, T., Weiss, S., Ladkani, D., & Grp, P. R. T. S. (2009). Glatiramer acetate treatment in PPMS: Why males appear to respond favorably. *Journal of the Neurological Sciences*, 286(1-2). doi: 10.1016/j.jns.2009.04.019
- Yu, P., Gregg, R. K., Bell, J. J., Ellis, J. S., Divekar, R., Lee, H. H., . . . Zaghouani, H. (2005). Specific T regulatory cells display broad suppressive functions against experimental allergic encephalomyelitis upon activation with cognate antigen. *Journal of Immunology*, 174(11), 6772-6780.
- Ziehn, M. O., Avedisian, A. A., Dervin, S. M., O'Dell, T. J., & Voskuhl, R. R. (2012). Estriol preserves synaptic transmission in the hippocampus during autoimmune demyelinating disease. *Laboratory Investigation*, 92(8), 1234-1245. doi: 10.1038/labinvest.2012.76
- Ziehn, M. O., Avedisian, A. A., Dervin, S. M., Umeda, E. A., O'Dell, T. J., & Voskuhl, R. R. (2012). Therapeutic Testosterone Administration Preserves Excitatory Synaptic Transmission in the Hippocampus during Autoimmune Demyelinating Disease. *Journal of Neuroscience*, 32(36), 12312-12324. doi: 10.1523/jneurosci.2796-12.2012